

**NON-LINEAR FINITE ELEMENT ANALYSIS OF THE  
EFFECTS OF FIRE PROTECTION ON A TOP AND  
SEATED ANGLE BOLTED STEEL CONNECTION WITH  
DOUBLE WEB ANGLES**

by

**Iksha Singh**

Submitted in fulfilment of the requirements for the degree of  
Master of Science in Civil Engineering

College of Agriculture, Engineering and Science  
University of KwaZulu-Natal  
Durban

01 December 2017

Supervisor: Dr. Georgios A. Drosopoulos

# Preface

---

The work presented in this dissertation was performed through the School of Engineering, Civil Engineering Programme, University of KwaZulu-Natal, Durban, from January 2017 to December 2017, under the supervision of Dr. Georgios. A Drosopoulos.

As the candidate's Supervisor I agree to the submission of this thesis.

 signed at UKZN on 29/11/2017

# Declaration - Plagiarism

---

I, Iksha Singh, declare that:

1. The research reported in this dissertation, except where otherwise indicated, is my original research.
2. This dissertation has not been submitted for any degree or examination at any other university.
3. This dissertation does not contain other persons' data, pictures, graphs or other information, unless specifically acknowledged as being sourced from other persons.
4. This dissertation does not contain other persons' writing, unless specifically acknowledged as being sourced from other researchers. Where other written sources have been quoted, then:
  - a. Their words have been re-written but the general information attributed to them has been referenced.
  - b. Where their exact words have been used, then their writing has been placed in italics and inside quotation marks, and referenced.
5. This dissertation does not contain text, graphics or tables copied and pasted from the Internet, unless specifically acknowledged, and the source being detailed in the thesis and in the References sections.

Signed



.....

Iksha Singh

**Dedicated to my parents – Sunil and Shamini Singh**

Words cannot express my profound gratitude for all that you have done and continue to do for me. Thank you.

# Acknowledgements

---

I would like to express my sincere thanks and appreciation to my supervisor, Dr. Georgios Drosopoulos, for his time, guidance, support and encouragement that has facilitated the successful completion of this dissertation. Thank you for the wisdom you have imparted on me, your willingness in assisting my endeavours and your instrumental supervision throughout the course of this year.

I would also like to express my gratitude to:

- Professor Georgios E. Stavroulakis, Technical University of Crete (Greece), for providing the remote access to engineering software and computer hardware that allowed the completion of this dissertation.
- My family: Sunil, Shamini and Sanav Singh for their invaluable love, blessings, sacrifices, assistance and unwavering support. I would not be who I am or where I am today, without you.
- Mr Nitesh Jaganik for his patience, constant encouragement and immeasurable help and support. Thank you for always having faith in me.
- Miss Cerissa Ramsumer for her assistance, encouragement, reassurance and most of all, her friendship.
- The South African Institution of Civil Engineering (SAICE) for awarding me the postgraduate bursary that aided and further motivated my pursuit of a Master's degree.

# Abstract

---

This study was aimed at investigating the performance of steel structures, towards improving fire design, by examining the effects of fire protection on a steel connection exposed to elevated temperatures. A literature review formed the keystone of the study, whereby relevant principles were contextualised. Two steel I-sections formed a cantilever beam-column connection that was selected as a relevant substructure to form the crux of the analyses. The modelling and numerical analysis of the steel connection was performed using Abaqus, Finite Element Analysis (FEA) computer software. In particular, a three-dimensional, non-linear, finite element model was developed for the simulation of the structural behaviour of the steel connection. The developed models accounted for the semi-rigid behaviour of the connection using contact mechanics laws between the interfaces of all the contacting parts. A proper plasticity model was used to depict damage of the structural steel. Two types of analyses were conducted: steady-state simulations with sequential thermal and thermomechanical analyses, as well as transient simulations with coupled temperature-displacement analyses. The former approach was adopted to gauge the effect of thermal protection and associated variables on the steel connection under fire. The latter approach considered the gradual delamination and deterioration of the protection due to elevated temperatures. A procedure for the numerical implementation of this idea was considered and presented. In both approaches, the steel connection was modelled separately with and without fire protection, in order to provide comparable results. The types of fire protection investigated were concrete and gypsum board. Variables of the fire protection under examination were the thicknesses and extent of coverage thereof, located initially on the top flange of the beam and progressing onto the overall structure. The steady-state analysis results indicated that fire protection offered an improved behaviour of the steel connection under fire. The role of the fire resistant materials became increasingly important for more severe fire phenomena, indicating a significant increase in strength of the fire-protected models. The transient analysis results deemed that progressive delamination has detrimental effects on the performance of the steel structure and fire protection mitigates these effects for a limited period of time.

# Table of Contents

---

Preface.....	i
Declaration - Plagiarism .....	ii
Acknowledgements .....	iv
Abstract.....	v
Table of Contents.....	vi
List of Figures.....	ix
List of Tables.....	xiii
List of Abbreviations .....	xv
Chapter 1 .....	1
1. Introduction .....	1
1.1 Motivation for the Research .....	1
1.2 Research Questions.....	2
1.3 Aims.....	3
1.4 Objectives .....	3
1.5 Structure of the Dissertation.....	4
Chapter 2 .....	5
2 Literature Review .....	5
2.1 Introduction .....	5
2.2 The Incidence of Fire .....	5
2.2.1 Introduction .....	5
2.2.2 Fire in Engineering Structures.....	7
2.3 Properties of Steel.....	11
2.3.1 Structural Steel as a Building Material.....	11
2.3.2 Thermal Properties of Steel.....	11
2.3.3 Thermomechanical Properties of Steel.....	14
2.4 Fire Design of Structural Steel.....	19
2.4.1 Approaches for Structural Fire Design.....	20
2.4.2 Codes of Practice.....	21
2.4.3 Fire Resistance .....	22

2.4.4	Fire Testing and Fire Curves .....	25
2.4.5	Finite Element Analysis .....	29
2.4.6	Behaviour of Steel Substructures under Fire .....	31
2.5	Fire Protection .....	34
2.5.1	Active and Passive Systems .....	34
2.5.2	Types of Fire Protection .....	34
2.5.3	Comparison of Fire Protection Materials .....	34
2.6	Transient Delamination .....	39
2.6.1	Definition .....	39
2.6.2	Causes of Delamination .....	39
2.6.3	Effects and Consequences of Delamination .....	40
2.6.4	Limitations of Current Research .....	41
2.7	Summary .....	43
Chapter 3	.....	44
3	Methodology for Finite Element Analysis .....	44
3.1	Introduction .....	44
3.2	The Research Process .....	44
3.3	Abaqus Analyses .....	45
3.3.1	Steady-State Analysis .....	45
3.3.2	Transient Analysis .....	46
3.4	Abaqus Simulation .....	47
3.5	Abaqus Steady-State Models .....	56
3.5.1	Assigning Material-Specific Properties .....	57
3.5.2	Modelling Fire Protection .....	61
3.5.3	Load Cases and Boundary Conditions .....	62
3.6	Abaqus Coupled Transient Delamination Models .....	67
3.6.1	Assigning Material-Specific Properties .....	67
3.6.2	Model Specifics .....	68
3.6.3	Load Cases and Boundary Conditions .....	70
3.7	Limitations .....	72
3.8	Summary .....	73
Chapter 4	.....	74
4	Steady-State Analysis Results and Discussion .....	74
4.1	Introduction .....	74
4.2	Chapter 4 List of Abbreviations .....	74

4.2.1	Steady-state Models and Thermal Load Cases.....	74
4.3	Mechanical Model .....	75
4.4	Thermal Models – Qualitative Results .....	79
4.5	Uncoupled Thermomechanical Models – Quantitative Results .....	83
4.5.1	Results for BM Coverage – Load Case 1 .....	84
4.5.2	Results for FULL Coverage – Load Case 1 .....	90
4.5.3	Results for FULL Coverage – Load Case 2 .....	95
4.5.4	Results for FULL Coverage – Load Case 3 .....	101
4.5.5	Results for Fire Resistance Offered by Protection Materials.....	107
4.6	Summary.....	113
Chapter 5	.....	115
5	Transient Analysis Results and Discussion .....	115
5.1	Introduction .....	115
5.2	Chapter 5 List of Abbreviations .....	115
5.2.1	Transient Models and Thermal Load Case.....	115
5.3	Control Model – No Fire Protection .....	115
5.4	Initial Fire-Protected Model .....	121
5.5	Final Fire-protected Model – Fire Curve Steel .....	127
5.6	Summary.....	134
Chapter 6	.....	135
6	Conclusions and Recommendations .....	135
6.1	Introduction .....	135
6.2	Steady-State Analyses .....	135
6.3	Coupled Transient Analyses .....	137
6.4	Recommendations for Further Research.....	139
References	.....	141
Appendix A	.....	146
A.1	Geometry of the Steel Connection Parts .....	146
Appendix B	.....	147
B.1	Raw Data .....	147
Appendix C	.....	154
C.1	Sample Calculation.....	154

# List of Figures

---

Figure 2-1: Illustrative comparison of death rate per 100,000 worldwide and quantitative rank and rate of South Africa (Source: after World Life Expectancy, 2014) .....	6
Figure 2-2: Fire incidents in the United States of America in 2015 per sector (Source: NFPA, 2016) .....	8
Figure 2-3: Thermal elongation of steel as a function of temperature (Source: EN1993-1-2, 2005).....	12
Figure 2-4: Thermal conductivity of steel as a function of temperature (Source: EN1993-1-2, 2005).....	13
Figure 2-5: Specific heat of steel as a function of temperature (Source: EN1993-1-2, 2005).....	14
Figure 2-6: Stress-strain relationship for steel at elevated temperatures (Source: EN1993-1-2, 2005).....	15
Figure 2-7: Reduction factors for the stress-strain relationship of steel with respect to temperature (EN1993-1-2, 2005).....	17
Figure 2-8: Deterioration of the stress-strain relationship of steel due to elevated temperatures ( $\theta$ ) (Source: EN1993-1-2, 2001; cited by Kalogeropoulos et al., 2011) ..	19
Figure 2-9: Standard time-temperature curves (Source: Phan et al., 2010) .....	26
Figure 2-10: Comparison of standard fire curve and parametric fire curve (Winestone, 2010).....	27
Figure 2-11: Steel connection in the finite element model (Source: Abdalla et al., 2015) .....	32
Figure 2-12: Steel beam-column finite element model with predetermined delamination region (Source: Arablouei and Kodur, 2016).....	41
Figure 3-1: Abaqus steps for numerical model simulations .....	48
Figure 3-2: Two-dimensional diagram of assembled steel connection (After Abdalla et al., 2015) .....	49
Figure 3-3: Assembly of steel connection in Abaqus .....	51
Figure 3-4: Overall geometry and point of application of 200kN concentrated load (Source: Abdalla et al., 2015) .....	54
Figure 3-5: Common boundary conditions .....	54
Figure 3-6: Overall steel connection depicting the 8-node brick finite element mesh with 167,785 finite elements .....	55

Figure 3-7: Deterioration of the stress-strain relationship of steel due to elevated temperatures ( $\theta$ in °C) (Source: EN1993-1-2, 2001; cited by Kalogeropoulos et al., 2011).....	60
Figure 3-8: Overall connection with 50mm Concrete/ Gypsum board fire protection for: (a) BM coverage; (b) FULL coverage .....	62
Figure 3-9: Overall connection with 30mm Gypsum board fire protection for: (a) BM coverage; (b) FULL coverage .....	62
Figure 3-10: BM fire protection coverage with applied LC1.....	63
Figure 3-11: FULL fire protection coverage with applied LC1 .....	64
Figure 3-12: FULL fire protection coverage with applied LC2 .....	64
Figure 3-13: FULL fire protection coverage with applied LC3 .....	65
Figure 3-14: Zero temperature BC at the base of the column for all models .....	66
Figure 3-15: Zero temperature BC at ends of BM fire protection.....	66
Figure 3-16: Zero temperature BC at partitioned surface edges of FULL fire protection .....	67
Figure 3-17: Standard Fire Curve for 90 minutes (Source: after EN1991-1-2, 2002) ...	71
Figure 4-1: Force-displacement diagram for the mechanical model.....	76
Figure 4-2: Superimposed original shape (grey) and final deformed (green) shape of steel beam under structural loading.....	77
Figure 4-3: Steel connection indicating: (a) yielding at failure (in red); (b) openings at failure .....	78
Figure 4-4: Yielding (in red) of steel connection at: (a) column and angles; (b) beam..	78
Figure 4-5: Representative, general temperature distribution for BM-LC1 fire-protected models .....	81
Figure 4-6: Representative, general temperature distribution for FULL-LC1 fire-protected models.....	82
Figure 4-7: Representative, general temperature distribution for FULL-LC2 fire-protected models.....	82
Figure 4-8: Representative, general temperature distribution for FULL-LC3 fire-protected models.....	83
Figure 4-9: Temperature distribution (°C) in the BM-LC1-CONTROL model at failure .	85
Figure 4-10: Temperature distribution (°C) in the BM-LC1-CONC50 model at failure ..	85
Figure 4-11: Temperature distribution (°C) in the BM-LC1-GYP50 model at failure .....	86
Figure 4-12: Temperature distribution (°C) in the BM-LC1-GYP30 model at failure .....	86
Figure 4-13: Force-displacement curves for steady-state Thermomechanical BM-LC1 models .....	87
Figure 4-14: Equivalent Plastic Strains for BM-LC1 unprotected model.....	90

Figure 4-15: Equivalent Plastic Strains for BM-LC1-GYP30 fire-protected model .....	90
Figure 4-16: Temperature distribution (°C) in the FULL-LC1-CONTROL model at failure .....	91
Figure 4-17: Temperature distribution (°C) in the FULL-LC1-CONC50 model at failure .....	91
Figure 4-18: Temperature distribution (°C) in the FULL-LC1-GYP50 model at failure ..	92
Figure 4-19: Temperature distribution (°C) in the FULL-LC1-GYP30 model at failure ..	92
Figure 4-20: Force-displacement curves for steady-state Thermomechanical FULL-LC1 models .....	93
Figure 4-21: Temperature distribution (°C) in the FULL-LC2-CONTROL model at failure .....	96
Figure 4-22: Temperature distribution (°C) in the FULL-LC2-CONC50 model at failure .....	96
Figure 4-23: Temperature distribution (°C) in the FULL-LC2-GYP50 model at failure ..	97
Figure 4-24: Temperature distribution (°C) in the FULL-LC2-GYP30 model at failure ..	97
Figure 4-25: Force-displacement curves for steady-state Thermomechanical FULL-LC2 models .....	98
Figure 4-26: Temperature distribution (°C) in the FULL-LC3-CONTROL model at failure .....	101
Figure 4-27: Temperature distribution (°C) in the FULL-LC3-CONC50 model at failure .....	102
Figure 4-28: Temperature distribution (°C) in the FULL-LC3-GYP50 model at failure ..	102
Figure 4-29: Temperature distribution (°C) in the FULL-LC3-GYP30 model at failure ..	103
Figure 4-30: Force-displacement curves for steady-state Thermomechanical FULL-LC3 models .....	104
Figure 4-31: Equivalent Plastic Strains for FULL-LC3 unprotected model .....	107
Figure 4-32: Equivalent Plastic Strains for FULL-LC3-GYP30 fire-protected model ..	107
Figure 4-33: Fire resistance offered by protection materials for BM-LC1 .....	108
Figure 4-34: Fire resistance offered by protection materials for FULL-LC1 .....	110
Figure 4-35: Fire resistance offered by protection materials for FULL-LC2 .....	111
Figure 4-36: Fire resistance offered by protection materials for FULL-LC3 .....	112
Figure 5-1: General temperature distribution for TRANS-BM-LC1 control model .....	116
Figure 5-2: Temperature distribution (°C) in the TRANS-BM-LC1 control model at: (a) 0 minutes; (b) 6 minutes; (c) 11 minutes; (d) 18 minutes, at failure .....	117
Figure 5-3: Force-displacement curve for coupled Thermomechanical TRANS-BM-LC1 control model .....	119

Figure 5-4: Superimposed undeformed shape (grey) and final deformed (green) shape after 18 minutes of the steel connection for TRANS-BM-LC1 control model.....	120
Figure 5-5: Equivalent Plastic Strains for TRANS-BM-LC1 unprotected model at 18 minutes .....	121
Figure 5-6: Temperature distribution for TRANS-BM-LC1 initial fire-protected model after complete GYP30 delamination, at 41 minutes .....	122
Figure 5-7: Temperature distribution (°C) and progressive delamination in the initial TRANS-BM-LC1 fire-protected GYP30 model at: a) 0 minutes; (b) 15 minutes; (c) 30 minutes; (d) 41 minutes, after complete delamination.....	123
Figure 5-8: Force-displacement curves for coupled Thermomechanical TRANS-BM-LC1 control and initial fire-protected model .....	125
Figure 5-9: Equivalent Plastic Strains for TRANS-BM-LC1 initial fire-protected model at 41 minutes .....	127
Figure 5-10: Temperature distribution for TRANS-BM-LC1 final fire-protected model after complete GYP30 delamination and additional fire applied to steel beam, at 22 minutes .....	129
Figure 5-11: Temperature distribution (°C) and progressive delamination in the final TRANS-BM-LC1 fire-protected GYP30 model at: a) 11 minutes; (b) 14 minutes; (c) 16 minutes; (d) 22 minutes, after complete delamination.....	130
Figure 5-12: Force-displacement curves for coupled Thermomechanical TRANS-BM-LC1 control and fire-protected models.....	132
Figure 5-13: Equivalent Plastic Strains for TRANS-BM-LC1 final fire-protected model at 22 minutes .....	134
Figure A-1: Geometry of the column and beam steel elements in millimetres.....	146
Figure A-2: Geometry of the steel angle elements in millimetres.....	146

# List of Tables

---

Table 2-1: Fire losses in South Africa 2013-2015 (Source: after FPASA, 2017) .....	7
Table 2-2: Summary of multi-story World Trade Centre building fires with collapses in the United States of America in 2001 (Source: after Beitel and Iwankiw, 2004).....	10
Table 2-3: Reduction factors for the stress-strain relationship of steel at elevated temperatures (after EN1993-1-2, 2005).....	16
Table 2-4: Reduction factors (RF) for steel bolts at elevated temperatures (after EN1993-1-2, 2005).....	18
Table 2-5: Approaches and descriptions for fire design to EN and ISO (Source: after Winestone, 2010) .....	21
Table 2-6: Three alternative methods of comparing fire severity with fire resistance (Source: Phan et al., 2010).....	23
Table 2-7: Typical fire resistance requirements (after Winestone, 2010) .....	24
Table 2-8: Summarised description and comparison of four main types of fire protection materials (Source: As shown).....	37
Table 3-1: Material properties for mechanical models (Source: As shown).....	58
Table 3-2: Material properties for thermal models (Source: As shown).....	58
Table 3-3: Combined material properties for thermomechanical models (Source: EN1993-1-2, 2005).....	59
Table 3-4: Reduction of elasticity modulus with temperature (Source: As shown) .....	60
Table 3-5: Summary of investigated fire protection and various contributing factors....	61
Table 3-6: Material properties for transient thermomechanical model (Source: As shown) .....	68
Table 4-1: Compilation of steady-state thermal and thermomechanical models .....	80
Table 4-2: Summarised comparison of fire protection materials for BM-LC1 models ...	88
Table 4-3: Summarised comparison of fire protection materials for FULL-LC1 models	94
Table 4-4: Summarised comparison of fire protection materials for FULL-LC2 models	99
Table 4-5: Summarised comparison of fire protection materials for FULL-LC3 models .....	105
Table 5-1: Observations and description of initial and final fire-protected models .....	128
Table B-1: Plasticity properties for mechanical model.....	147
Table B-2: Thermal conductivities of fire protection materials for thermal mode.....	147
Table B-3: Plasticity properties for steel parts in thermomechanical model.....	148

Table B-4: Plasticity properties for steel bolts in thermomechanical model.....	149
Table B-5: Specific heat of steel (after EN1993-1-2, 2005) and gypsum.....	149
Table B-6: Data for the standard fire curve.....	150
Table B-7: Data for force-time curve.....	152
Table C-1: Sample calculation for force-displacement curve in mechanical model.....	154

# List of Abbreviations

---

BC	Boundary Conditions
BM	Fire protection coverage to steel beam top flange only
CF	Concentrated Force
CONC50	Concrete fire protection of 50mm thickness
EN	Eurocode
FEA	Finite Element Analysis
FPASA	Fire Protection Association of Southern Africa
FRR	Fire Resistance Rating
FULL	Fire protection coverage applied to overall steel connection
GYP30	Gypsum board fire protection of 30mm thickness
GYP50	Gypsum board fire protection of 50mm thickness
ISO	International Organisation for Standardisation
LC	Load Case
LC1	Surface heat flux applied to steel beam/ protection material top flange
LC2	Surface heat flux applied to all steel beam and column/ protection material flanges
LC3	Surface heat flux applied to all external steel/ protection material surfaces
NBRs	National Building Regulations
NFPA	National Fire Protection Association

NT	Nodal Temperatures
PEEQ	Equivalent Plastic Strain
RF	Reduction Factor
SA	South Africa
SAISC	Southern African Institute of Steel Construction
SANS	South African National Standards
T	Thermal analysis without fire protection
TM	Thermomechanical analysis without fire protection
TMR	Thermomechanical analysis with fire protection
TR	Thermal analysis with protection
TRANS-BM-LC1	Transient models with thermo-structural loading
U	Vertical Displacement

# Chapter 1

---

## 1. Introduction

### 1.1 Motivation for the Research

Designing for fire in buildings and civil engineering structures is both a critical and mandatory process not only in South Africa, but worldwide (Franssen and Real, 2015). The occurrence of fires in buildings is usually unpredictable and destructive. While the causes of fires vary, the resulting consequences can include environmental damage, destruction of property and most significantly, loss of human life. Therefore, there is a need to constantly improve and contribute to the knowledge of the behaviour of structures under fire, in order to build safer structures and mitigate the threat of fire (Franssen et al., 2009).

The Fire Protection Association of Southern Africa (FPASA, 2017) estimated the total number of fire-related deaths in 2015 to be 436 people, of which 23 per cent were attributed to the structural sector. A total number of 45,784 fires were recorded in South Africa in 2015, indicating a 42 per cent increase from the 26,475 fires recorded in 2006 (FPASA, 2017). Moreover, these findings are conservative as they only depict the documented data of *'fires attended by reporting fire services'* (FPASA, 2017). These statistics motivate the need for the design of appropriate and effective fire protection for structural members. In this research, fire protection of steel structures is investigated.

Zingoni (2006) states that with the ever-growing structural use of steel, new challenges constantly arise. This warrants research into the performance of steel structures under excessive temperature conditions. When exposed to fire, steel becomes increasingly vulnerable over time, consequently losing strength and stiffness at elevated temperatures (Winestone, 2010). Although widely researched, there is potential for innovation in providing fire resistance to steel members, thereby allowing the structure to resist failure and collapse and maintaining its structural integrity as far as possible (Zingoni, 2006). Steel structures range from small-scale commercial buildings to large industrial buildings and multi-storey assemblies. Two-dimensional modelling and single element analysis of structural members is simply insufficient, in that the analysis fails to provide adequate assessment of the actual behaviour of the global structure (Gentili, 2013). Thus, the crux of this study is based on the behaviour of a relevant steel

substructure under fire. A three-dimensional, non-linear, finite element model is developed that incorporates material plasticity, large deflections, principles of contact mechanics and temperature dependence. Furthermore, few investigations into the delamination failure mechanism that occurs between fire protection and steel structures at elevated temperatures exist. Moreover, this phenomenon is not distinctly provided for in national building regulations and design codes. This dissertation aims to contribute towards and address this deficiency in research by providing non-linear, time-dependent analyses examining delamination and the eventual destruction of the fire protection material.

Provisions for the fire design of structures (including steel structures) are made through design codes and regulations in both local and international capacities. One of the South African codes that enforce fire safety in building design is SANS 10400 Part T: Fire Protection (2011). However, it can be seen from the aforementioned data that despite the existence of a national code, the occurrence of fires and fire-related deaths involving structural entities remains extensive. This is due to the fact that even in conjunction with international design codes, such as the Eurocode (EN), the documented regulations fail to fully encompass the numerous loading combinations and fire scenarios that occur in reality. As a result, solutions and innovations in designing for structures under fire are constantly sought after, thus presenting the purpose of this research. This study strives to bring awareness to the paramount importance of fire safety in building design and deliver insight into the provision of fire protection for steel structures, towards ultimately improving fire design.

## 1.2 Research Questions

- What is the effect of fire protection on a steel connection when exposed to elevated temperatures?
- What is the effect of delamination between fire protection and a steel connection at elevated temperatures, over time?

The ancillary investigation of the delamination phenomenon was to study the effect of the gradual deterioration and eventual destruction of the thermal protection due to elevated temperatures, resulting in direct contact of the fire event and the steel after some time.

### 1.3 Aims

The aims of the study are:

- To investigate the influence of fire protection on a steel connection under elevated temperatures, towards improving fire design of steel structures.
- To determine and compare the effect of different fire protection materials and the extent of coverage of the protection on the steel substructure, under fire conditions.
- To investigate the role and effect of delamination between fire protection and a steel connection at elevated temperatures, accounting for damage or destruction of the protection, over time.

### 1.4 Objectives

The objectives forming the crux of the study are:

- Compile and critically evaluate existing literature relevant to the study, to provide context to the research.
- Select appropriate and available computer software for modelling and conducting finite element analyses.
- Import an existing steel connection and design three-dimensional, non-linear models for the connection using the computer software, Abaqus.
- Compute the steady-state analysis models (no real time considered) to validate the outcomes against established research and compare the results of the fire protected and unprotected models.
- Compute the transient analysis models (considering evolution of the fire event in real time) that depict the delamination failure mechanism over time and compare the results of the protected and unprotected models.
- Analyse and evaluate the steady-state analysis and transient analysis results in the form of comparative force-displacement diagrams and temperature distributions to draw meaningful conclusions about the investigated types and placement of fire protection.
- Comment on the potential for improved fire design of steel structures and provide recommendations for further research of the topic.

## 1.5 Structure of the Dissertation

The dissertation consists of six chapters and is structured to provide a progressive and comprehensive understanding of the research undertaken in the study. The contents of each chapter are further elaborated on:

**Chapter 1** contextualises the pivotal concepts of the study and provides a motivation for the research. The research questions, aims and objectives are stated.

**Chapter 2** consists of a literature review that provides a synthesised progression of information relevant to the study. Insight is given into the broad topics including fire safety, engineering structures under fire, steel as a building material and the fire design of steel structures. These topics converge to detailed literature focusing on the different types of fire protection materials, locations of fire protection and the occurrence of delamination of the fire protection materials over time.

**Chapter 3** describes the methodology adopted in achieving the aims and objectives of the study. This includes a description of the research process followed in conducting the literature review. The steps taken in modelling the Abaqus finite element analysis (FEA) simulations and designing the various numerical models are expressed. The modelled scenarios under investigation are described. Both steady-state analysis and transient analysis procedures are discussed. The limitations experienced in using the Abaqus software and conducting the study are presented.

**Chapter 4** presents the results of the steady-state analyses performed with the Abaqus numerical models. The results of the models with and without fire protection are quantified and compared; evaluations of the comparative analyses are made.

**Chapter 5** provides the results obtained from the transient analyses performed with the Abaqus numerical models and the outcomes of the delamination failure mechanism and gradual destruction of the fire protection material are presented.

**Chapter 6** offers the main conclusions and final remarks drawn from assessing the results of the study and aforementioned analyses. This chapter discusses the extent to which the research questions, aims and objectives stated in Chapter 1 are achieved and recommendations for further research into the topic are advised.

# Chapter 2

---

## 2 Literature Review

### 2.1 Introduction

The purpose of this chapter is to provide insight into the pivotal concepts of fire in engineering structures, steel and its material properties and the fire design of structural steel. This lays the foundation of the dissertation and creates the context in which the research is based. Relevant literature regarding methods of structural numerical analysis, fire resistance and delamination of fire protection is considered and critically evaluated.

### 2.2 The Incidence of Fire

#### 2.2.1 Introduction

The Geneva Association (2014) considers fire safety of paramount importance. The countless deaths, injuries and significant other losses are evidence of the destructive impacts of infernos. This is aligned with the view of ‘*fire as vulnerability*’ (Geneva Association, 2014). The prevention and control of fires is critical, especially considering the effects of climate change and increasing occurrence of natural disasters, which can trigger blazes in the wake of an aftermath (Geneva Association, 2014). Mitigating the potentially disastrous consequences of fire should be considered a priority worldwide.

The occurrence of fires poses a dire threat to humankind and is one of the leading causes of death in South Africa (SA) and internationally (World Life Expectancy, 2014). Out of the top 86 causes of death worldwide in 2014, World Life Expectancy (2014) ranks fires at 41. Furthermore, fires rank at 23 out of the top 50 causes of death in South Africa in 2014 (World Life Expectancy, 2014). Figure 2-1 indicates an illustrative, worldwide comparison of mortality rates per 100,000 in 2014 due to fire, as well as a quantitative rank and rate of South Africa.

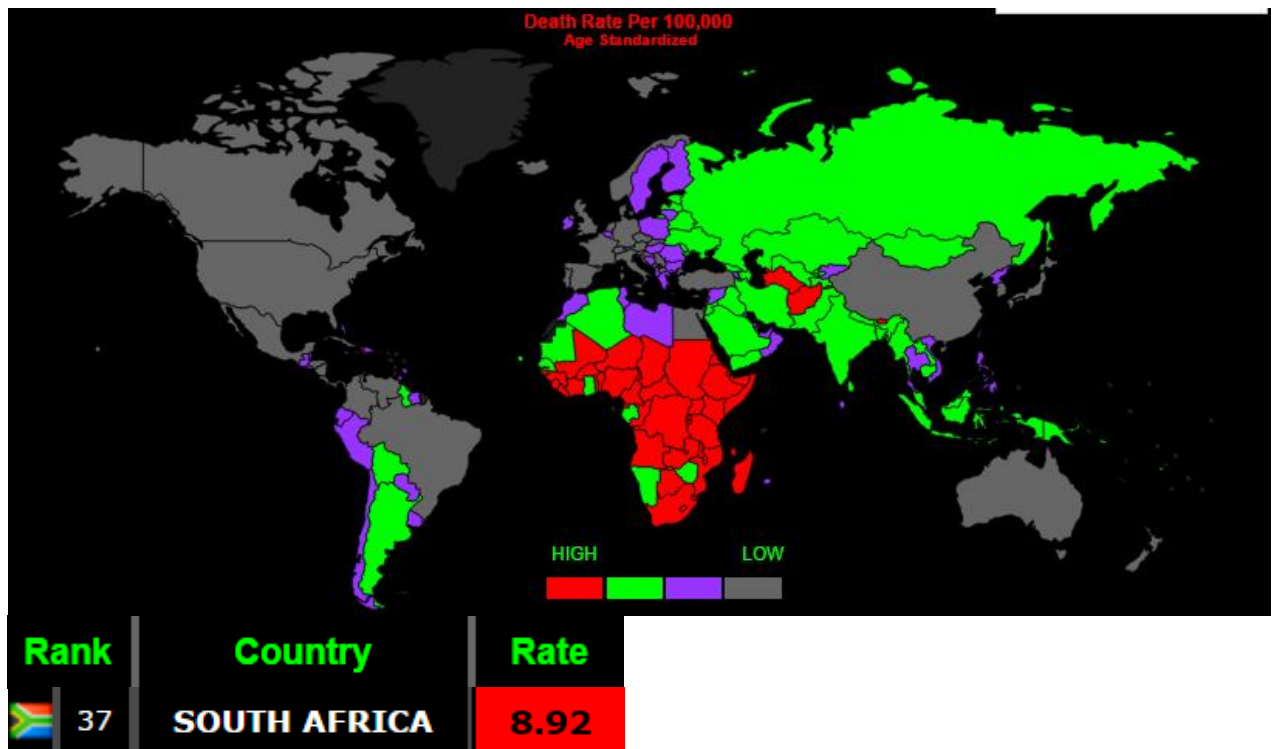


Figure 2-1: Illustrative comparison of death rate per 100,000 worldwide and quantitative rank and rate of South Africa (Source: after World Life Expectancy, 2014)

According to Figure 2-1, the South African mortality rate of 8.92 per 100,000, as a result of fire, is categorised as ‘high’ in comparison to the rest of the world. The death rate in SA is at an ominously high position of 37 out of a total of 172 documented countries. It can be conjectured that with an increase in world population and constant development of infrastructure, the frequency of blazes and resulting mortality figures would increase over the years.

The National Fire Protection Association (NFPA, 2016) states that 1,345,500 fires occurred in the United States of America in 2015, resulting in property damage of an estimated 14.3 billion dollars (approximately 205.5 billion rand). However, the United States of America is regarded as a developed country, which alludes to the fact that more infrastructure increases the probability of a fire, since each new development carries the potential risk of a fire hazard. Comparatively, South Africa, as a third-world developing country, incurred significantly fewer fire losses. The accuracy of the recorded data in South Africa is limited, as certain circumstances of fire incidents were not reflected (FPASA, 2017). Nevertheless, the losses suffered from blazes remain extensive and *‘fires continue to plague the country’* (FPASA, 2017). The fire losses suffered over the period of three years in South Africa can be seen in Table 2-1.

Table 2-1: Fire losses in South Africa 2013-2015 (Source: after FPASA, 2017)

	2013	2014	2015
<b>Total Loss in Rands (in millions)</b>	2158	1847	2732
<b>Gross National Income (GNI) (in thousand millions)</b>	3441	3694	3913
<b>Fire Loss as a % of GNI</b>	0,62%	0,05%	0,69%
<b>No. of Fires (in thousands)</b>	42,3	46,1	45,7
<b>Population (in millions)</b>	52,9	53,5	54,3

The trend with an increasing occurrence of infernos and subsequent millions of rands amassed in fire losses is, at the very least, problematic. South Africa continues to contribute to the tens of billions in accumulated costs due to the impact of fire (Geneva Association, 2014). One per cent of global Gross Domestic Product (GDP) per year is attributed to the costs generated from blazes, according to the Geneva Association (2014), which has the potential to be lowered through research into the field of fire safety. These statistics highlight the imperative need to prioritise fire safety and enact measures to safeguard citizens against the hazard of fire.

### 2.2.2 Fire in Engineering Structures

*'Fire represents one of the most severe conditions encountered during the life-time of a structure...'* (Franssen et al., 2009). The occurrence of this hazard, particularly in structures, is potentially an even greater threat to human life and property, considering the additional risk of structural instability and collapse. Despite the innovations in engineering, science and technology, the incidence of fires in structures is still widespread in South Africa and internationally (FPASA, 2017).

In the United States of America in 2015, a total of 501,500 structure fires were recorded; one structure-related fire was reported every 63 seconds (NFPA, 2016). It is documented by the NFPA (2016) that, on average, fire caused the death of nine people every day in 2015, of which the majority of the United States civilian deaths and injuries were attributed to structure infernos. Furthermore, 10.3 billion dollars (approximately 150.1 billion rand) in fire damage to buildings and other properties was estimated over

the one-year period (NFPA, 2016). This constituted 72 per cent of the total damage expense due to fires in the United States of America (NFPA, 2016). Figure 2-2 graphically compares the fire occurrences in the United States over a one-year period, per sector.

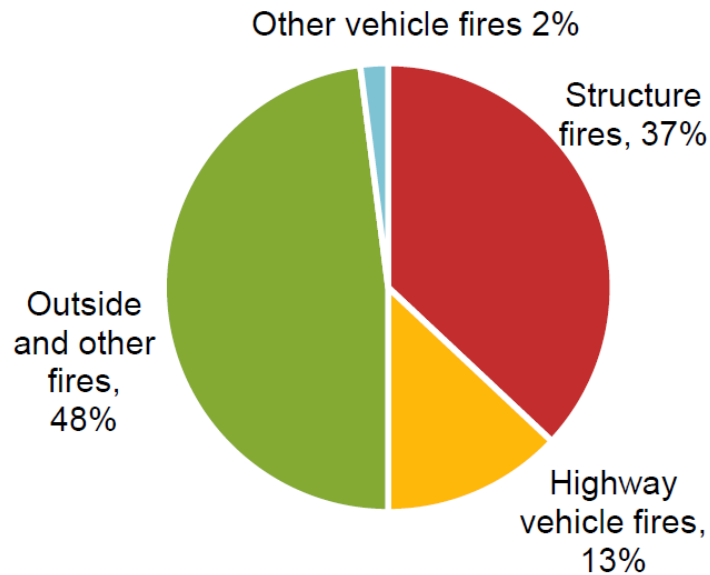


**Figure 2-2: Fire incidents in the United States of America in 2015 per sector (Source: NFPA, 2016)**

From Figure 2-2, it can be seen that in the United States of America, 37 per cent of all fires in 2015 were structure fires. Comparatively, in South Africa, almost 19 per cent of recorded fires in 2015 relate to structures, including industrial buildings (FPASA, 2017). The financial losses incurred in SA in 2015 from structural infernos reached approximately 1.67 billion rand, contributing 77 per cent of the total cost of damage from fires (FPASA, 2017). This relatively large contribution of structural blazes to overall fire incidents and excessive cost implications affirms the need to investigate means to improve the protection of structures. The risk of fire in structures is further compounded by the fact that the event of this hazard is not limited to a specific type of building or assembly; fires can extend to various properties such as residential, commercial, institutional, public assembly, storage facilities or a combination (FPASA, 2017).

#### **2.2.2.1 Composite Structures**

A vast amount of structures in the civil engineering industry constitute a combination of two or more construction materials, such as concrete, steel, timber etc. These materials can also be amalgamated to form a stronger building resource, compared to

the strength that each component would offer individually, such as reinforced concrete. While each of the constituents may react differently under fire conditions, all are susceptible to fire-induced failure and possible collapse (Beitel and Iwankiw, 2004). These structural failures and collapses may be partial or complete, and can occur during construction, while the structure is in use or while under renovation (Beitel and Iwankiw, 2004).

The London Grenfell Tower fire of 2017 is one of the most recent tragedies. The primarily concrete-constructed Tower experienced a fire disaster that led to numerous deaths. Potentially, this could have been avoided if the building had been designed to contain and survive internal fires (Slater, 2017), although much of the controversy of the calamity surrounds the external cladding of the building. The Torch Tower in Dubai also experienced a fire disaster and consisted of similar cladding materials; however, no lives were lost during that particular fire (Henderson and Graham, 2017). Thus, effective structural fire design of buildings can make a crucial difference towards mitigating the effect of fire, to ensure the structural integrity of the building is the last line of defence (Franssen et al., 2009).

#### **2.2.2.2 Predominantly-Steel Structures**

Steel is used extensively as a building material for both composite and homogenous structures in South Africa and across the world. Favourable design characteristics of the material permit its use in a range of structures with varying occupancies. The primary occupants of these structures extend from people, to assets, to machinery, all of which require a stable structure. This is especially critical under extreme conditions, such as exposure to fire.

In South Africa, an extensive fire in a Cape Town warehouse is one of the latest fire incidents (Nombembe, 2017). The blaze compromised the steel structure of the warehouse, consequently resulting in structural failure and the loss of millions of rands (Nombembe, 2017). However, this is an example of local, relatively small-scale fire destruction. On a global scale, the collapse of the World Trade Centre complex in the United States of America is one of, if not the most, notable catastrophes of the twenty-first century. This tragedy in 2001 brought focus to the failure of structural steel under fire (Beitel and Iwankiw, 2004). Table 2-2 relays a summary of the World Trade Centre buildings that suffered partial and complete collapse.

**Table 2-2: Summary of multi-story World Trade Centre building fires with collapses in the United States of America in 2001 (Source: after Beitel and Iwankiw, 2004)**

<b>Building Name</b>	<b>Type of Construction, Material, and Fire Resistance</b>	<b># Of Floors and Occupancy</b>	<b>Date, Approximate Time of Collapse</b>	<b>Nature and Extent of Collapse (Partial or Total)</b>
World Trade Centre 7	Steel moment frame with composite beam and deck floors; fire resistive with sprinklers	47 Office	Sept. 11, 2001	Total
World Trade Centre 2	Structural steel tube lateral system with composite floor truss system; fire resistive with retrofitted sprinklers	110 Office	Sept. 11, 2001 After 1 hour of fire following jet impact and damage	Total
World Trade Centre 1	Structural steel tube lateral system with composite floor truss system; fire resistive with retrofitted sprinklers	110 Office	Sept. 11, 2001 After 1.5 hours of fire following jet impact and damage	Total
World Trade Centre 5	Steel moment frame with composite beam and deck floors; fire resistive with sprinklers	9 Office	Sept. 11, 2001 Unknown time, fire burned uncontrolled for more than 8 hours	Partial collapse of 4 stories and 2 bays

Table 2-2 shows that the blazes persisted for an extended period of time, despite the steel buildings having active fire resistance in the form of sprinklers. Some form of collapse, either partial or total, was suffered, thereby motivating further research into preventative fire protection of structural steel members.

## 2.3 Properties of Steel

### 2.3.1 Structural Steel as a Building Material

The Southern African Institute of Steel Construction (SAISC) (2016) defines structural steel as ‘*steel used for elements whose primary purpose is to support loads or resist forces which act on a structure.*’ As a construction material, steel offers valuable design qualities to engineers, such as being versatile, economical, light-weight and most significantly, offering strength in tension and compression (Zingoni, 2006). However, Zingoni (2006) states that contrary to the advantages of steel, the material also possesses substantial challenges in terms of ‘*slenderness, stability, fire resistance and other structural requirements.*’

### 2.3.2 Thermal Properties of Steel

#### 2.3.2.1 Thermal Expansion

Thermal expansion, also referred to as thermal strain, occurs in steel when it is exposed to elevated temperatures, thereby causing elongation of the steel (EN1993-1-2, 2005). It is possible for this thermal property to significantly influence and contribute to the failure of steel members (Baetu et al., 2017).

According to EN1993-1-2 (2005), the equations that determine the thermal elongation of steel are:

- For steel temperatures from (including) 20°C to (excluding) 750°C:

$$\frac{\Delta l}{l} = 1.2 \times 10^{-5} \theta_a + 0.4 \times 10^{-8} \theta_a^2 - 2.416 \times 10^{-4} \quad (2-1)$$

- For steel temperatures from (including) 750°C to (including) 860°C:

$$\frac{\Delta l}{l} = 1.1 \times 10^{-2} \quad (2-2)$$

- For steel temperatures from (excluding) 860°C to (including) 1200°C:

$$\frac{\Delta l}{l} = 2 \times 10^{-5} \theta_a - 6.2 \times 10^{-3} \quad (2-3)$$

Where:

$\frac{\Delta l}{l}$  = Thermal elongation of steel

$l$  = Length at 20°C

$\Delta l$  = Temperature induced expansion

$\theta_a$  = Steel temperature [°C]

The variation of thermal elongation with respect to temperature, represented by equations (2-1), (2-2) and (2-3), is displayed in Figure 2-3.

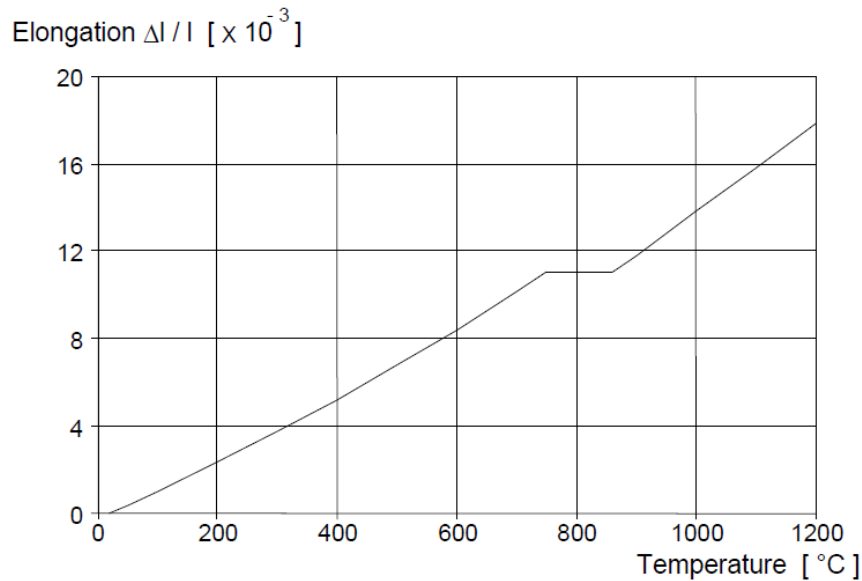


Figure 2-3: Thermal elongation of steel as a function of temperature (Source: EN1993-1-2, 2005)

### 2.3.2.2 Thermal Conductivity

Thermal conductivity, assigned the constant  $k$  or denoted by  $\lambda_a$ , is a material's ability to conduct heat (Encyclopaedia Britannica, 2017). It follows that a substance with a high thermal conductivity is a good conductor of heat; while conversely, a low thermal conductivity indicates a poor heat conductor. Additionally, this thermal material property is temperature dependent (Encyclopaedia Britannica, 2017).

From EN1993-1-2 (2005), the thermal conductivity of steel is calculated thus:

- For steel temperatures from (including) 20°C to (excluding) 800°C:

$$\lambda_a = 54 - 3.33 \times 10^{-2} \theta_a \text{ W/mK} \quad (2-4)$$

- For steel temperatures from (including) 800°C to (including) 1200°C:

$$\lambda_a = 27.3 \text{ W/mK} \quad (2-5)$$

Where:

$\lambda_a$  = Thermal conductivity [W/mK]

$\theta_a$  = Steel temperature [°C]

The variation of thermal conductivity with respect to temperature, denoted by equations (2-4) and (2-5) is displayed in Figure 2-4.

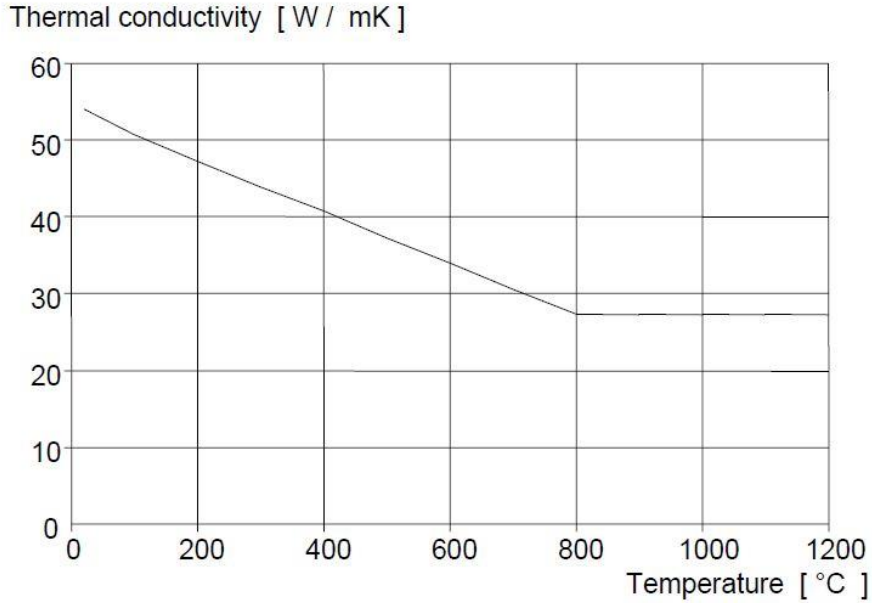


Figure 2-4: Thermal conductivity of steel as a function of temperature (Source: EN1993-1-2, 2005)

### 2.3.2.3 Specific Heat

Encyclopaedia Britannica (2017) defines specific heat as ‘the amount of heat, in calories, required to raise the temperature of one gram of a substance by one Celsius degree.’ This thermal quality of steel is temperature dependent (Encyclopaedia Britannica, 2017).

The specific heat of steel is determined using the equations presented in EN1993-1-2 (2005), thus:

- For steel temperatures from (including) 20°C to (excluding) 600°C:

$$c_a = 425 + 7.73 \times 10^{-1}\theta_a - 1.69 \times 10^{-3}\theta_a^2 + 2.22 \times 10^{-6}\theta_a^3 \quad \text{J/kgK} \quad (2-6)$$

- For steel temperatures from (including) 600°C to (excluding) 735°C:

$$c_a = 666 + \frac{13002}{738 - \theta_a} \quad \text{J/kgK} \quad (2-7)$$

- For steel temperatures from (including) 735°C to (excluding) 900°C:

$$c_a = 545 + \frac{17820}{\theta_a - 731} \quad \text{J/kgK} \quad (2-8)$$

- For steel temperatures from (including) 900°C to (including) 1200°C:

$$c_a = 650 \quad \text{J/kgK} \quad (2-9)$$

Where:

$c_a$  = Specific heat of steel [J/kgK]

$\theta_a$  = Steel temperature [°C]

The variation of specific heat with respect to temperature expressed by equations (2-6), (2-7), (2-8) and (2-9) is illustrated in Figure 2-5.

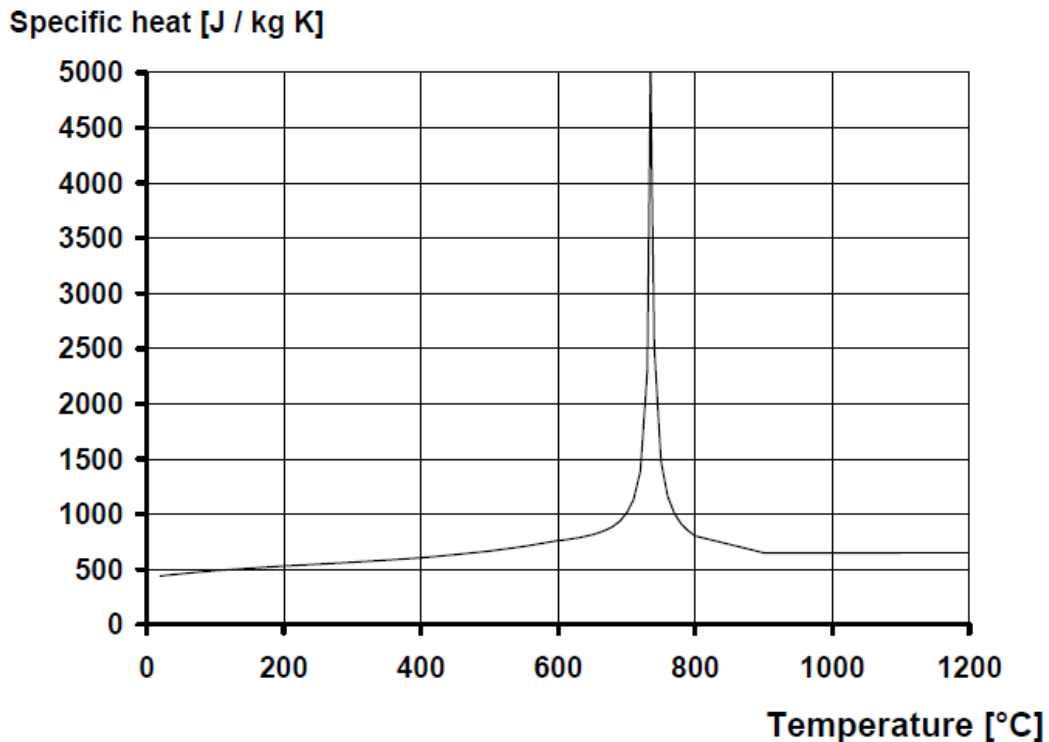


Figure 2-5: Specific heat of steel as a function of temperature (Source: EN1993-1-2, 2005)

From Figure 2-5, a surge in the specific heat of steel is observed at a temperature slightly higher than 700°C. This peak results from a metallurgical change in the crystal structure of the material, thereby amplifying the specific heat value to a maximum of 5000J/kgK at a corresponding temperature (EN1993-1-2, 2005).

### 2.3.3 Thermomechanical Properties of Steel

#### 2.3.3.1 Stress-Strain Relationship of Steel

EN1993-1-2 (2005) provides insight into the behaviour of structural steel under excessive heat. The strength and deformation characteristics of steel at elevated temperatures are presented in the stress-strain relationship depicted by Figure 2-6. This relationship is derived from, and valid for, heating rates between 2K/min and 50K/min (EN1993-1-2, 2005).

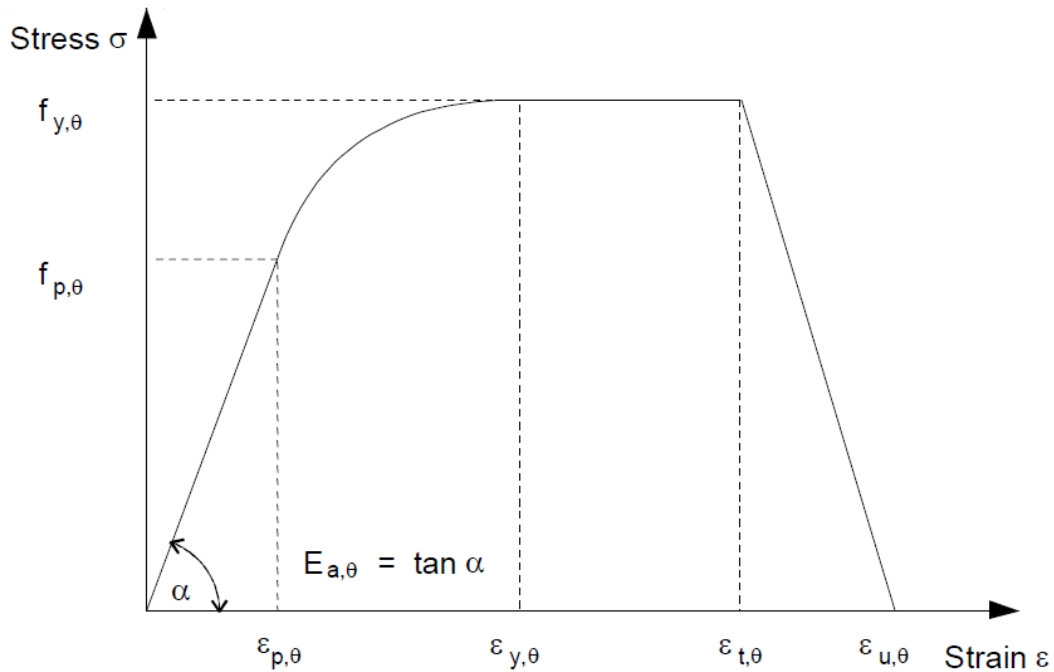


Figure 2-6: Stress-strain relationship for steel at elevated temperatures (Source: EN1993-1-2, 2005)

Where:

- $f_{y,\theta}$  = Effective yield strength
- $f_{p,\theta}$  = Proportional limit
- $E_{a,\theta}$  = Slope of the linear elastic range
- $\varepsilon_{p,\theta}$  = Strain at the proportional limit
- $\varepsilon_{y,\theta}$  = Yield strain
- $\varepsilon_{t,\theta}$  = Limiting strain for yield strength
- $\varepsilon_{u,\theta}$  = Ultimate strain

### 2.3.3.2 Reduction Factors

At elevated temperatures, the strength and stiffness of steel is significantly diminished. (SAISC, 2016). Therefore, reduction factors for steel parts are derived for the stress-strain relationship portrayed in Figure 2-6. These factors are presented in Table 2-3, while the temperature-dependent variation of the factors is graphically displayed in Figure 2-7.

EN1993-1-2 (2005) defines the reduction values relative to steel as indicated:

- $k_{y,\theta} = f_{y,\theta}/f_y$  : Effective yield strength, relative to yield strength at 20°C (2-10)
- $k_{p,\theta} = f_{p,\theta}/f_y$  : Proportional limit, relative to yield strength at 20°C (2-11)
- $f_{E,\theta} = E_{a,\theta}/E_a$  : Slope of linear elastic range, relative to slope at 20°C (2-12)

**Table 2-3: Reduction factors for the stress-strain relationship of steel at elevated temperatures (after EN1993-1-2, 2005)**

Steel Temperature $\theta_a$	Reduction factors (RF) at temperature $\theta_a$ relative to the value of $f_y$ or $E_a$ at 20°C		
	<i>RF for Effective yield strength</i> $k_{y,\theta} = f_{y,\theta}/f_y$	<i>RF for Proportional limit</i> $k_{p,\theta} = f_{p,\theta}/f_y$	<i>RF for Slope of linear elastic range</i> $f_{E,\theta} = E_{a,\theta}/E_a$
20°C	1.000	1.000	1.000
100°C	1.000	1.000	1.000
200°C	1.000	0.807	0.900
300°C	1.000	0.613	0.800
400°C	1.000	0.420	0.700
500°C	0.780	0.360	0.600
600°C	0.470	0.180	0.310
700°C	0.230	0.075	0.130
800°C	0.110	0.050	0.090
900°C	0.060	0.0375	0.0675
1000°C	0.040	0.0250	0.0450
1100°C	0.020	0.0125	0.0225
1200°C	0.000	0.000	0.000

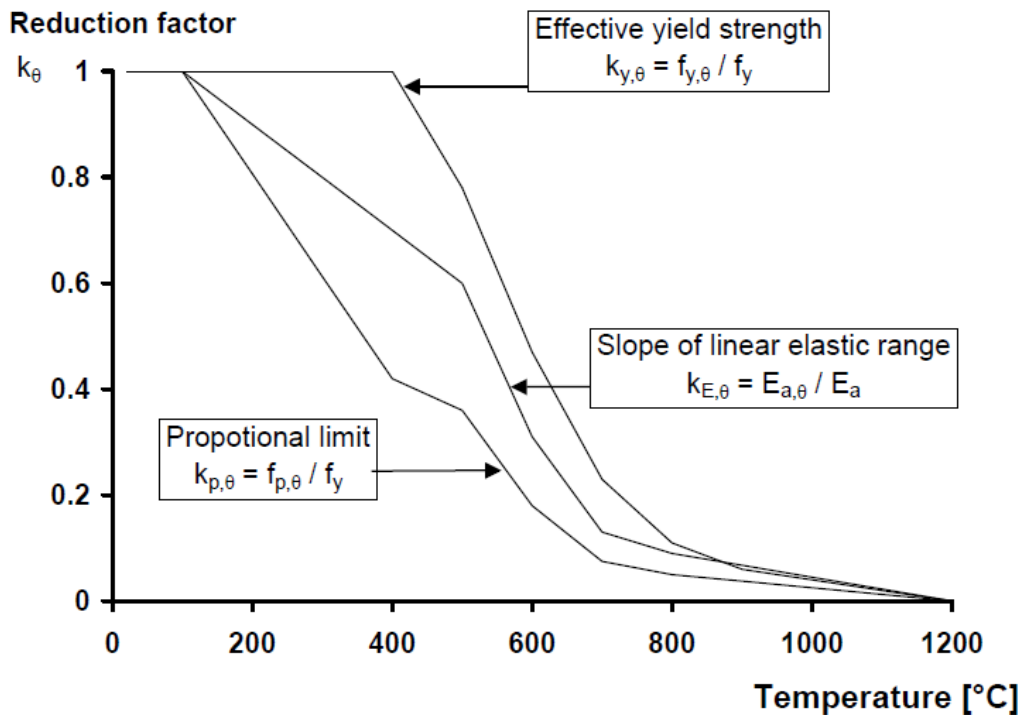


Figure 2-7: Reduction factors for the stress-strain relationship of steel with respect to temperature (EN1993-1-2, 2005)

Among the observations made from Figure 2-7, it can be seen that despite the Young's modulus being influenced by temperatures beyond 100°C, the effective yield strength of steel does not experience any loss at temperatures from 0°C to at least 400°C (Baetu et al., 2017). Thereafter, for a smaller increase in temperature, the initial value of the yielding strength drops by approximately 50 per cent at 600°C, while the elasticity modulus is estimated at 35 per cent of its original value (Baetu et al., 2017).

For a bolted connection, such as the case under investigation in this research, the reduction in strength of bolts under fire conditions is accounted for in EN1993-1-2 (2005). The reduction factors for bolts relative to elevated temperatures are displayed in Table 2-4.

EN1993-1-2 (2005) prescribes the reduction values relative to steel bolts as:

- $k_{b,2} = f_{y,\theta} / f_y$  : Effective yield strength, relative to yield strength at 20°C (2-13)
- The reduction factor for the modulus of elasticity remains as presented in (2-12)

Table 2-4: Reduction factors (RF) for steel bolts at elevated temperatures (after EN1993-1-2, 2005)

Temperature $\theta_a$	RF for Effective yield strength $k_{b,2} = f_{y,\theta}/f_y$	RF for Modulus of elasticity $f_{E,\theta} = E_{a,\theta}/E_a$
20°C	1.000	1.000
100°C	0.968	1.000
200°C	0.935	0.900
300°C	0.903	0.800
400°C	0.775	0.700
500°C	0.550	0.600
600°C	0.220	0.310
700°C	0.100	0.130
800°C	0.067	0.090
900°C	0.033	0.0675
1000°C	0.000	0.0450

### 2.3.3.3 Plasticity

The plastic stress-strain relationship of structural steel is similarly influenced by elevated temperatures. Thus, the values of the plastic stresses and strains are reduced by the factors given in Tables 2-3 and 2-4. The degradation in stress-strain laws of steel under fire conditions is illustrated in Figure 2-8. The plasticity model governed by these values represents the von Mises theory for ductile materials. Logan (2007) states that the von Mises theory predicts failure of the material when the effective stress (von Mises stress) reaches the yield strength of the material. Hence, *'for yielding to occur, the von Mises stress must become equal to or greater than the yield strength of the material...'* (Logan, 2007).

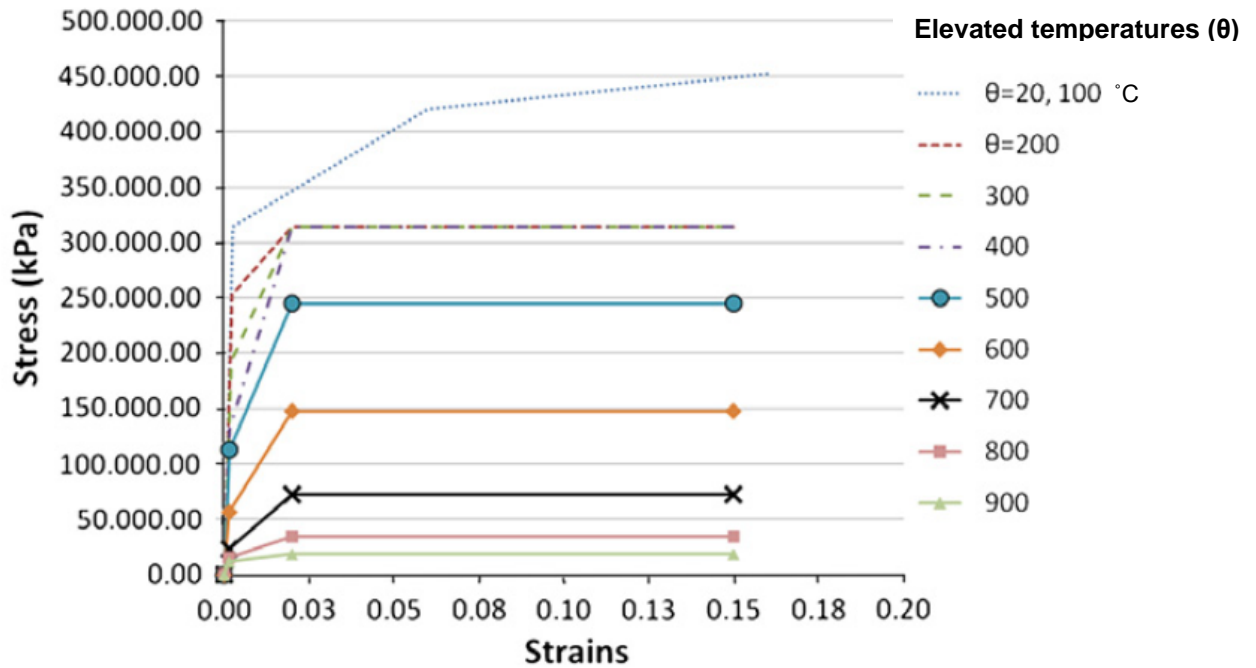


Figure 2-8: Deterioration of the stress-strain relationship of steel due to elevated temperatures ( $\theta$ ) (Source: EN1993-1-2, 2001; cited by Kalogeropoulos et al., 2011)

## 2.4 Fire Design of Structural Steel

Structural fire engineering design aims at analysing the behaviour of structures under fire conditions, towards achieving fire safety in buildings and other assemblies. Designing steel structures for fire requires consideration of the impacts of thermal expansion, reduction in strength of the material and large deflections at elevated temperatures (Franssen et al., 2009). According to EN1990 (2002); cited by Winestone (2010), fire design may proceed by considering the following:

1. Fire behaviour. This determines the thermal actions or loads applied to the structure from a selected approach and corresponding temperature-time curve.
2. Thermal response of the structure. An appropriate thermal analysis should be performed to deduce the temperature-time history of the structure.
3. Mechanical behaviour of the member. This is defined through analysis or testing to determine the fire resistance of a structural member, given its assessed thermal response. Further criteria, stipulated by EN1990 (2002); cited by Winestone (2010), for evaluating acceptable mechanical behaviour of structural elements are:

- *Load bearing resistance* – The structural member should maintain stability under its specified applied loads, for the duration of the time required under fire conditions.
- *Insulation* – The structural element should confine the temperatures experienced during a fire and limit the rise in temperature of the unexposed side to below an average of 140°C and a maximum of 180°C. Any heat conducted through the cold side above these temperatures could ignite a fire in adjacent spaces.
- *Integrity* – The member should prevent and inhibit the development of any cracks, holes or openings that may allow hot gas or fire to progress into adjoining spaces.

#### 2.4.1 Approaches for Structural Fire Design

According to Winestone (2010), two approaches exist for conducting structural fire engineering design, namely: a prescriptive approach and a performance-based approach. The former refers to fire resistance of structural members governed by national regulations or design codes, such as those given by the International Organisation for Standardisation (ISO). The performance-based approach relies on the discernment of the designer in quantifying the risk of fire in a scenario. Although, the use of advanced rules and models in both approaches is governed by physical models and finite element analysis (FEA) (Winestone, 2010). Irrespective of the procedure selected, the design is required to comply with national regulations to some extent. Table 2-5 provides a basic summary of the two methods for fire design according to the Eurocode, as referenced.

**Table 2-5: Approaches and descriptions for fire design to EN and ISO (Source: after Winestone, 2010)**

<b>Approach</b>	<b>Tools</b>	<b>1. Thermal action</b>	<b>2. Thermal response</b>	<b>3. Mechanical behaviour</b>
<b>Prescriptive</b> (Standard fire methods)	Pre-engineered data sheets (tabulated data)	Standard ISO fire tests to EN1363-1; EN1365-2	Relevant information covered in EN1994-1-2, documents and packages provided by fire protection manufacturers	
	Simple rules and models	Standard ISO fire calculations to EN1991-1-2	Steel members to EN1993-1-2	
	Advanced rules and models		Physical models for heat transfer; FEA	Physical models for structural response; FEA
<b>Performance-based</b> (Natural fire methods)	Simple rules and models	Parametric fire	Steel members to EN1993-1-2	
	Advanced rules and models	Natural fire to EN1991-1-2	Physical models for heat transfer; FEA	Physical models for structural response; FEA

Numerous factors influence the selection of an optimal approach for fire design of buildings, which includes the geometry, intended functionality and structural features of the building (Winestone, 2010). The ideal approach, described by Winestone (2010), for fire design of multi-storey structures is predominantly aligned with the most economical solution, which varies with building size and height. For the investigations presented in this research, the thermal, mechanical and thermo-mechanical behaviours of steel are determined from advanced rules and models using FEA.

#### **2.4.2 Codes of Practice**

Various design codes are used around the world for structural fire design; however, the aims to prevent loss of human life and property due to fire are inherently similar (Buchanan and Abu, 2017). Prescriptive-based codes have been the historical basis of structural design for fire resistance, thereby limiting the provision of rational fire design, whereas many countries have recently adopted performance-based building codes

(Buchanan and Abu, 2017). *'A performance-based approach to fire safety often facilitates innovative, cost-effective and rational designs'* (Franssen et al., 2009).

The fire sections of the Eurocode, particularly EN1993-1-2 (2005), present a comprehensive and improved understanding of the fire design of structures, including steel assemblies. The motivation for the use of the Eurocode in fire design extends to the fact that the code contains information that is not readily available in other fire codes (Phan et al., 2010). This information includes topics such as the stress-strain relationships of materials at elevated temperatures, as previously mentioned in the chapter. The fire design methodology of EN1993-1-2 (2005) allows for logical and flexible analysis of single members, substructure assemblies and entire structures subject to fire, with simple or advanced calculation models (Franssen and Real, 2015). However, the application of the Eurocode methodologies is hindered by the lack of detailed explanations for the procedures and specifications (Franssen et al., 2009).

In contrast to the fire design specifications of the EN1993-1-2 (2005), *'South Africa currently lacks a structural fire loading and basis for design code for buildings...'* (Walls and Botha, 2016). Currently, prescriptive design for fire in structures is followed through standard fire tests and equations, due to inadequate knowledge and ability to design for fire (Walls and Botha, 2016). Nevertheless, there is scope for performance-based fire design to be conducted with the adoption of the Eurocode, in accordance with the existing codes of the country. SANS 10400 encompasses the South African National Building Regulations (NBRs), where the standard fire times of buildings is consistent with international codes, including the British Standard 9999 (Walls and Botha, 2016). This establishes the consistency between the NBRs and the rational fire design of the Eurocode, permitting the use of both codes, relevant to the fire design of structures.

### **2.4.3 Fire Resistance**

Technically, Phan et al. (2010) defines fire resistance as: *'A measure of the ability of a structure to resist collapse, fire spread or other failure during exposure to a fire of specified severity.'* Designing members and structures to resist fire is in alignment with the overall objective of achieving fire safety in a building, such that the structural stability thereof is maintained for a certain required period (Franssen and Real, 2015). Thus, fire resistance is significant in protecting occupants of a building, allowing access for fire rescue services and protection of the property itself in preventing collapse

(Buchanan and Abu, 2017). The requirement of designing fire resistance is vital and inclusive of structural steel members and assemblies.

The most common method, described by Franssen and Real (2015), for the fire design of steel structures follows two basic steps; namely: designing the structure for fire loading from the ambient temperature and subsequently using appropriate fire protection materials to conceal the steel elements (beams, columns etc.). This inhibits the development of excessively high temperatures within the members. The disadvantage of this approach is the risk of under-designing or over-designing for fire since the ‘*survival time*’ of the steel structure in the standard fire test could be inaccurate in real fire conditions, depending on the severity of the fire (Franssen and Real, 2015). The fire resistance that a structure or element offers under elevated temperatures should exceed the severity of the fire it experiences (Phan et al., 2010). Table 2-6 provides three alternative methods for comparing fire severity with fire resistance offered by the steel structure.

**Table 2-6: Three alternative methods of comparing fire severity with fire resistance (Source: Phan et al., 2010)**

Domain	Units	Fire Resistance	≥	Fire Severity
<b>Time</b>	Minutes or hours	Time to failure (Fire Resistance Rating, FRR)	≥	Fire duration as calculated or specified by code
<b>Temperature</b>	°C	Steel temperature to cause failure	≥	Maximum steel temperature reached during the fire
<b>Strength</b>	kN or kN.m	Load capacity (strength/stability) at elevated temperature	≥	Applied load during the fire

#### **2.4.3.1 Fire Resistance Rating (FRR)**

The FRR is the time to failure of a structure or structural element, under standard fire conditions, where the majority of the ratings are deduced from previous fire testing (Phan et al., 2010). Various countries, all with different design codes for fire resistance, offer FRRs categorised by type of structural element, occupancy classification of a

building, type and thickness of fire protection materials among other criteria. An example of fire resistance requirements in the United Kingdom is shown in Table 2-7.

**Table 2-7: Typical fire resistance requirements (after Winestone, 2010)**

	Fire resistance (minutes) for height of top storey (metres)			
	< 5	≤ 18	≤ 30	> 30
Residential (non-domestic)	30	60	90	120
Office	30	60	90	120*
Shops, commercial, assembly & recreation	30	60	90	120*
Closed car parks	30	60	90	120
Open-sided car parks	15	15	15	60
*Sprinklers are required, but the fire resistance of the floor may be 90 minutes only				

As an illustration of the differences between FRRs prescribed by design codes, the SANS 10400-T: Fire protection (2011), provides the following for offices:

- Single-storey building : 30 minutes stability
- Double-storey building : 30 minutes stability
- 3 to 10 storey building : 60 minutes stability
- 11 storeys and more : 120 minutes stability
- Basement in any building : 120 minutes stability

The variation in FRRs of offices from practice in the United Kingdom, observed in Table 2-7, and from SANS 10400-T is noticeable. The criteria for the stability FRR differs in terms of the classification of the storeys of the building, as well as the fire resistance offered in minutes. It can be argued that while these FRRs are accurate in their own right and validated from extensive testing, discrete research of scenarios for steel structures and substructures under fire is required for greater accuracy. The conclusions from individual research, such as the current study, determine scenario-based results that can assist structural design for fire.

## 2.4.4 Fire Testing and Fire Curves

### 2.4.4.1 Standard Fire

The standard fire tests determine the fire action and thermal reaction of structural members in response to a specified rate of heating, which is determined by corresponding fire design codes of various countries (Winestone, 2010). The standard fire, represented by a time-temperature curve, is used in full-scale resistance tests to account for the impacts of thermal expansion, shrinkage, local damage and deflections under loading in fire conditions (Phan et al., 2010). Physical experimental tests and numerical software can integrate the standard fire curve in the analysis of the behaviour of structural elements under elevated temperatures, such as that incorporated in the transient analyses performed in this study.

ISO fire curves and tests, mentioned previously in Table 2-5, prevail as an international standard for time-temperature curves. In South Africa, the ISO 834 standard fire curve is implemented in design and testing pertaining to fire (Walls and Botha, 2016). The ISO 834 standard time-temperature curve is derived from the following relationship:

$$\bullet \quad T = 345 \log_{10}(8t + 1) + T_0 \quad (2-14)$$

Where:

$T$	=	Temperature [°C]
$t$	=	Time [min]
$T_0$	=	Ambient temperature [°C]

Figure 2-9 depicts a comparison of standard time-temperature curves from various international standards, including ISO 834, ASTM E119 (an American standard curve) and the nominal curves to EN1991-1-2 (2002).

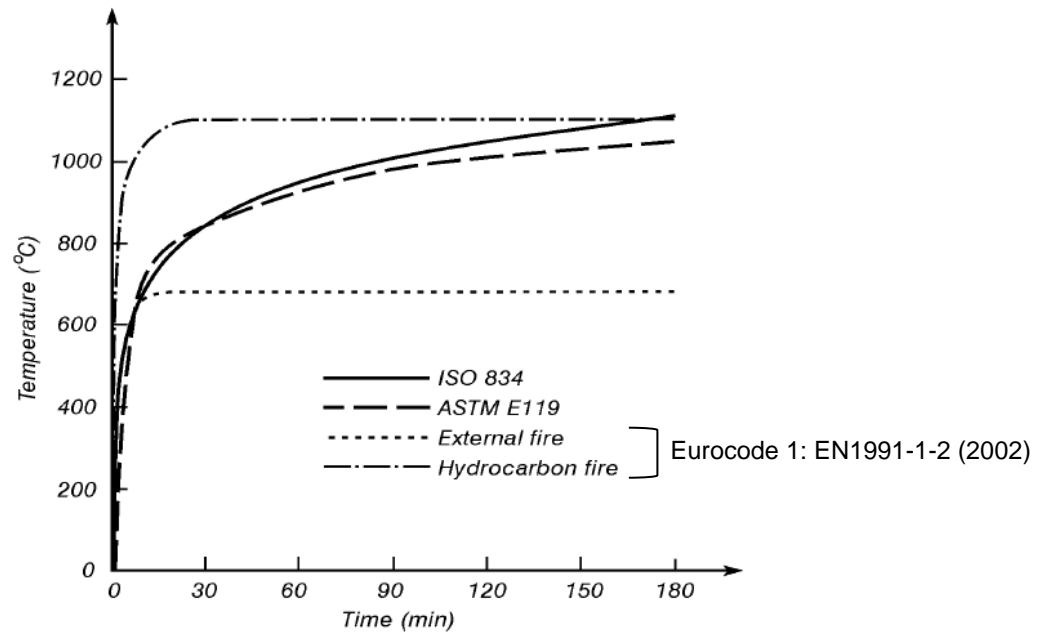


**Figure 2-9: Standard time-temperature curves (Source: Phan et al., 2010)**

It can be perceived from Figure 2-9 that the ISO 834 and ASTM E119 fire curves are relatively similar and are therefore used extensively in many countries. The external fire and hydrocarbon fire curves are intended for use in designing external structural members under fire and structural members engulfed by flames respectively (Phan et al., 2010). According to Phan et al. (2010), similar time-temperature curves to those portrayed in Figure 2-9 are derived by ‘*all other international fire resistance test standards.*’

While the ISO 834 curve is commonly implemented in South Africa, Walls and Botha (2016) predict that dependency on purely the ISO 834 curve will become unsatisfactory. Furthermore, while ISO 834 presents a single curve, EN1991-1-2 (2002) offers multiple nominal curves such as the standard temperature-time curve, external fire curve and hydrocarbon fire curve, where the latter two curves are displayed in Figure 2-9. Thus, the current study utilises the EN1991-1-2 (2002) standard temperature-time curve for classification and verification of fire resistance of the steel connection in the transient analyses. According to Eurocode standards, EN1991-1-2 (2002) describes the standard temperature-time curve as ‘*a nominal curve defined in prEN13501-2 for representing a model of a fully developed fire in a compartment.*’

The EN1991-1-2 (2002) standard time-temperature curve is derived from the following relationship, similar to that of the ISO 834 curve:

- $\theta_g = 20 + 345 \log_{10} (8 t + 1)$  (2-15)

Where:

- $\theta_g$  = Gas temperature in the fire compartment [°C]
- $t$  = Time [min]
- $T_0$  = Ambient temperature [°C]

#### 2.4.4.2 Parametric Fire

While a standard fire is used in standard fire tests to determine the capability of structural materials and elements under fire, a parametric fire incorporates various phases of fire development (Winestone, 2010). Thus, a parametric fire curve tends to depict the thermal action of a real-life, natural fire in a structure. The heating, cooling and residual phases of the parametric fire are determined by and dependent on factors such as fire load, thermal characteristics of boundary conditions and aeration conditions (Winestone, 2010). The three phases of a parametric fire can be observed graphically in Figure 2-10, in comparison to a standard fire curve.

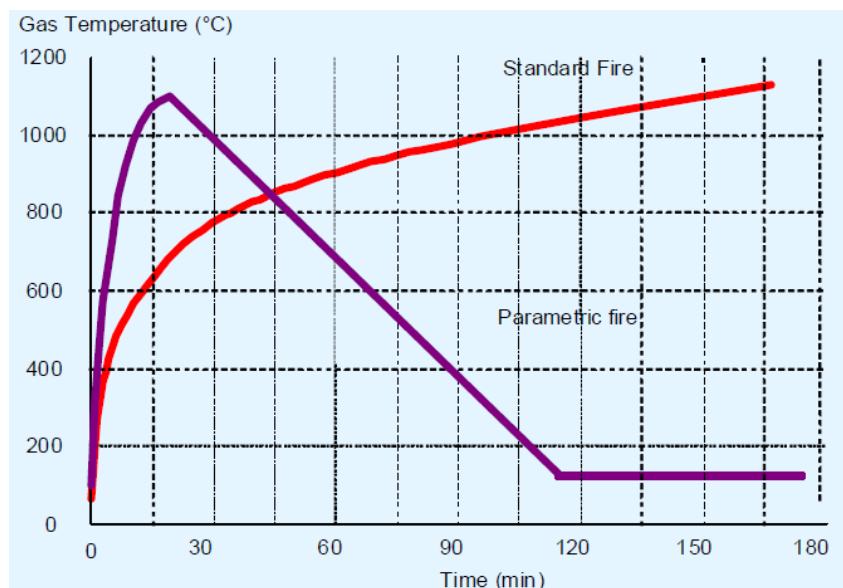


Figure 2-10: Comparison of standard fire curve and parametric fire curve (Winestone, 2010)

While a parametric fire curve may offer a more accurate scenario of an actual fire situation in a known building, the derivation of an accurate curve requires consideration of specific parameters, such as dimensions of openings and size of the enclosure in which the fire is occurring (Phan et al., 2010). The standard fire curve is acceptable in numerical analyses, such as the transient analyses performed in this study, to investigate the behaviour of a relevant substructure where the aforementioned building parameters are unknown. Accordingly, the substructure analysis may be considered in a range of buildings of various sizes and openings.

#### **2.4.4.3 Cardington Fire Tests**

Prescriptive approaches and simple calculation models evaluate the fire resistance of an unprotected multi-storey steel building at a maximum period of 30 minutes (Winestone, 2010). However, fire tests carried out on an eight-storey steel-composite framed building in Cardington (in the United Kingdom) determined that the performance of unprotected steel members in framed buildings surpass the expectations documented from standard fire tests (Winestone, 2010). The Cardington building comprised of unprotected steel beams and composite slabs. The tests indicated parallel conclusions to those of real fire investigations: the thermal response of entire steel-framed buildings differs significantly from that of individual steel elements (Phan et al., 2010). This means that the analysis of substructures and entire structures under fire is essential in obtaining accurate and realistic outcomes.

Results from a representative, secondary beam were selected from the eight-storey, 6m x 9m x 6m grid-shaped structure in the Cardington fire tests. The outcomes demonstrated that the structure maintained its stability up to a peak temperature of 954°C, contrary to anticipated collapse from standard fire tests (Winestone, 2010). At the peak temperature of 954°C, the vertical displacement experienced in the beam was 428mm (Winestone, 2010). The final vertical displacement of the beam after cooling was measured at 296mm, indicating a recovery in the displacement of the beam by 132mm (Winestone, 2010). From this, it can be inferred that steel-framed buildings may offer greater fire resistance than expected and extensive fire protection may be unnecessary. However, the large reserves of fire resistance observed in the Cardington fire tests may not be true for pure steel structures, as the steel-composite flooring aided the performance of the overall building (Winestone, 2010). Therefore, numerical analysis and testing of steel substructures is crucial in determining the exact impact and response of steel elements under fire.

### 2.4.5 Finite Element Analysis

Computer analysis of fire-exposed structures is categorised as an advanced calculation method, according to the Eurocode (Phan et al., 2010). Such software modelling is advantageous over simple method analyses since substructures and entire structures are able to be accurately analysed, in terms of thermal and thermomechanical behaviour (Phan et al., 2010). Such computer modelling is based on finite element analysis (FEA) to determine the mechanical and thermal actions and responses of structures.

The finite element method involves separating a body into an equivalent system of interconnected smaller entities, known as finite elements (Logan, 2007). This process is called “discretisation” and allows the formulation of a ‘*system of simultaneous algebraic equations for solution*’ pertaining to each finite element (Logan, 2007). Thus, instead of solving the problem of a whole body in a single operation, the system of equations for each finite element can be combined to attain a solution for the entire body (Logan, 2007). Solutions using FEA are obtained by determining unknowns at points common to two or more finite elements, known as “nodes”. The unknowns can range from displacements and stresses for structural problems, to temperatures and thermal fluxes for thermal analyses. The compact matrix form of the equations underpinning the finite elements and global structure in FEA are presented in Equations (2-15) and (2-16) respectively, from Logan (2007):

- Element equations in the compact matrix form:

$$\{f\} = [k]\{d\} \quad (2-15)$$

Where:

$\{f\}$  = Vector of element nodal forces

$[k]$  = Element stiffness matrix

$\{d\}$  = Displacement vector for unknown element nodal degrees of freedom

- Global equation generated from the element equations:

$$\{F\} = [K]\{d\} \quad (2-16)$$

Where:

$\{F\}$  = Vector of global nodal forces

$[K]$  = Global stiffness matrix

$\{d\}$  = Displacement vector of known and unknown structure nodal degrees of freedom

Once boundary conditions are incorporated, the displacement vectors can be solved for using the Equations (2-15) and (2-16) for structural analyses. Thereafter, stresses and strains can be deduced from the relationships between strain and displacement.

According to a study carried out by Daryan and Yahyai (2009), FEA is an accurate and preferred method for simulating structural behaviour under fire conditions, due to the high cost in conducting practical experiments and the limitations experienced with numerous parameters, complicated geometries, etc. Additionally, the numerical modelling of bolted angle connections in fire conducted by Daryan and Yahyai (2009), proved to be consistent with experimental data. This indicates that FEA of structures under elevated temperatures is both warranted and precise to an acceptable degree.

The computer modelling, also used to interpret the results from the Cardington fire tests, allows for three-dimensional modelling of non-linear analyses that takes into account the non-linear behaviour of steel at elevated temperatures (Phan et al., 2010). The non-linear analysis permits actual material behaviour to be determined by incorporating material plasticity, large deformations and temperature dependence (Rogers and Medonos, n.d.). These analyses can be carried out using finite element programmes. The programmes available are considered either special-purpose programmes such as SAFIR and VULCAN, or general-purpose finite element programmes, namely Abaqus, Ansys or LS-DYNA (Phan et al., 2010). For the purposes of this research, general-purpose programmes are accurate and sufficient. A comparison of 78 mechanical FEA programmes indicates that Abaqus and ANSYS Mechanical contain all the necessary features to conduct this study, including (FEACcompare, 2017):

- Non-linear – large displacements
- Transient non-linear
- Heat transfer
- Plasticity
- Contact mechanics

In Abaqus, the Newton-Raphson procedure that is followed allows for solving non-linear problems incrementally through an iterative process (Abdalla et al., 2015). Abaqus is a suitable computer programme for analyses in this study, since it is extensively used in FEA of structures under fire conditions and due to the availability of the license for the programme.

#### 2.4.6 Behaviour of Steel Substructures under Fire

Single element analysis is considered the most basic form of structural analysis (Rogers and Medonos, n.d.). The importance of considering loading, mechanical or thermal, on whole or significant parts of structures is discussed earlier in the chapter. Furthermore, the behaviour of restrained members is dissimilar to that of unrestrained members under elevated temperatures, where restraint and the degree of restraint affects distribution of internal forces (Baetu et al., 2017). Furthermore, the study determined three types of failure of a restrained beam under fire conditions: yielding failure due to a low slenderness ratio, buckling failure due to a high slenderness ratio and a combination of the two failures depended on the slenderness of the member.

Key findings in a study undertaken by Gentili (2013) stated various factors that could affect the behaviour of a single storey steel structure, which are aligned with the present study. This includes determining that an analysis of a three-dimensional model is typically the only method of achieving a reliable assessment of collapse mechanisms in the structure. Additionally the study stated that the response of the structure varies with the location of the fire load applied, hence this dissertation considers multiple load cases.

Many investigations into the behaviour of steel structures and sub-assemblies under fire focus on the joints of beam-to-column connections, specifically bolted angle joints. One such investigation conducted by Daryan and Yahyai (2008) using experimental and numerical analyses, examined a connection with top and seat angles, with and without web angles and attached with M16 bolts. The study deduced that bolts play an important role in the failure mechanism of steel structures under fire. Additionally, the study concluded that using bolts of a higher steel grade increased the temperature resistance of the connection and verified that the stiffness and temperature capacity of common steel connections decline at 900°C. However, the effects of fire protection on the overall behaviour under fire were not taken into consideration. Furthermore, the study done by Daryan and Yahyai (2008) affirmed that the structural connections were not the deciding components of failure: *‘the connections fail at the same temperature at which the frame beams are assumed to fail.’*

A similar deduction was made in research conducted by Kalogeropoulos et al. (2011), in that the failure of steel members occurred prior to the failure of bolts under elevated temperatures. Additionally, in this particular research of an extended end-plate steel connection under fire, a critical observation was made with respect to the sequence of

thermal and mechanical loading. It was documented that the connection displayed improved behaviour if mechanical loading was applied during the application of the thermal load, or if a diminished mechanical load was assigned prior to thermal loading.

A separate study by Abdalla et al (2015) was executed on a steel connection consisting of a HEA 400 x 350 column and an IPE 360 x 170 beam, which is presented in Figure 2-11. The column and beam joint consisted of a top angle, a seat angle and two web angles, bolted with 17 M20 high-strength bolts. The non-linear, three-dimensional model was subject to an applied static point load on the beam and incorporated unilateral contact-friction interfaces between the angles and steel parts. Abaqus software was employed in conducting large displacement analyses, considering von Mises plasticity. Experimental tests confirmed the numerical results which, in comparison, displayed that Eurocode 3 results are more conservative. Thus, conducting numerical analyses, as performed in this study, is both valid and accurate. Furthermore, the steel connection incorporated in this dissertation, presented in Chapter 3, was adopted from this research as a means to verify the analyses and results against current literature.

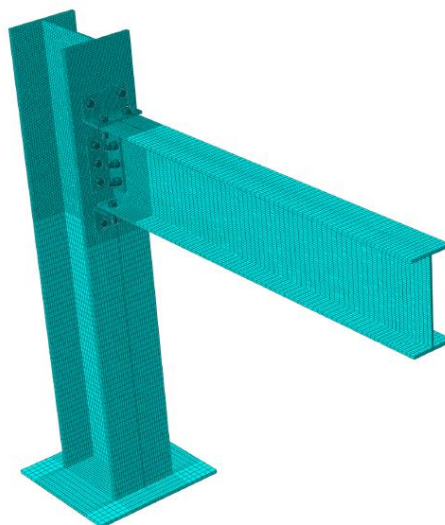


**Figure 2-11: Steel connection in the finite element model (Source: Abdalla et al., 2015)**

The aforementioned research indicates the limited investigations into the effect of fire protection materials on the overall steel assembly. One such investigation was conducted by Tsapara et al (2013), considering the effect of gypsum and concrete protection on the mechanical behaviour of steel joints in an end-plate steel connection. Sequential thermal and thermomechanical analyses were performed on the connection, with protection covering the column and bolted parts of the assembly.

While the effect of the protection materials on the behaviour of the joint was determined, the effect on the beam and column steel elements were not considered. Furthermore, the application of the fire protection was only investigated for one scenario; coverage of the column and bolts and variation of thicknesses of fire protection were not accounted for. Thus, the current study proposes to review and contribute to this research deficit by ascertaining the behaviour of the steel elements as a whole, as well as examining variables of the applied fire protection.

Further motivation for the present study is offered by means of experimental verification of the steel connection modelled in this dissertation that was used in research conducted by Badarneh (2004) and Abdalla et al (2015), displayed in Figure 2-11. Badarneh (2004) performed an experimental investigation on a top and seated angle bolted connection with double web angles, under a static vertical applied load. The results of the experimental investigation were compared and authenticated by a subsequent FEA of the steel connection, which focused on determining the moment-carrying capacity of the steel joint and the prying forces present therein. Thus, the behaviour of the steel connection under conditions of fire and the effects of fire protection were not accounted for, providing opportunity for research to be conducted on this topic.

Considering the research presented in this chapter, there is scope for continued and improved studies of steel substructures under fire. The investigations of Gentili (2013) on a single storey structure motivate the consideration of various fire scenarios, which is presented in this dissertation. In addition, research is required into the analysis of steel substructures that consider factors such as the effects of thermal expansion, large deformations and thermo-plastic behaviour of the connection (Gentili, 2013); such analyses are performed in this study. The various studies of Badarneh (2004), Daryan and Yahyai (2008; 2009), Kalogeropoulos et al (2011) and Abdalla et al (2015) specifically focus on the analysis and behaviour of joints in a steel connection. This indicates the need for research into the analysis of the behaviour of an overall steel substructure under fire conditions, which forms part of the purpose of the current study. Additionally, current research provides limited or no insight into fire protection materials widely used in industry and their effect on the behaviour of the steel structure. This dissertation aims to address this deficiency by modelling a steel connection, presented in the studies done by Badarneh (2004) and Abdalla et al (2015), and conducting relevant analyses of the connection under fire, with various applied protection materials.

## 2.5 Fire Protection

### 2.5.1 Active and Passive Systems

As previously discussed, steel members and assemblies possess an inherent, but limited, fire resistance. This fire resistance may be insufficient in achieving overall fire safety in a building, thereby relying on other methods of resistance. These other methods can be either active or passive fire protection methods (Buchanan and Abu, 2017). Active fire protection systems, according to Buchanan and Abu (2017), refer to the action taken by an individual or automatic device in controlling a fire or effects of a fire once erupted, thereby focusing on management of the fire. Alternatively, the main aim of passive systems is based on prevention, where passive fire protection is built into the structure from the outset and is designed to prevent the spread of fire and premature structural collapse (Buchanan and Abu, 2017).

### 2.5.2 Types of Fire Protection

A comprehensive and conservative effort to design for fire safety in structures would incorporate the use of both passive and active fire protection systems; however, this could become a costly (but necessary) exercise. This prompts the need to identify efficient mechanisms of fire protection, which is undertaken in this study. Active fire protection measures stated by Winestone (2010) include installation of fire detectors or alarms and fire sprinklers, such as the ones equipped in the World Trade Centre buildings. Passive fire protection is associated primarily with the provision of fire protection materials, which can be classified as reactive or non-reactive, depending on the protecting mechanism of the material (Steelconstruction, 2017). These materials can include boards, sprays, encasements and intumescent coatings that insulate steel structures from the effects of fire, thereby maintaining structural stability for a required period of time (Winestone, 2010). This is achieved through the designed thickness of fire protection materials and their intrinsic properties such as low thermal conductivity, heat-absorbing reactions and intumescence (Phan et al., 2010).

### 2.5.3 Comparison of Fire Protection Materials

Numerous protection materials have varied performances and mechanisms of protection. The selection thereof depends on the design constraints and building requirements of a structure. The most common non-reactive fire protection materials are boards and sprays, *which maintain their properties when they are exposed to a*

*fire*' (Winestone, 2010). Conversely, the constituents of reactive protection materials undergo alteration under fire conditions, such as intumescent coatings.

As reported by Steelconstruction (2017), the use of on-site applications of intumescent coatings was the preferred method of fire protection for steel frames in the United Kingdom in 2016, with a market share of approximately 62 per cent. Off-site intumescent coatings shared the second-largest market share percentage at an estimated 18 per cent, followed by the use of fire-protecting boards at around 17 per cent (Steelconstruction, 2017). Sprays and other forms of protection of steel frames constituted the rest of the market.

Investigation into current data on the use of fire protection materials in South Africa yields that steel and fire protection companies utilise a variety of materials and methods in providing passive fire protection to a structure. Pyro-cote (2015) selects the type of fire protection material (to be used on structural steel elements) based on various factors, which include a calculation of the rate at which steel heats, whether the structure being protected is directly exposed to weather elements, the type of building requiring protection (commercial, industrial, etc.), the time period required for fire resistance and the level of aesthetic appeal required. According to Pyro-cote (2015), fire protection options range from a light or medium density spray (depending on the aforementioned factors), to intumescent coatings.

While intumescent coatings remain a popular choice of fire protection in South Africa and abroad, Lafarge (2017) argues that gypsum fire protection systems are *'more economical and practical to install on-site than alternative constructions.'* Furthermore, Lafarge gypsum plasterboards adhere to regulatory fire resistance standards and the thickness of the plasterboards can be altered to suit the level of fire protection required. (Lafarge, 2017). Further motivation for the use of and research into gypsum fire protection, as performed in this study, is provided by Gyproc South Africa (2017), in describing the versatility of gypsum plasterboard as material: the composition of gypsum board protection can be varied to satisfy numerous applications, such as providing efficient fire, moisture, impact and acoustic resistance (Gyproc, 2017).

Besides gypsum board fire protection, adapted concrete-based or cementitious fireproofing materials are also used in South Africa. A vermiculite cement premix substance is used as a spray-applied fire protection material for structural columns and beams, where the vermiculite material expands when contact with fire is made, forming

a type of encasement around the member (Mandoval, 2017). Additionally, Mandoval (2017) offers fire protection in another form of encasement of a structure, with a cast-in-place fire protection material. Furthermore, the use of concrete as passive fire protection is growing in industry, with adaptations to its material composition to enhance its fire resistance capability (Engineering News, 2017). These adaptations include the addition of specialised fibres to the concrete mix, where there exists 'substantial scope in South Africa' for the use of these fibres in concrete as passive fire protection (Engineering News, 2017). Thus, studying the effects of protection in the form of encasement, specifically concrete protection, is both relevant and significant in terms of its growing use in industry.

A summarised description and comparison of four main types of fire protection is presented in Table 2-8. In this study, the fire protection materials considered are gypsum boards and concrete protection, due to the aforementioned motivation of these materials and the ability to model the protection accurately in Abaqus numerical analyses.

Table 2-8: Summarised description and comparison of four main types of fire protection materials (Source: As shown)

FIRE PROTECTION MATERIALS	REACTIVE	NON-REACTIVE		
	<i>Intumescent Coatings</i>	<i>Encasement</i>	<i>Boards</i>	<i>Spray-Applied Fire-Resistive Materials (SFRM)</i>
<b>Description</b>	Thin or thick film coatings are paint-like materials that react chemically with fire, to provide insulation by expanding (Steelconstruction, 2017)	Concrete encasement allows for fire protection through its thickness and low conductivity (Phan et al., 2010)	Gypsum boards are widely used since the water content allows for delay in transfer of heat to steel (Phan et al., 2010)	SFRM are primarily cement or gypsum based, such as mineral fibre protection, applied in-situ to insulate steel (Phan et al., 2010)
<b>Advantages</b>	<ul style="list-style-type: none"> <li>- Fire resistance of 30-120 mins for 0.25 - 2.5 mm thickness</li> <li>- Simple installation and aesthetically appealing finish</li> <li>- Suitable for complex shapes</li> <li>- Off-site application allows quicker construction (Steelconstruction, 2017; Winestone, 2010)</li> </ul>	<ul style="list-style-type: none"> <li>- Main advantage is its durability where resistance is required for exposure to impact damage, abrasion and weather conditions</li> <li>- Useful in external structures and internal buildings (warehouses etc.) (Steelconstruction, 2017)</li> </ul>	<ul style="list-style-type: none"> <li>- Can achieve 30-120 minute fire resistance for 15-50 mm thickness</li> <li>- Guaranteed quality and thickness</li> <li>- Decorative finishes improve aesthetic appeal</li> <li>- Easily attachable (Winestone, 2010)</li> </ul>	<ul style="list-style-type: none"> <li>- Can achieve 30-120 minutes fire resistance for 10-35 mm thickness</li> <li>- In-situ application</li> <li>- Easy and quick application</li> <li>- Low material cost</li> <li>- Suitable for complex shapes (Steelconstruction, 2017; Winestone, 2010)</li> </ul>
<b>Disadvantages</b>	<ul style="list-style-type: none"> <li>- Relatively costly option</li> <li>- Lengthy installation to accommodate drying time of multiple coats</li> <li>- Off-site application leads to potential damage during transit</li> <li>- Requires regular maintenance (Steelconstruction, 2017; Phan et al., 2010)</li> </ul>	<ul style="list-style-type: none"> <li>- High cost of use compared to lightweight materials</li> <li>- Extensive space required to accommodate large protection thicknesses</li> <li>- Heavy material weight adds to structure weight</li> <li>- Laborious installation (Steelconstruction, 2017)</li> </ul>	<ul style="list-style-type: none"> <li>- More costly if decorative</li> <li>- Longer installation time induces more construction costs and affects programme</li> <li>- Difficult installation for complex shapes</li> <li>- Cracks may occur under fire due to shrinkage (Winestone, 2010)</li> </ul>	<ul style="list-style-type: none"> <li>- High labour and equipment costs</li> <li>- Wet trade thus potentially messy installation</li> <li>- Shielding of other elements required in case of over-spraying</li> <li>- Visually unappealing (Steelconstruction, 2017)</li> </ul>

In terms of general fire testing of a building, Pyro-cote (2015) determined that structural steel members in a commercial building fails at a temperature of approximately 550 Celsius degrees, 'which is reached within 5 minutes of a standard time temperature building fire.' However, fire protection materials are tested to offer fire resistance for time periods of up to 240 minutes, in maintaining the stability of the structure (SANS 10400-T: Fire protection, 2011). From the results of fire testing performed to South African National Standards (SANS), the following comparison between gypsum and concrete fire protection is presented in Table 2-9, extracted from SANS 10400-T: Fire protection (2011).

**Table 2-9: Comparative fire resistances of materials for structural steel columns and beams**  
(Source: After SANS 10400-T: Fire protection, 2011)

Fire Protection Material		Fire Resistance (minutes)					
		240	180	120	90	60	30
		Minimum Thickness of Protection (mm)					
Structural steel columns	Non-structural Reinforced Concrete (minimum 25 MPa)	50	38	25	25	25	25
	Structural Reinforced Concrete (minimum 25 MPa)	75	50	50	50	50	50
	Metal lath with Gypsum plaster	-	-	45	30	20	12.5
	19mm Gypsum plasterboard (with 1.6mm wire binding) with vermiculite gypsum plaster of thickness:	32*	19	10	10	7	7
Structural steel beams	Non-structural Reinforced Concrete (minimum 25 MPa)	63	50	25	25	25	25
	Structural Reinforced Concrete (minimum 25 MPa)	75	50	50	50	50	25
	Metal lath with Gypsum plaster	-	-	22	19	16	12.5
*Light mesh reinforcement is required 12.5mm to 19mm below the surface.							

Table 2-9 indicates that an increase in thickness of protection material, results in a greater fire resistance offered by that material, for the same fire condition. This can be seen with 50 millimetre non-structural reinforced concrete, which offers 240 minutes of fire resistance to steel columns, compared to 25 millimetres of the same protection that offers half the fire resistance. Thus, investigating the effect of varying thicknesses of fire protection materials, as performed in this study, is relevant and imperative.

Furthermore, 19 millimetres gypsum plasterboard with vermiculite gypsum plaster of thickness 32 millimetres (a total of 51 millimetres of protection) requires the addition of light mesh reinforcement, in order to provide the same fire resistance as that of non-structural concrete, of the same thickness (50 millimetres). For structural steel beams, non-structural concrete and metal lath with gypsum plaster of approximately the same thickness (25 and 22 millimetres respectively) provide the same resistance to fire. However, non-structural concrete of 25 millimetres affords double the resistance to that of gypsum plaster for relatively the same thickness (20 millimetres), in steel columns. This indicates the necessity for further fire testing experiments to be conducted on various fire protection materials and the need for research into these materials, which is offered by this dissertation.

## 2.6 Transient Delamination

### 2.6.1 Definition

A rudimentary definition of delamination, provided by the Oxford English Dictionary (2017), means to '*divide into layers.*' In terms of structural analysis, it is understood that delamination refers to the potential of connected surfaces to separate. These surfaces or elements can be two or more different materials that detach, either partially or completely, from one another. This occurs under specific circumstances and as a gradual effect over time.

### 2.6.2 Causes of Delamination

The phenomenon of delamination between protection materials and the structure they are applied to is not widely researched, even less so under the effects of elevated temperatures. A few studies conducted focus on delamination as a mode of failure of composite structures. One such study performed by Garg (2003) specified mechanical causes of delamination as stresses at the material interfaces, originating from high impacts, structural load eccentricities or structure discontinuities. Garg (2003) also

documented the potential of elevated temperatures to result in delamination from stresses, but did not investigate the thermal aspects of delamination any further.

Gu and Kodur (2011) accounted for the detachment of insulating Spray-applied Fire Resistive Materials (SFRM) in a six-storey, two-bay, steel framed building. The reasons for the separation of insulation included various factors such as corrosion of steel, poor application of the material to the steel surface and high stress levels from loading events such as explosions (Gu and Kodur, 2011). An alternative cause of the delamination phenomenon was attributed to cracks that developed from loading, which propagated through the interface between the protection material and steel, causing a division between material surfaces (Arablouei and Kodur, 2015). In a separate study, Kodur and Arablouei (2015) examined two structural assemblies, of which one consisted of a beam-column connection in a moment-resisting frame. Three governing factors for the delamination of SFRM from steel were determined as: 'elastic modulus of fire insulation (E), thickness of insulation (t) and the interfacial fracture energy ( $G_c$ ).'

Research conducted from four separate studies, by Kodur and Arablouei (2015), Gu and Kodur (2011) and Arablouei and Kodur (2015; 2016) respectively, examined delamination occurrence between SFRM and steel structures. The latter three studies focused on the separation of the protection material from the steel due to impact, dynamic or extreme loading. However, delamination caused by static loading is also relevant, which can account for the additional loading onto members from failure of other elements during a fire. Furthermore, while SFRM is a relevant protection material, there is a lack of investigation into separation of both board and encasement fire protection materials from steel substructures. This study attempts to address this issue.

### **2.6.3 Effects and Consequences of Delamination**

While the causes of delamination of insulation from steel structures under fire can be argued, the effects thereof are unanimously documented as detrimental. Partial or complete loss of fire-protecting material can significantly lower the fire resistance of the protected steel members by exposing them to direct fire (Gu and Kodur, 2011). The subsequent rise in temperatures of steel members increases the vulnerability of the structure and escalates the risk of failure, posing a threat to the safety of occupants. This necessitates the need for research into the occurrence of delamination of fire protection, particularly due to the fact that specifications in design codes do not provide adequate information on this incidence.

The study conducted by Gu and Kodur (2011) on a six-storey steel frame with SFRM protection indicated that under the effect of a Eurocode design fire, column and beam members with no protection and a 20 per cent protection material loss reached a failure temperature of 704°C. However, the effect of the thickness of the fire protection material and location, investigated in the current study, was not considered. Furthermore, Kodur and Arablouei (2015) state various researches regarding the delamination of SFRM from steel columns in particular, rather than steel beams. One such study investigated a steel column with 25 mm applied SFRM protection. A 5 per cent loss in fire protection resulted in significantly reduced plastic capacity of the column and reduced the fire resistance thereof by half, from 180 minutes to 90 minutes (Dwaikat and Kodur, 2012; cited by Kodur and Arablouei, 2015).

#### 2.6.4 Limitations of Current Research

In addition to the limited research probing the delamination of insulating material from steel structures, there exist limitations in the available studies relating to the FEA modelling of the phenomenon. In research undertaken by Arablouei and Kodur (2016), a sequential thermal-structural analysis was performed on beam-column assemblies to investigate effects of delamination. The analysis comprised of a beam-column connection and a beam-column moment-resisting frame, insulated by SFRM under fire conditions from seismic and blast events. The delamination region was predetermined using a prior fracture mechanics approach. The finite element model created for analysis of the effect of SFRM delamination is shown in Figure 2-12.

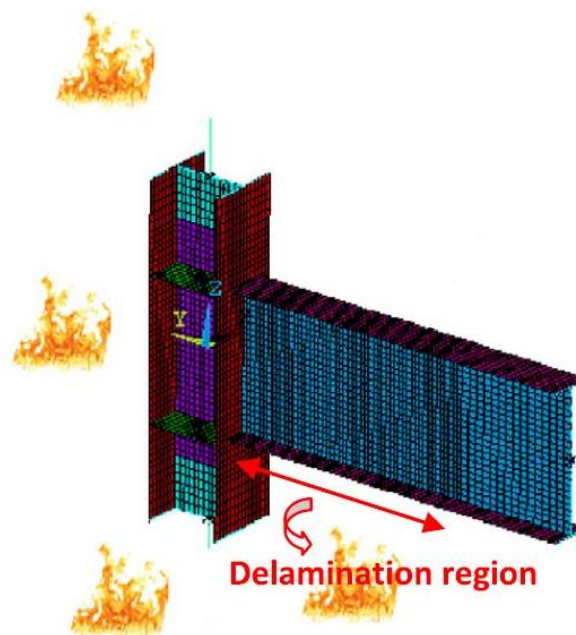


Figure 2-12: Steel beam-column finite element model with predetermined delamination region (Source: Arablouei and Kodur, 2016)

While the model depicted in Figure 2-12 establishes a delamination region prior to structural and thermal analysis, this dissertation aims at improving this approach by allowing the effects of delamination to occur naturally and simultaneously with structural and thermal loading. This represents a more accurate and realistic scenario of a real-life fire where the separation of protection materials would occur while under conditions of thermal and mechanical loading. Furthermore, the thermal action imposed on the beam-column assembly of the frame in this study, is only applied to the specific region experiencing delamination.

There is no indication that the scenario investigated by Arablouei and Kodur (2016) considered the semi-rigid behaviour of the steel connection, taking into account the relevant contact conditions present in structural connections. The present research endeavours to include all the interactions between contacting bodies using unilateral contact-friction interfaces. A further limitation of the study by Arablouei and Kodur (2016) is apparent in the sequential thermal-structural analysis performed using ANSYS programme. This uncoupled analysis did not encompass the complexities of a coupled temperature-displacement analysis, offering a less-than-realistic approach to examining the effects of delamination on the steel structure under fire. The current study aims to refine this by investigating a coupled thermo-structural analysis and incorporating time-dependent delamination of protection materials from the steel surface. Thus, the FEA model developed for transient analyses in this study attempts to describe real delamination within the particular fire scenario and parameters under investigation.

Besides the limitations experienced with numerical modelling using FEA, there exists a deficiency in experimental data on the topic of delamination. As mentioned previously, Badarneh (2004) conducted an experimental and subsequent numerical investigation into the effect of unilateral contact on the structural response of a steel connection under a vertical static applied load, similar to that presented in this dissertation. However, the study by Badarneh (2004) did not consider the fire condition and therefore, did not present findings on fire protection of the steel connection or delamination thereof.

## 2.7 Summary

This chapter provided a review of the fire problem in the context of South Africa and worldwide. The relevant and critical properties of steel in thermal and thermomechanical analyses were discussed, with consideration given to the reduction in mechanical properties under fire. The current approaches to the fire design of structures and steel structures were presented and input from both the Eurocode and the South African design codes were evaluated. The requirement of designing fire resistance for buildings was assessed and deemed adequate for conventional design purposes, though discrete research of structural steel assemblies under fire should be conducted for greater accuracy. The concepts underlying fire testing and design using finite element analysis methods were contextualised, indicating the relevance of conducting numerical analyses with computer software. Current literature on the performance of steel structures under fire was presented and it was determined that there exists a deficiency in research regarding the behaviour of beam and column elements in a steel connection under fire conditions, with a tendency to focus on the joints in the connection. The necessity of analysing a three-dimensional, non-linear model subject to a variety of fire scenarios with multiple fire protection variables was outlined, thus indicating the relevance of this dissertation. The application of numerous fire protection materials was evaluated, where the current use of gypsum board and concrete encasement protection in industry prompts research into these materials, which is investigated in this study. The phenomenon of delamination was discussed; the causes and effects thereof were presented. The existing limitations experienced in modelling simultaneous thermo-structural actions onto a steel connection, towards simulating delamination, were assessed. This issue is addressed in the present dissertation, noting the current lack of experimental data. The methodology adopted in conducting the numerical analyses of a steel connection under fire and the effect of delamination thereon, will be provided in Chapter 3.

# Chapter 3

---

## 3 Methodology for Finite Element Analysis

### 3.1 Introduction

The initial procedure followed in conducting the study was research-based. A fundamental understanding of the topic of finite element analysis was required and achieved using relevant textbooks based on the topic. A literature review, presented in the preceding chapter, was carried out to gain understanding of other key components related to the research and to contextualise key concepts underpinning the crux of the study. The procedures followed in conducting the study will be described in this chapter and the numerical simulations executed with Abaqus FEA software will be presented. The steps followed in creating and running the numerical models will be outlined. Furthermore, the level of accuracy obtained from the analyses and limitations experienced in performing the investigation will be expressed and discussed.

### 3.2 The Research Process

Based on background research presented in the literature review and in this chapter, and availability of resources, a FEA method for performing the numerical analyses of the study was determined and Abaqus was selected as the means of running the analyses. The relevant material properties of the steel connection adopted for the study was investigated during the research process and the data obtained was used in the preparation of the numerical models in Abaqus. The scenarios investigated in the study were ascertained from an evaluation of deficiencies in current literature provided in Chapter 2, surrounding the topic of steel structures under fire conditions and the delamination of fire protection materials.

The FEA models presented in this study were developed in an attempt to investigate the real behaviour of a specific beam-to-column bolted steel connection in various fire scenarios, with and without fire protection. The significance of using accurate numerical models to analyse such behaviour was documented in a study performed by Daryan and Yahyai (2009) and discussed in Chapter 2, subsection 2.4.5. A comparison between results of experimental data and FEA models in the study by Daryan and Yahyai (2009) determined that '*FE technique is capable of predicting connection*

*response at elevated temperatures to an acceptable degree of accuracy.*' This statement, together with several researches related to FEA in steel connections, support the fact that similar numerical tools can adequately be adopted to conduct this type of research.

### 3.3 Abaqus Analyses

Abaqus is computer software that runs numerical analyses based on the finite element method, as discussed in the previous chapter. Details about FEA and justifications for adopting this software are presented in Chapter 2. Two types of analyses were executed with Abaqus, namely steady-state and transient analyses. Relevant models were developed pertaining to each type of analysis to conduct the investigation and achieve the results.

#### 3.3.1 Steady-State Analysis

Steady-state analyses were conducted based on three types of models: mechanical, thermal and thermomechanical models. Each setup required different inputs and produced distinct results corresponding to the method of analysis, described as follows:

- *Mechanical model* – This model was based on a purely structural analysis of the system. Material properties relating to the mechanical behaviour of elements and structural loads were considered in the analysis. The effects of fire were not considered. The baseline result used for verification of the subsequent results was obtained from the analysis of this model.
- *Thermal models* – In this model, only the thermal effects on the system from thermal load, in the form of surface heat flux, was considered. Thus no structural loads or components were analysed. Thermal properties of the materials, heat flux loading and thermal boundary conditions were applied. Results for temperature distributions and developments were obtained from these analyses.
- *Thermomechanical models* – This model was a combination of input from both the mechanical and thermal models, in terms of material properties, loading, boundary conditions and output criteria. The main results of the study were obtained from force-displacement diagrams derived from these analyses.

The steel substructure used in the analyses was modelled separately with and without fire protection in order to provide comparable results for two analyses: a thermal

analysis and a subsequent thermomechanical analysis. Each analysis was conducted twice, as follows:

- (T) – A thermal analysis without fire protection was computed.
- (TM) – Results of (T) imported into a thermomechanical analysis without fire protection.
- (TR) – A thermal analysis with fire protection was performed.
- (TMR) – Thermal output of (TR) was transferred into a corresponding thermomechanical analysis.

An important factor that was considered in executing the analyses was that while the TMR analysis implies the addition of fire protection in the model, this analysis only considered the thermal impacts of the fire protection from the analogous TR analysis. In the TMR model, the temperature distribution obtained in the TR model is imported; however, the fire protection material itself has not been included. Thus, the TMR model and results were not influenced by any additional support or strength originating from importing the fire protection; numerically, importing the protection into the TMR model would increase the strength of the connection. This is unrealistic since the fire protection material does not offer additional stability or support to the system structurally. Hence, the effect of fire protection is only considered in the capacity of the TR models and the results thereof were exported to the TMR model.

### **3.3.2 Transient Analysis**

The investigation into the delamination of fire protection materials required the development of thermomechanical models. The analyses conducted were coupled stress-temperature analyses on models with and without fire protection, which accounted for the realistic, simultaneous impact of structural and thermal loading. These models examined the delamination phenomenon over time, hence transient analyses were conducted. The transient thermomechanical models follow a similar description to the aforementioned steady-state thermomechanical models, with a few differentiating features that are further expanded on later in the chapter. The main distinguishing factor is that the fire protection material is imported into the transient thermomechanical models, while protection is not incorporated in the TMR steady-state analyses, as discussed previously. In the transient fire-protected models, this could not be avoided since the simultaneous effects of elevated temperatures and structural loading on delamination was inspected, thus requiring the incorporation of the fire protection. However, the models were developed in a manner that prevented the

structural performance of the fire protection material from influencing the structural behaviour of steel. Hence, only the thermal performance of fire protection was taken into account in these models. Transient thermomechanical analyses were conducted on a model with fire protection and on a model with no fire protection (the control model).

### **3.4 Abaqus Simulation**

The various analyses conducted with the Abaqus models followed a standard procedure in creating and running the models. The baseline process of conducting Abaqus simulations is displayed in Figure 3-1, followed by explanations of the principal steps adhered to in steady-state and transient analyses of relevant mechanical, thermal and thermomechanical models.

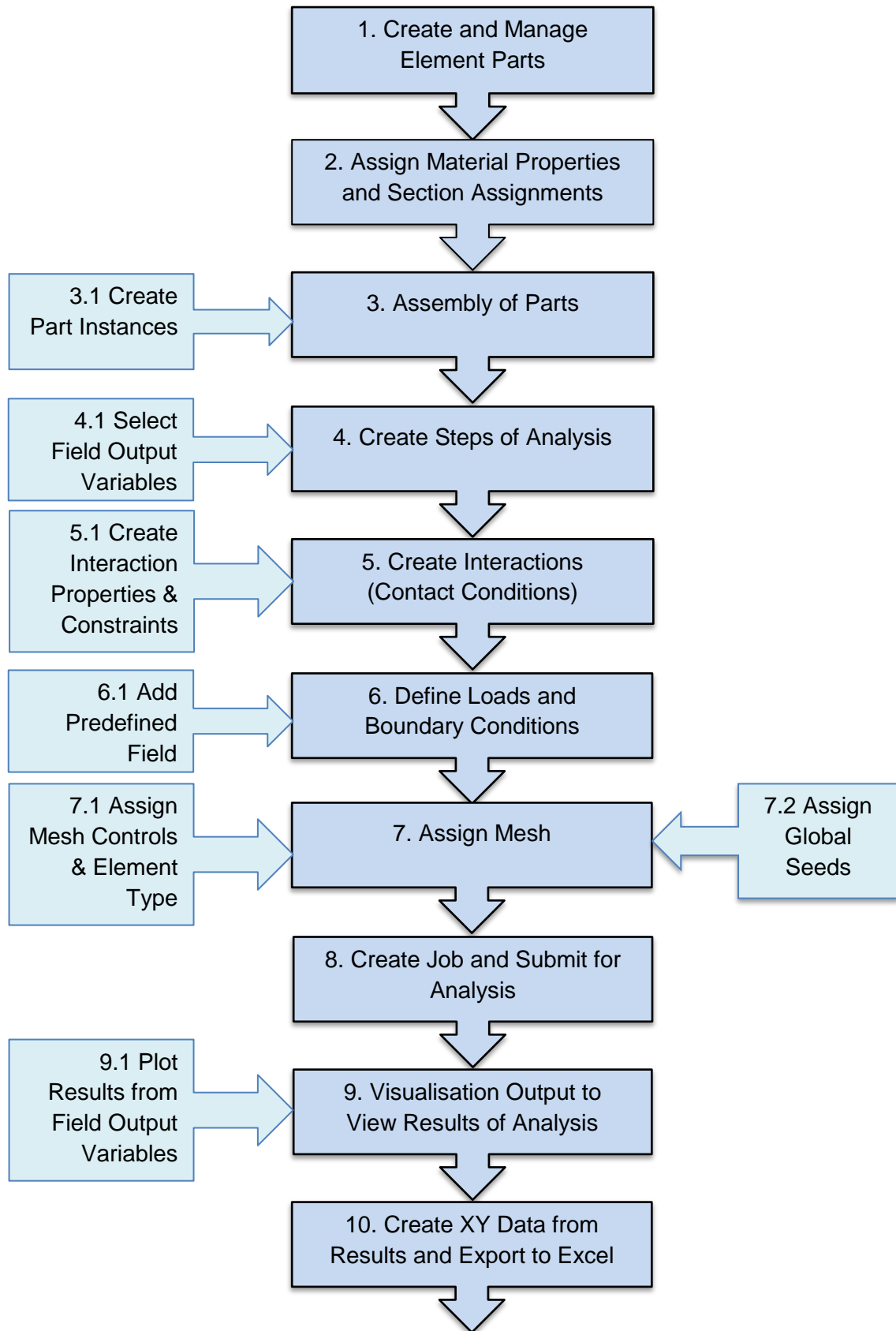


**Figure 3-1: Abaqus steps for numerical model simulations**

## 1. Create and Manage Element Parts

The geometry of the steel substructure was first created in AutoCAD and thereafter imported into Abaqus as individual parts. A three-dimensional model, consisting of a beam, a column, angles, bolts and washers was developed in AutoCAD rather than in Abaqus, due to the simpler and more familiar interface of AutoCAD. The steel connection that forms the basis of the numerical models in this study was adopted from experimental and FEA research conducted by Badarneh (2004) and Abdalla et al (2015). This was done to verify the initial results and FEA model of this study, in the absence of resources to experimentally design and test a steel substructure. The geometry of the column, beam and angles are displayed in an assembled connection shown in Figure 3-2. The bolts used to connect the steel elements were seventeen M20 high-strength grade 8.8 bolts (Abdalla et al., 2015). Detailed geometry of the structural steel elements of the connection is depicted in Appendix A: Figure A-1 and A-2.

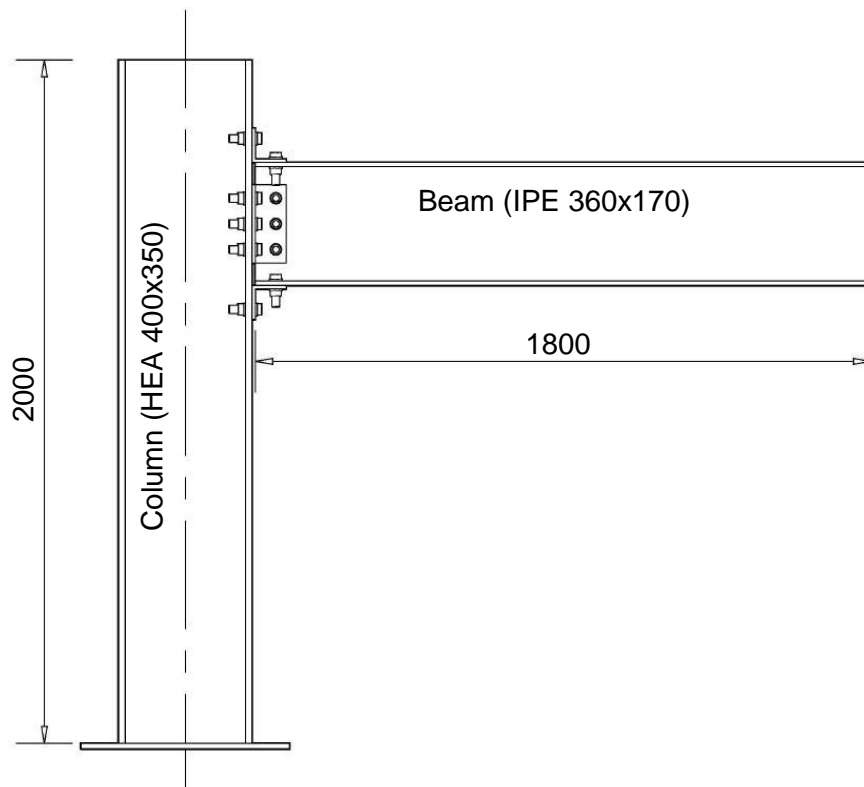


**Figure 3-2: Two-dimensional diagram of assembled steel connection (After Abdalla et al., 2015)**

The units of Figure 3-2 indicate the dimensions in millimetres; however, the drawing in AutoCAD was done in metres to comply with Abaqus, since the software detects units from user-defined material properties. The AutoCAD drawing parts were converted to

Standard ACIS Text (SAT file) and imported into Abaqus, where the elements were managed as three-dimensional, deformable parts.

## **2. Assign Material Properties and Section Assignments**

In order to accurately model the behaviour of the elements and parts in Abaqus, material properties were defined for the steel parts and, where necessary, for fire protection. The properties specific to each material include general, mechanical, thermal, electrical or other properties. Particular material behaviours under each of the properties were specified according to the relevant model under investigation. In the mechanical models, these behaviours were: density, elasticity (Young's modulus and Poisson's ratio) and plasticity (yield stresses with corresponding plastic strains). Thermal models required only thermal conductivity and thermal expansion properties of the materials, while the thermomechanical models were assigned a combination of temperature-dependent mechanical and thermal behaviours. In the thermomechanical setup, material behaviour data accounted for the reduction in strength of some properties with an increase in temperature, as discussed in the literature review, in subsection 2.3.3. The aforementioned models refer to steady-state conditions; however, the transient thermomechanical models required the additional input of the specific heat properties of the materials. Each steel element and fire protection material, where applicable, was assigned as a solid, homogenous section in all models.

## **3. Assembly of Parts**

The separate parts imported into Abaqus were assigned independent instances and positioned relative to each other in a global coordinate system, thus creating an overall main assembly. A part instance is the name given to a copy or representation of the original element imported into Abaqus (Abaqus User's Guide, 2014). The instances also allow a mesh to be generated for each steel part or fire protection element. Figure 3-3 displays the final assembly of the steel parts.

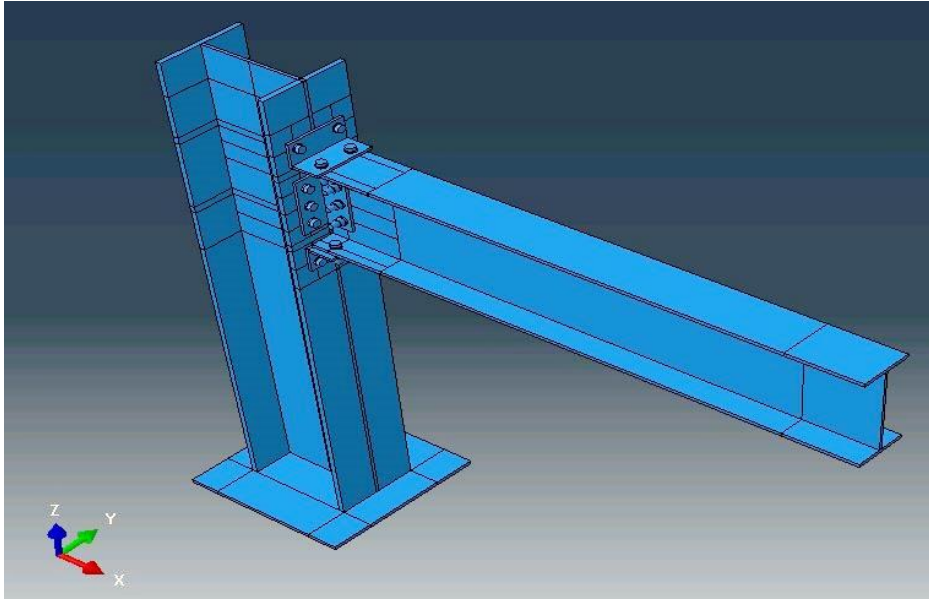


**Figure 3-3: Assembly of steel connection in Abaqus**

#### **4. Create Steps of Analysis**

The method of analysis of each step of the numerical models was defined at this stage. The steady-state mechanical and thermomechanical models followed a static, general procedure due to the structural nature of the models. These thermal models incorporated a heat transfer analysis step. The transient thermomechanical models progressed, initially, with a static, general step and thereafter progressed into a transient coupled temperature-displacement analysis. This type of analysis coordinated thermal and structural effects on the system. The analysis steps, especially pertaining to the structural models, accounted for non-linear geometry and used the Newton-Raphson iterative method for solving the analysis, as mentioned in the preceding chapter.

The selected field output variables for the mechanical models included: stresses, strains and plastic strains (PEEQ), translations and rotations (U), concentrated forces (CF), reaction forces, contact stresses, displacements and contact forces. The nominated thermal model output variables were nodal temperatures (NT), element temperatures and heat flux variables. The thermomechanical output variables stipulated for both the steady-state and transient analyses were a combination of the above-mentioned mechanical and thermal variables.

## **5. Create Interactions (Contact Conditions)**

Contact conditions and interactions were created and assigned in this step. Abaqus requests input for interaction types, interaction properties and interaction constraints. For all contact conditions, standard surface-to-surface contact was selected and for each pair of interacting surfaces, a 'master' and 'slave' surface was assigned. All the interactions between contacting bodies in the main assembly of the models, namely the beam, column and angle cleats, were considered using unilateral contact-friction interfaces with a friction coefficient of 0.4. Hence, the interaction properties assigned were normal and tangential (friction) behaviours. The friction coefficient value of 0.4 was selected based on research done by Abdalla et al (2015), where a particular model of the steel connection was tested with variable friction coefficients of 0.2, 0.4 and 0.6. The resulting force-displacement diagrams for each coefficient lead to the conclusion that *'an increase of the friction coefficient of the connected parts from 0.2 to 0.6 leads to a small increase in the maximum load of the connection'* (Abdalla et al., 2015). Thus, the average friction coefficient value (0.4) was assigned to the unilateral contact-friction interfaces in the steel connection of this dissertation.

The interface between the bolts-to-holes and bolts-to-angle surfaces were regarded as frictionless contact, allowing sliding without resistance, thus no penetration. Tie constraints were assigned for the interfaces between washers and steel parts, preventing opening-sliding behaviour and inhibiting the separation of the surfaces during analysis. With models incorporating fire protection in the assembly, normal and tangential behaviour was allocated in the standard surface-to-surface contact, where the master and slave surfaces were assigned to the fire protection and connecting steel surface respectively. In addition to the above-mentioned interaction properties, thermomechanical models were assigned thermal conductance contact properties for each material.

## **6. Define Loads and Boundary Conditions**

The loads that ultimately determined the behaviour of the structural connection were defined in the load module of Abaqus. The steady-state mechanical and thermomechanical model loads were initially specified as a stabilising gravity load, based on the self-weight of the assembly. Thereafter, a concentrated force of 200kN was applied at 1.58 metres along the beam, as shown in Figure 3-4, and remained unchanged across the steady-state structural analyses. The magnitude of the 200kN point load was initially selected based on the results of the study conducted by Abdalla

et al (2015), where the steel connection under investigation yielded a maximum load of approximately 100kN. Following this knowledge and considering that the steel connection from Abdalla et al (2015) was adopted in the current study, a value reasonably higher than 100kN was chosen for the concentrated applied force. This was done to ensure that the analysis would progress from linear to non-linear and eventually, damage of the steel connection would be depicted. It is noted that the value of 200kN was only used by the software for the initiation of the incremental Newton-Raphson analysis. Thus, the force of 200kN followed this Newton-Raphson FEA procedure and was applied incrementally according to Abaqus. The vertical load was applied in time steps (not real time), where, for example, a time step of 0.01 was set in the Abaqus step module of a model. The time steps were selected within a reasonable range. Thereafter, the force would be applied as follows:

- $0.01 \text{ (time step)} \times 200 \text{ (force in kN)} = 2\text{kN}$  increments per time step and the applied force in the first step is 2kN.

From this, it was understood that selecting a force less than 100kN would not have achieved the required output in terms of reaching post-elastic behaviour of the steel connection. Furthermore, selecting a substantially higher force value such as 200,000kN would result in increments of 2000kN per 0.01 time step, which exceeds the capacity of the Newton-Raphson FEA iterative procedure.

The thermal heat flux load was used to represent the connection under fire conditions. The heat action was applied at varying positions, thereby creating multiple and comparable load cases. The results of the T and TR models were imported into the corresponding TM and TMR models as a predefined field, at the relevant step in the analysis. The structural and thermal loading of the transient models was based on ramped loading according to a force-time curve and the standard temperature-time curve, discussed in Chapter 2.

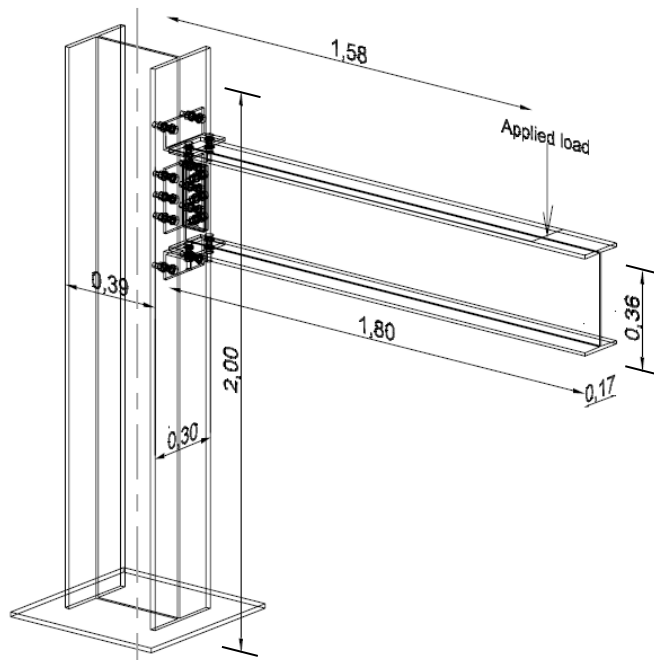


Figure 3-4: Overall geometry and point of application of 200kN concentrated load (Source: Abdalla et al., 2015)

The common boundary conditions set across the models included fixing the bottom of the column to prevent displacement and rotation in all directions (BC1) and assigning symmetry along the Y-axis of the beam to prevent twisting (BC2). These boundary conditions are shown in Figure 3-5. The boundary conditions in the steady-state thermal models and transient thermomechanical models were defined as zero temperatures at strategic places (end sections of the protection), to demonstrate the temperature development and distribution in the model, as well as to provide the necessary temperature restraint in the developed models.

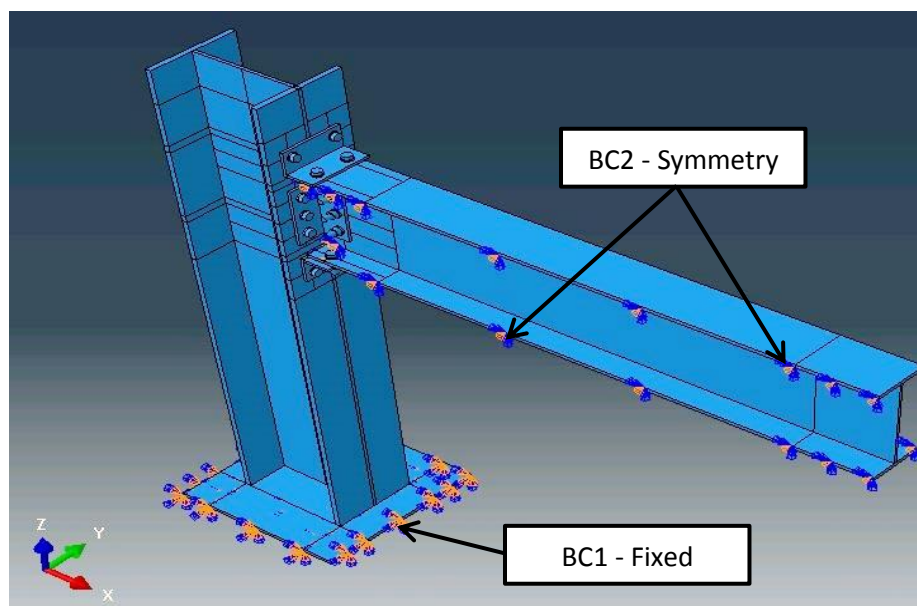
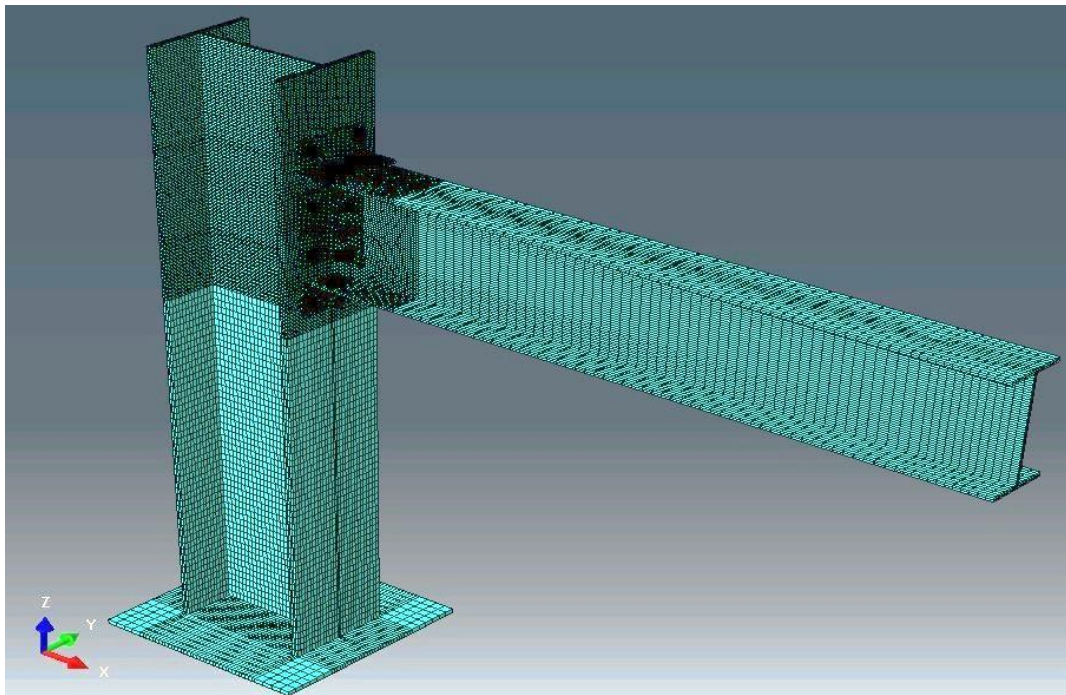


Figure 3-5: Common boundary conditions

## 7. Assign Mesh

A mesh was generated for each of the elements in the connection, as well as the fire protection when applicable. The mesh allows for computing the numerical model using FEA. Denser meshes provide more accurate results; however, this requires a significant amount of computational time and memory. To generate the mesh, three mesh features were assigned, namely: mesh controls, element type and global seeds. To satisfy the mesh controls, hexagonal mesh elements were chosen. The element types of the mesh varied depending on the type of analysis being conducted, such that the element types of mechanical and steady-state thermomechanical models were assigned as three-dimensional stress elements (displacement degrees of freedom), thermal models were defined by heat transfer elements (temperature degrees of freedom) and the transient thermomechanical models were allocated coupled temperature-displacement elements (displacement and temperature degrees of freedom). The approximate global seed sizes that determine the number of elements per thickness of the assembly parts varied across the models. However, a general rule of two, three or four elements per thickness was abided by in order to create a dense enough mesh to obtain a satisfactory level of accuracy, while not inducing excessively long computational times. Figure 3-6 illustrates the final mesh of the overall steel connection in Abaqus.



**Figure 3-6: Overall steel connection depicting the 8-node brick finite element mesh with 167,785 finite elements**

## **8. Create Job and Submit for Analysis**

After completing the aforementioned steps and defining the required data and information for analysis, a job was created in Abaqus to run the numerical models. Multiple jobs with various outputs were created for the range of models and the results thereof were viewed in the visualisation output module in Abaqus. The results presented after analysis were completed and aligned with the field output variables stipulated in step 4.

## **9. Visualisation Output to View Results of Analysis**

The visualisation output module was used to view the illustrative and quantitative results of the completed analyses. The progressive and final deformed shapes of the connection were viewed and the results of each of the field output variables were determined and extracted. The main results of the thermal models were the Nodal Temperatures (NT) outputs, while the results forming the focal point of the study were obtained from the Vertical Displacement (U), stresses, plastic strains and other outputs, from the thermomechanical analyses.

## **10. Create XY Data from Results and Export to Excel**

From the visualisation module in Abaqus, XY data was extracted from the point at which the concentrated force was applied. The generated XY data from Abaqus utilised the Vertical Displacement (U) and Concentrated Force (CF) output variable results to present corresponding displacement and loading results. This data was then exported to Microsoft Excel to create and illustrate force-displacement diagrams.

## **3.5 Abaqus Steady-State Models**

In order to achieve particular aims and objectives outlined in Chapter 1, steady-state numerical models were developed and analysed using FEA through Abaqus. As mentioned earlier in the chapter, the steel connection in this dissertation was adopted from the researches of Badarneh (2004) and Abdalla et al (2015). The results of the initial model in this study, namely the mechanical model, were verified by a similar structural analysis conducted by Abdalla et al (2015) on the steel connection. Thereafter, using the same connection, original models were developed for thermal and thermomechanical analyses, for the purposes of investigating the influence of fire protection on the connection under elevated temperatures in this study. These

investigations were achieved by modelling fire protection materials onto the steel connection and conducting thermal and subsequent thermomechanical analyses. As discussed previously, these models were analysed with and without fire protection to gauge the full impact of various protection materials on the steel connection.

### **3.5.1 Assigning Material-Specific Properties**

The material properties to run each model, specifically the mechanical, thermal and thermomechanical analyses, were defined at the beginning in building each model. Material properties for the steel connection components, as well as the fire protection materials, were assigned in the models accordingly. The fire protection materials selected were gypsum board and concrete. The modelling of these materials is discussed further in the chapter. Some of the material properties for steel parts, defined as the beam, column, angles and washers, differed slightly to those of the steel bolts and were accounted for from EN1993-1-2 (2005). Eurocode 3 information, specifically EN1993-1-2 (2005), was utilised, rather than South African data, since some pivotal steel properties are not comprehensively accounted for in South African codes as they are in the Eurocode. Furthermore, pivotal steel properties were defined in terms of EN1993-1-2 (2005) in this study, thus an effort was made to maintain uniformity throughout. These properties were presented in Chapter 2, of which, some include: thermal conductivity and specific heat of steel as a function of temperature (Figure 2-4 and 2-5 respectively), reduction factors for steel elements (Table 2-3 and 2-4) and the deterioration of the stress-strain relationship of steel at elevated temperatures (Figure 2-8).

#### **3.5.1.1 Mechanical Models**

The material properties required for the mechanical model simulations in Abaqus included defining the density, elasticity modulus, Poisson's ratio and plasticity of the material. The data input for these material behaviours is shown in Table 3-1.

**Table 3-1: Material properties for mechanical models (Source: As shown)**

Material Properties		Steel Connection	
		Steel parts	Steel bolts
Mass Density (kg/m <sup>3</sup> ) (EN1993-1-2, 2005)		7850	
Elasticity (Abdalla et al, 2015)	Young's modulus (kPa)	150000000	
	Poisson's ratio	0.3	
Plasticity	Yield stress (kPa)	Appendix B: Table B-1 and Figure 2-8 (Graph corresponding to 20°C, 100°C)	
	Plastic Strain		

The modulus of elasticity defined in Table 3-1 was selected as 150 GPa in accordance with the experimental and numerical study of Abdalla et al (2015), from which the steel connection was adopted. Although 150 GPa presents a relatively lower value than the common value used (200 GPa), it was determined that non-linear effects influence the results to a greater degree than Young's modulus (Abdalla et al., 2015). Therefore, a higher value would not significantly alter the measured outcomes.

### 3.5.1.2 Thermal models

The required material properties for the thermal models are indicated in Table 3-2. These included thermal conductivity and thermal expansion behaviours of the steel parts, steel bolts and respective fire protection materials.

**Table 3-2: Material properties for thermal models (Source: As shown)**

Material Properties		Steel Connection (EN1993-1-2, 2005)		Fire Protection (Tsapara et al, 2013)	
		Steel parts	Steel bolts	Gypsum	Concrete
Thermal Conductivity (kW/m°C)	20°C	0.045		0.000200	0.000988
	100°C			0.000183	0.000938
	20°C, 100°C -900°C			Appendix B: Table B-2	
Thermal Expansion: Coefficient of thermal expansion		1.2 x 10 <sup>-5</sup>	1.3 x 10 <sup>-5</sup>	1.8 x 10 <sup>-7</sup>	1.2 x 10 <sup>-5</sup>

The thermal conductivities of gypsum and concrete were varied with temperature from 20°C to 900°C. The values of thermal conductivities of the fire protection for gypsum and concrete are given in Table 3-2 for normal temperatures (20°C, 100°C). The full range of thermal conductivities of the protection materials is provided in Appendix B, as stated in Table 3-2. The thermal conductivity of steel was assigned as the average conductivity over the same range of temperatures, aligned with the initial thermal models adopted for analyses. A distinct model was analysed with temperature-dependent values of the thermal conductivity of steel and the effects were insignificant to the overall results. The lower values of the thermal conductivities of the fire protection, with respect to steel, indicates that fire due to conduction passes at a slower rate through these materials. Hence, these materials are used as thermal protection and afford the necessary fire resistance to the structure.

### 3.5.1.3 *Uncoupled Thermomechanical models*

The allocated material properties of the thermomechanical models were a combination of steel material behaviours from the mechanical and thermomechanical models; however, the reduction in strength of the materials with an increase in temperature was accounted for. The properties defined in these models are presented in Table 3-3. The behaviour of the fire protection materials is not included since the protection was not imported into the model, preventing the addition of pseudo-strength to the overall connection.

**Table 3-3: Combined material properties for thermomechanical models (Source: EN1993-1-2, 2005)**

Material Properties	Steel Connection	
	Steel parts	Steel bolts
Mass Density (kg/m <sup>3</sup> )	7850	
Temperature-dependent Elasticity (Young's modulus and Poisson's ratio)	As per Table 3-4	
Plasticity (Yield stress and Plastic strain)	Appendix B: Table B-3	Appendix B: Table B-4
Thermal Conductivity (kW/m°C)	0.045	
Thermal Expansion: Coefficient of thermal expansion	1.2 x 10 <sup>-5</sup>	1.3 x 10 <sup>-5</sup>

The degradation of the material properties of steel with increasing temperatures is in accordance with Figure 2-8, previously presented in the literature review and displayed in Figure 3-7. The reduction of the elasticity modulus, due to elevated temperatures, was accounted for in the material definitions of the steel parts in the relevant thermomechanical models and is presented in Table 3-4.

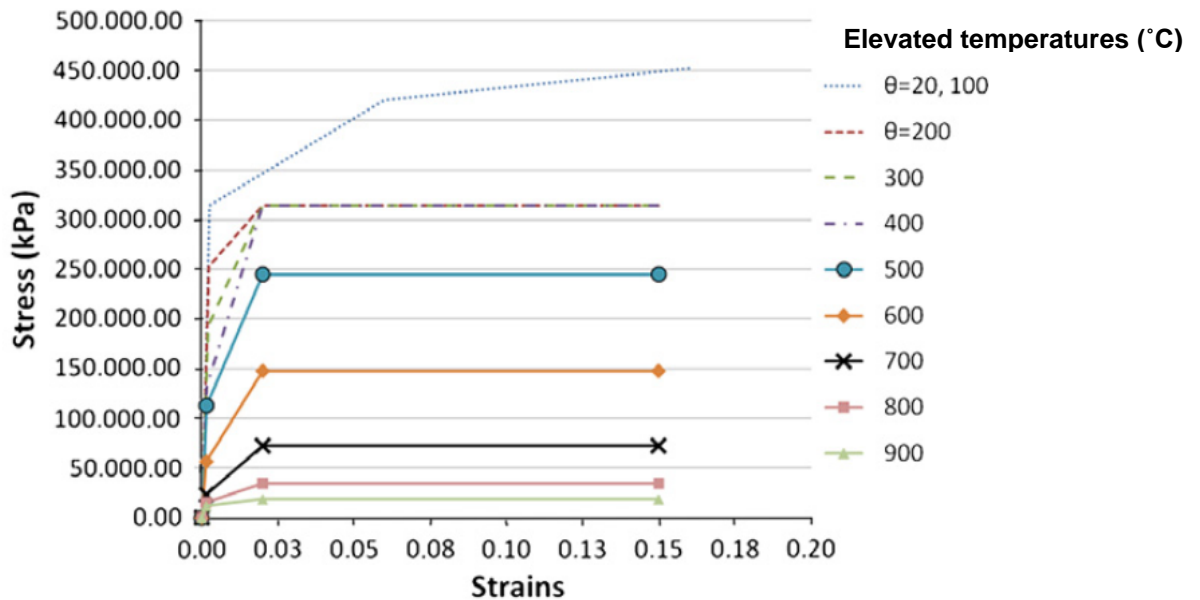


Figure 3-7: Deterioration of the stress-strain relationship of steel due to elevated temperatures ( $\theta$  in °C) (Source: EN1993-1-2, 2001; cited by Kalogeropoulos et al., 2011)

Table 3-4: Reduction of elasticity modulus with temperature (Source: As shown)

Temperature (°C)	Young's Modulus: Steel Parts and Bolts (GPa) (EN1993-1-2, 2005)	Poisson's Ratio (Abdalla et al, 2015)
20	150	0.3
100	150	0.3
200	135	0.3
300	120	0.3
400	105	0.3
500	90	0.3
600	46.5	0.3
700	19.5	0.3
800	13.5	0.3
900	10.125	0.3

### 3.5.2 Modelling Fire Protection

The effects of different fire protection materials on the steel connection under fire were examined. This was achieved by modelling two types of fire protection materials, namely concrete and gypsum, with varying thicknesses. Concrete was selected due to its favourable fire resistance material properties and since it presents a common construction material for composite steel and concrete structures. The relevance of gypsum board protection, discussed in Chapter 2, motivated an investigation into its influence on the steel connection.

The modelled thickness of concrete was selected as 50mm, as a common industry standard, while gypsum board protection thicknesses that were examined were 50mm (approximately three connected gypsum boards) and 30mm (roughly two attached gypsum boards). The 30mm gypsum board was chosen as a minimum thickness since one gypsum board, approximately 15mm, did not sufficiently cover the joint in the connection. Hence, such a setup is not relevant to this study.

Additionally, the effect of the location, or extent of coverage, of the fire protection was determined and compared. The aforementioned fire protection materials were modelled in two ways: along the full length of the top flange of the beam, presenting a simple scenario, and secondly, concealing the entire beam-to-column steel connection excluding the column base plate. The latter scenario depicts a more complicated and conservative protection mechanism. For simplicity, the simple situation of protecting the beam flange is specified as beam protection (BM), while the protection of the entire connection is elected as full protection (FULL). Moreover, where full fire protection was designed, three thermal load cases (LC) were investigated and described further in this chapter. Table 3-5 provides a compilation of fire protection materials, thicknesses and extent of coverage that was investigated in the study.

**Table 3-5: Summary of investigated fire protection and various contributing factors**

Protection Material	Thickness (mm)	Label	Coverage (Location)
Concrete	50	CONC50	BM
			FULL
Gypsum board	50	GYP50	BM
			FULL
	30	GYP30	BM
			FULL

Figure 3-8 (a) and (b) and Figure 3-9 (a) and (b) illustrate the finite element connection in Abaqus with relative fire protection comparisons, presented in Table 3-5.

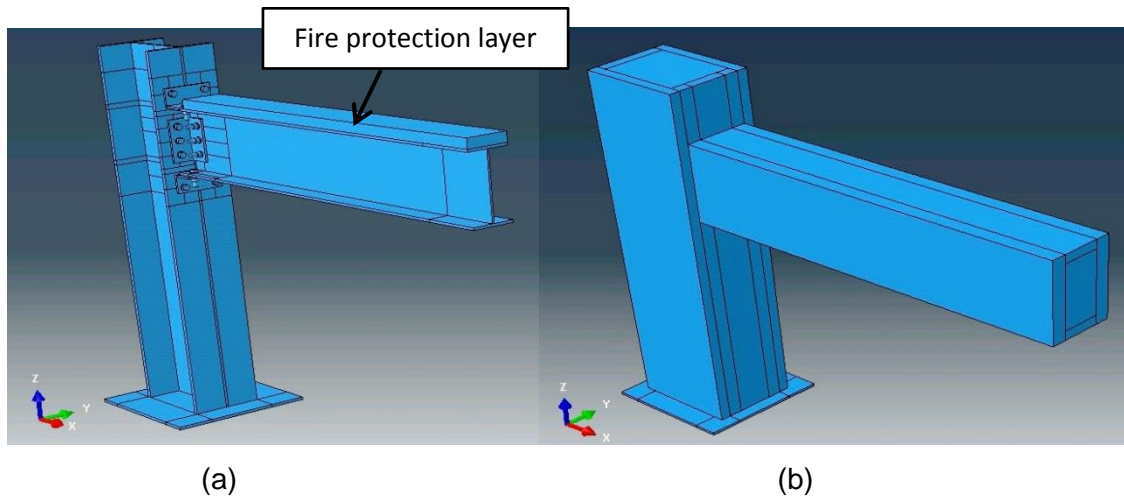


**Figure 3-8: Overall connection with 50mm Concrete/ Gypsum board fire protection for: (a) BM coverage; (b) FULL coverage**

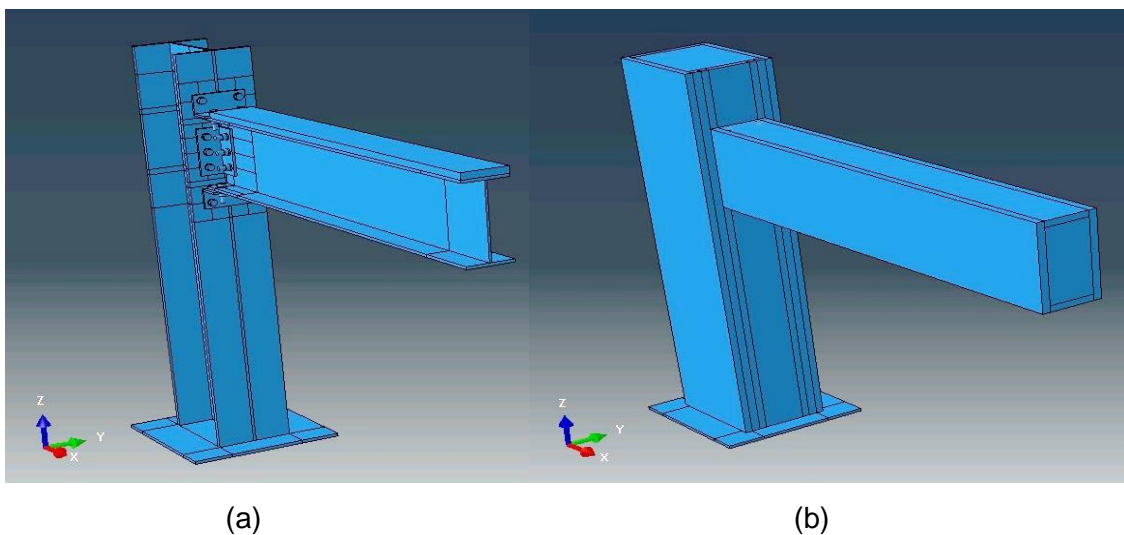


**Figure 3-9: Overall connection with 30mm Gypsum board fire protection for: (a) BM coverage; (b) FULL coverage**

Figures 3-8 (b) and 3-9 (b) that display FULL concealment of the connection were partitioned as shown, in order to create a hexagonal, structured mesh and define the global seeds per fire protection partition.

### 3.5.3 Load Cases and Boundary Conditions

The combination of structural and thermal loading defined the scenario-based analysis of the models. The structural loads on each of the models remained the same in the mechanical and thermomechanical analysis. Thus, the initial analysis step consisted of the force of gravity at  $9.81 \text{ m/s}^2$  on the entire model and thereafter, a concentrated load

of 200kN was applied to the beam as displayed in Figure 3-4. The explanation of this chosen magnitude of force was discussed earlier in this chapter, in subsection 3.4.

An explanation of the selected magnitude of the point load was presented earlier in the chapter, in subsection 3.4. Thermal load cases for the thermal models were chosen depending on the extent of fire protection coverage of the connection. A surface heat flux of  $2\text{kW/m}^2$  was applied throughout as the standard loading. The fire-protected thermal load cases with standard heat fluxes were defined as follows, and the corresponding illustrative loads are shown Figure 3-10, 3-11, 3-12 and 3-13 respectively:

*For BM coverage:*

- LC1 – thermal load applied to protection parallel to the top flange of the beam, displayed in Figure 3-10.

*For FULL coverage:*

- LC1 – fire applied to protection parallel to the top flange of the beam, extending over the joint connecting beam top flange to column flange (to be compared to BM-LC1), shown in Figure 3-11.
- LC2 – thermal load applied to protection concealing all flanges (beam and column), illustrated in Figure 3-12.
- LC3 – heat flux applied over the entire structure on all external protection surfaces, indicated by Figure 3-13.

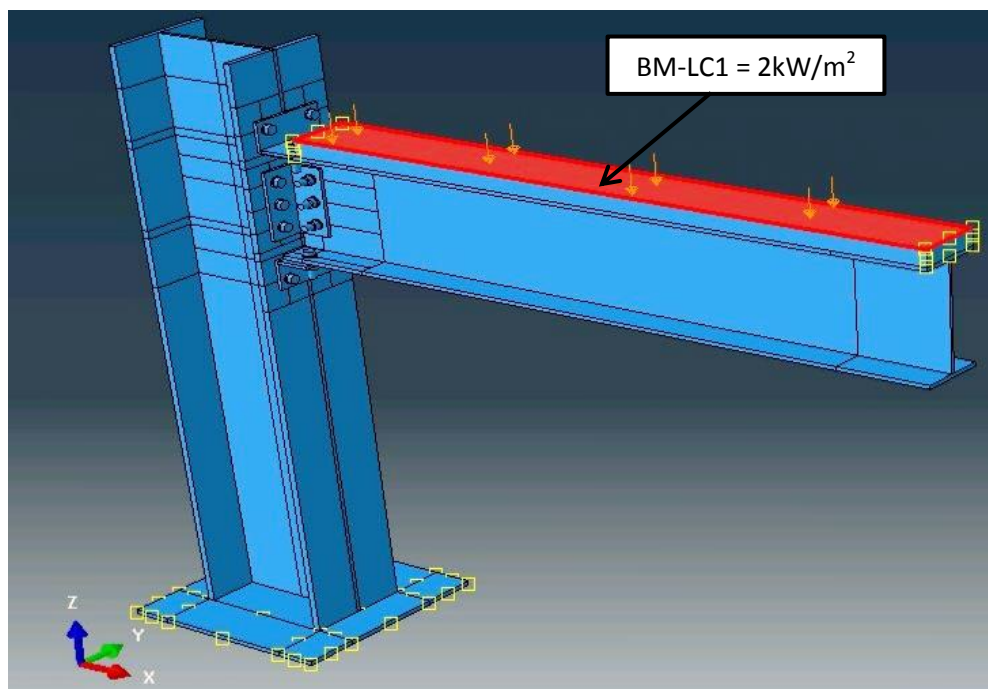


**Figure 3-10: BM fire protection coverage with applied LC1**

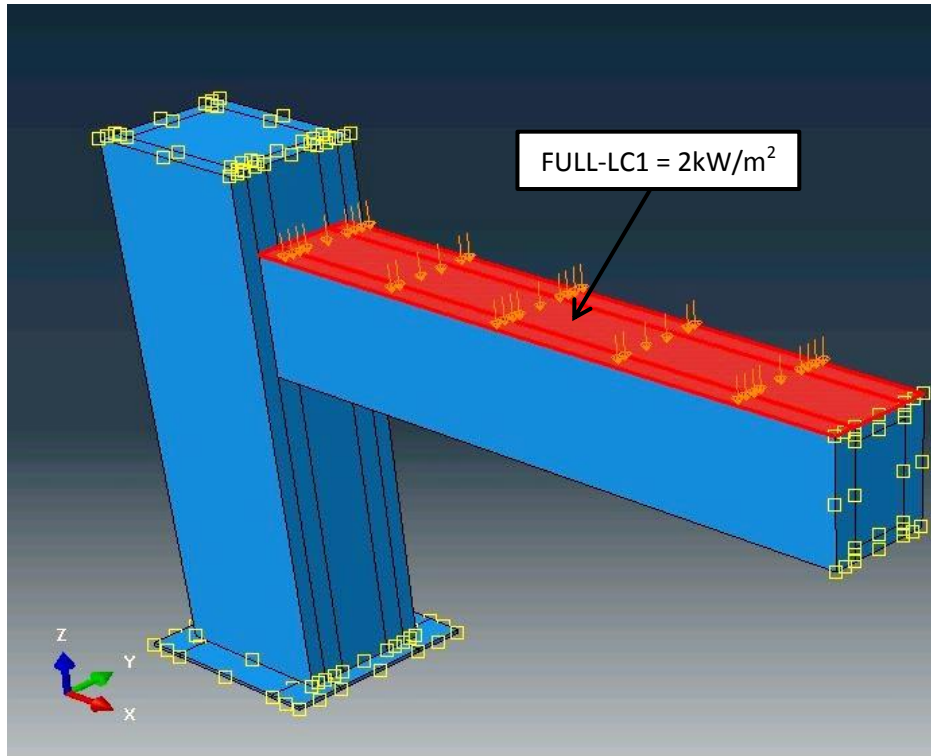


Figure 3-11: FULL fire protection coverage with applied LC1

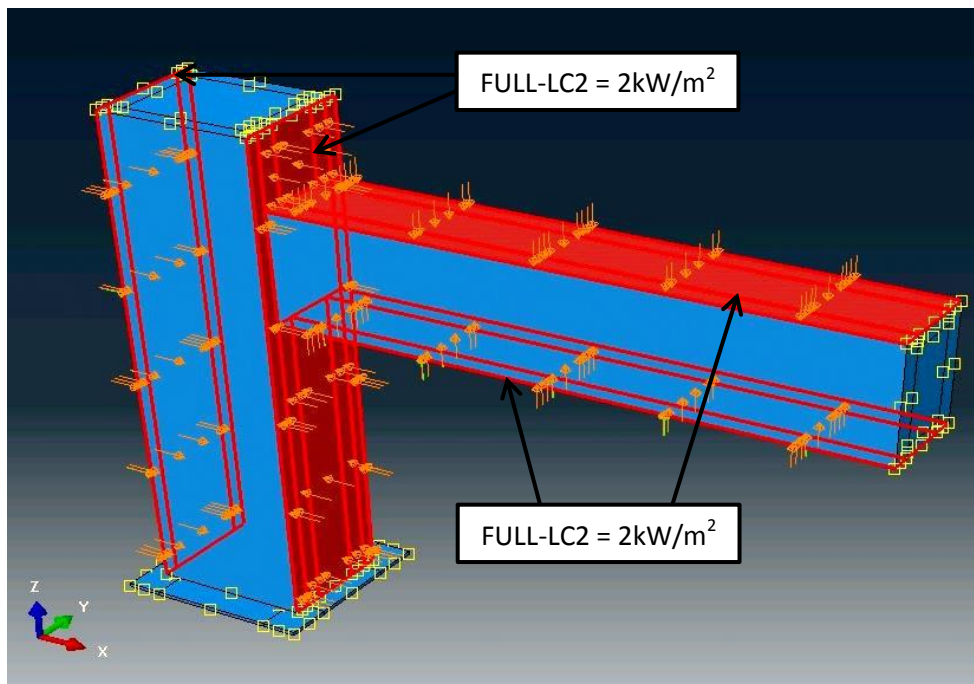
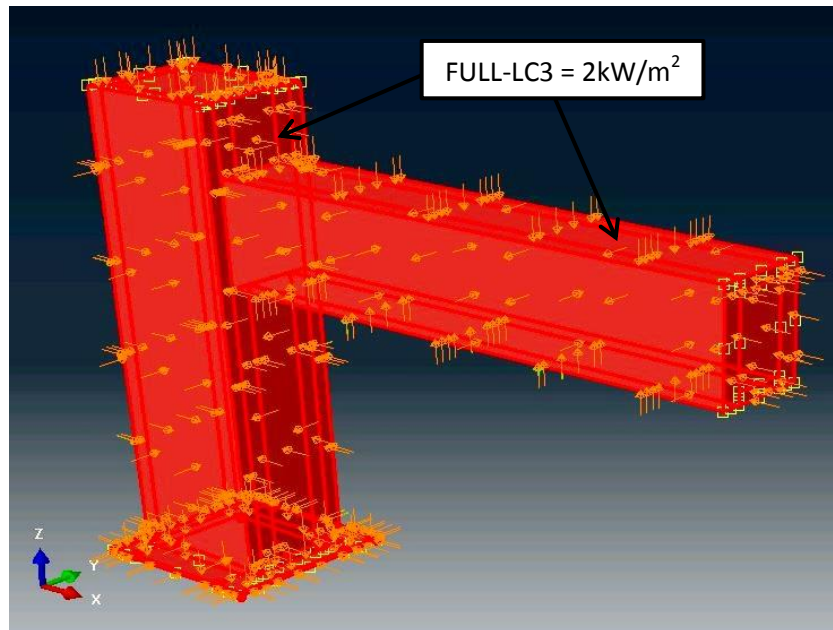


Figure 3-12: FULL fire protection coverage with applied LC2



**Figure 3-13: FULL fire protection coverage with applied LC3**

In the thermal models without fire protection, the load cases followed the same location of applied surface heat flux as the models with fire protection. The difference being that in the unprotected models, the thermal load was applied directly onto the steel for each load case, where the BM and FULL labels are used merely to distinguish the models by name, not to indicate protection coverage. The thermal load applied to the control models are as follows:

- BM-LC1-CONTROL model – thermal load applied to top flange of the steel beam
- FULL-LC1-CONTROL model – surface heat flux applied to the top flange of the beam, extending over the joint connecting beam top flange to column flange (to be compared to BM-LC1-CONTROL)
- FULL-LC2-CONTROL model – thermal load applied to all flanges of the steel beam and column
- FULL-LC3-CONTROL model – heat flux applied over the entire structure on all external steel surfaces

The supplementary boundary conditions (BC), to the fixed column base and symmetry assigned in the Y-axis, were zero temperatures that were applied at strategic surfaces in the model. This determined the heat development and nodal temperatures within the connection. These boundary conditions are displayed in Figures 3-14 and 3-15. In the case of FULL coverage, the zero temperature conditions were applied to the smaller exterior surfaces of each partitioned piece of the full fire protection. Figure 3-16

indicates one such boundary condition, which would be imitated at the opposite end of the beam, as well as the top and bottom of the column fire protection.

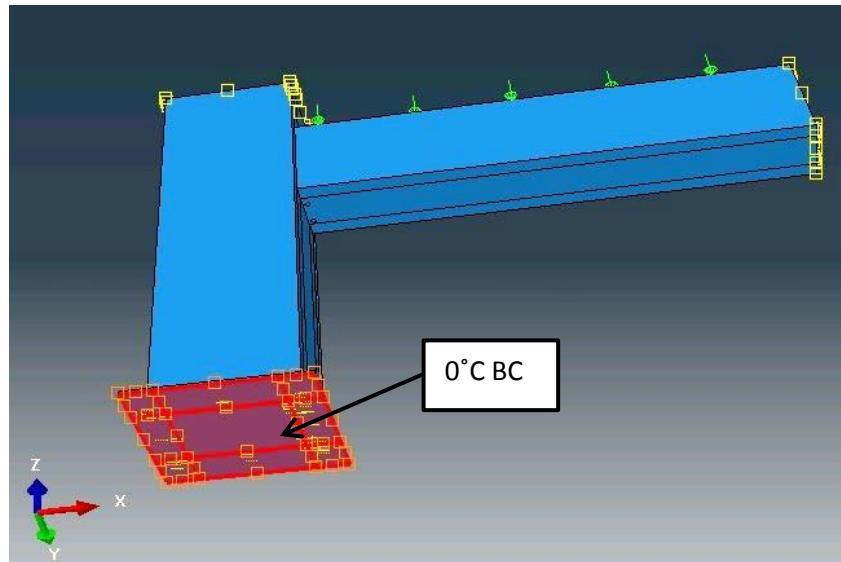


Figure 3-14: Zero temperature BC at the base of the column for all models

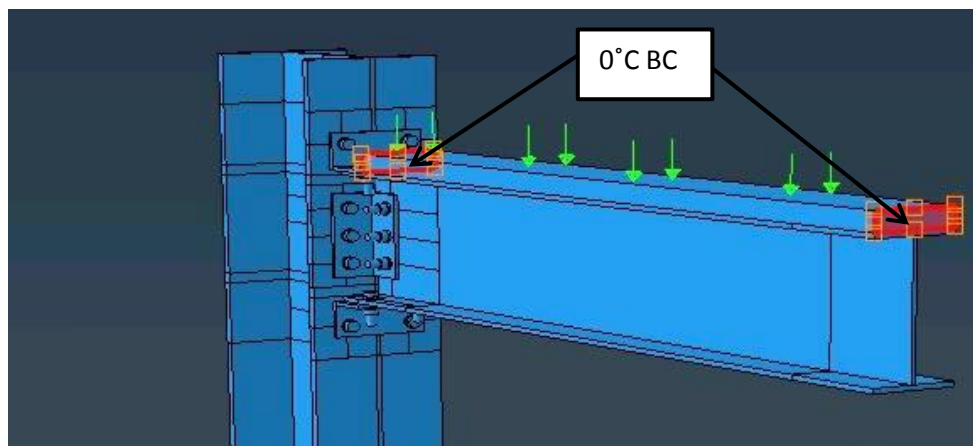
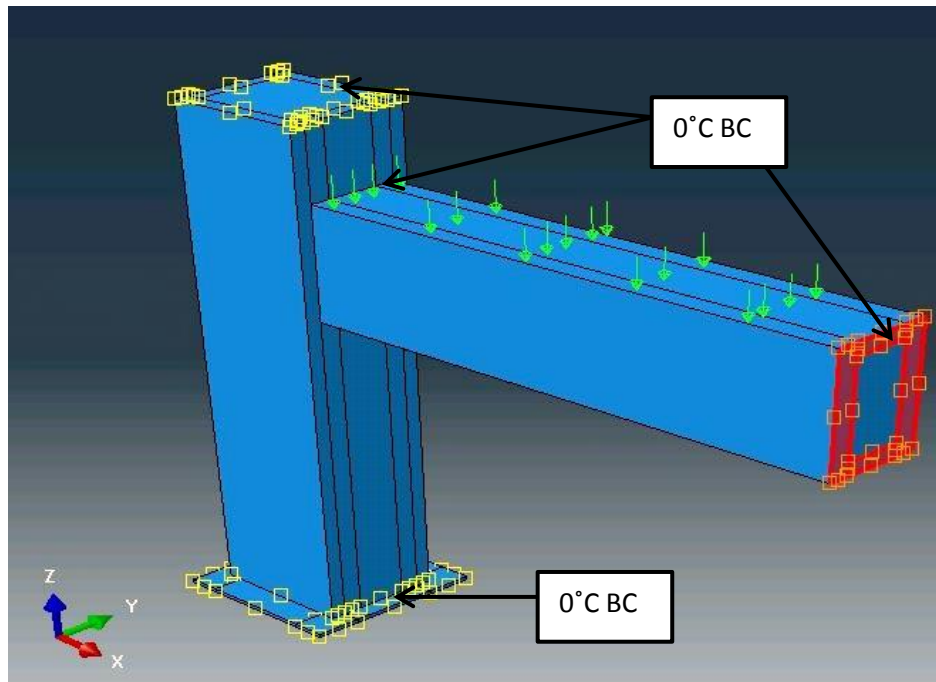


Figure 3-15: Zero temperature BC at ends of BM fire protection



**Figure 3-16: Zero temperature BC at partitioned surface edges of FULL fire protection**

### 3.6 Abaqus Coupled Transient Delamination Models

The process of creating and conducting transient analysis followed similar steps to the steady-state models. The transient models maintained the steps for Abaqus simulations from Figure 3-1, with alterations made for time-dependent analyses. The phenomenon of delamination is a pertinent one; a transient analysis was deemed the most accurate method of conducting a study into the delamination of protection materials from the steel connection. This is especially crucial in accounting for the complete loss of fire resistance offered by the fire protection due to damage or destruction sustained by the protection material during a fire. Thus in reality, after some time (in minutes), the steel connection would be exposed to direct fire and it was this time that was investigated in this study. In the framework of the coupled temperature-displacement analysis, both the temperature distribution due to fire and the structural behaviour are captured in the same simulation.

#### 3.6.1 Assigning Material-Specific Properties

The material properties for the entire steel connection, including steel column, beam, angles, washers and bolts, and the fire protection in the transient model was assigned similarly to those of the steady-state models. The most significant difference was that the fire protection material under investigation in the transient model, namely gypsum, was imported into the model and was assigned relevant mechanical and thermal

behaviours. Importing the fire protection into the transient model was required in order to conduct the coupled temperature-displacement analysis and the effects of delamination between the protection material and the steel under the coupled condition needed to be observed. An additional difference between the steady-state and transient models is the inclusion of a specific heat parameter for each material, in the transient analyses. Table 3-6 presents the material properties defined in the transient model, with much of the steel properties remaining the same as Table 3-3.

**Table 3-6: Material properties for transient thermomechanical model (Source: As shown)**

Material Properties	Steel Connection (EN1993-1-2, 2005)		Fire Protection (Hopkin et al, 2012)
	Steel parts	Steel bolts	Gypsum
Mass Density (kg/m <sup>3</sup> )	7850		648
Elasticity (Young's modulus and Poisson's ratio)	Table 3-4		Young's modulus = 1000000 kPa Poisson's ratio = 0.33
Plasticity (Yield stress and Plastic strain)	Appendix B: Table B-3	Appendix B: Table B-4	N/A
Thermal Conductivity (kW/m°C)	0.045		Appendix B: Table B-2
Thermal Expansion: Coefficient of thermal expansion	1.2 x 10 <sup>-5</sup>	1.3 x 10 <sup>-5</sup>	1.8 x 10 <sup>-7</sup>
Specific Heat (J/kgK)	Appendix B: Table B-5		

### 3.6.2 Model Specifics

The coupled temperature-displacement transient model was developed to analyse the effects of delamination, which could be clearly observed by focusing on a best-fit model. Characteristics of the transient model include the following:

- The fire-protected models used the optimal, simple and most common protection from the steady-state models, which was 30mm gypsum board covering the flange of the steel beam (TRANS-BM-LC1 with GYP30). Thus, the

finite element model depicted in Figure 3-8 (a) presented previously was adopted for this analysis.

- A time period of 5400 seconds, or 90 minutes, was considered in the analysis. This duration was selected based upon information gathered and examined in the literature review, subsection 2.4.3. From the fire resistance requirements in the United Kingdom (indicated in Chapter 2, Table 2-7), it was deduced that a 90 minute fire resistance period meets the requirements for structures less or equal to than 30 metres in height. Furthermore, for offices, shops, commercial assemblies and recreational structures greater than 30 metres in height, a fire resistance of 120 minutes is stipulated, but these also require sprinklers and *'the fire resistance of the floor may be 90 minutes only'* (Winestone, 2010). Additionally, from SANS 10400-T: Fire protection (2011), fire resistance for structural walls, for example, is provided for 30, 60, 90, 120 and 240 minutes. Thus, a 90 minute fire resistance period is a reasonable value as a time period; it is neither too conservative nor over-designed in the context of the South African code.
- Initially, a stabilising gravity load was applied to the overall structure at  $9.81\text{m/s}^2$ . Thereafter, the structural concentrated force was applied at the same position on the beam as previously indicated in Figure 3-4, with a magnitude defined by a force-time curve (described later in this chapter). This structural force was coupled with a thermal load, defined by the standard fire curve (presented in the literature review subsection 2.4.4.1 and later in this chapter) as an amplitude boundary condition.

Three transient models were created for one encompassing investigation into delamination effects and are described as follows:

- *Control Model* – A steel connection without fire protection was subjected to the coupled structural and thermal loads under transient conditions.
- *Initial Fire-Protected Model* – This model incorporated the BM-GYP30 protection under LC1, where the thermal loading was applied using a standard fire temperature-time curve (discussed in Chapter 2 subsection 2.4.4 and displayed in Figure 3-17) only to the surface of the GYP30 protection parallel to the top flange of the steel beam. An illustration of the surface of application of the thermal load is shown previously in Figure 3-10. Over time, the increasing opening between the steel beam and fire protection was observed.
- *Final Fire-Protected Model* – In this model, the same LC1 thermal action was applied at the top of the GYP30 protection; however, as openings occurred

between the fire protection and steel interface, the thermal load was applied directly onto the steel beam. This simulates the realistic spread of fire directly to the beam that would occur with the progressive delamination of the fire protection material.

### 3.6.3 Load Cases and Boundary Conditions

While the boundary conditions of the transient model remain the same as those described for the steady-state analysis, the application of the coupled structural-thermal loading was done with time curves. The thermal load was applied using the standard fire curve derived from EN1991-1-2 (2002), to account for the increase in temperature loading over time. The standard fire temperature-time curve for 90 minutes is displayed in Figure 3-17 and the data used to obtain the curve (from EN1991-1-2, 2002) is displayed in Appendix B: Table B-6. A description and derivation of the curve is presented in Chapter 2, subsection 2.4.4, with the equation (2-15) defined in the previous chapter and shown here:

- $\theta_g = 20 + 345 \log_{10} (8 t + 1)$  (2-15)

Where:

- $\theta_g$  = Gas temperature in the fire compartment [°C]
- $t$  = Time [min]
- $T_0$  = Ambient temperature [°C]

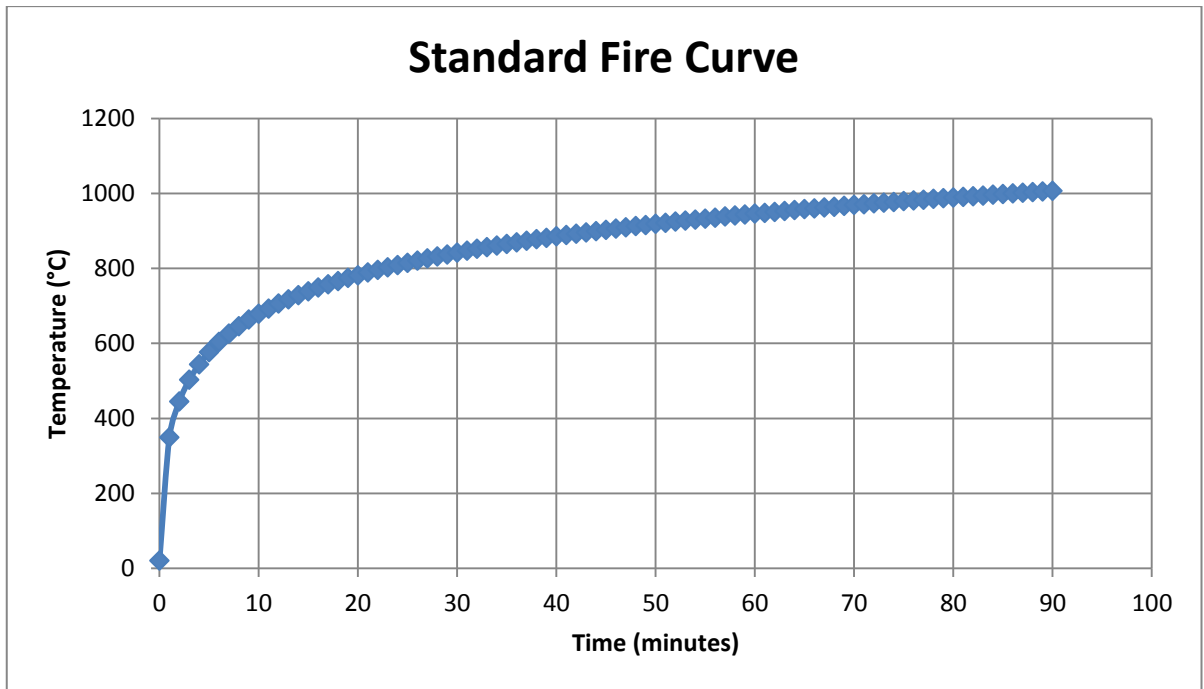


Figure 3-17: Standard Fire Curve for 90 minutes (Source: after EN1991-1-2, 2002)

The magnitude of the simultaneous structural point load applied to the beam was ramped linearly according to a force-time curve; the data of the force-time curve is presented in Appendix B as Table B-7. This force-time curve, also known as an amplitude force curve, was derived for the purposes of linking the coupled thermo-structural analysis. Since transient analysis considers the aforementioned standard fire curve and presents a temperature-time curve in real time, the simultaneously-applied structural force needed to be incorporated in real time as well. Thus, a force-time curve was developed to link the analyses over a 90 minute period. Previously, in steady-state analysis, un-coupled thermo-structural loading was investigated and Abaqus time steps were defined; therefore, a force-time curve was not required. In the steady-state analyses, the concentrated force was applied incrementally in accordance with Abaqus time steps (not real time).

The same boundary conditions were applied to the coupled transient models, regarding the fixed column base and symmetry assigned in the Y-axis in the steady-state models. In addition to this, the GYP30 protection on the top beam flange was fixed at one end since convergence issues arose when the fire protection was not fixed, due to the deformation and thermal expansion of the protection material.

### 3.7 Limitations

This study is limited to the investigation of one type of assembly of a steel connection. While this substructure is relevant and versatile in its use in multi-storey buildings and frames, other connection mechanisms could be examined to provide further comparisons and deductions on the behaviour of steel structures under fire. Furthermore, the study only focuses on a steel connection under elevated temperatures, without considering its effects on the overall stability of the structure. Composite structures are also not considered.

One of the constraints in the numerical modelling of the connection is related to the sequential analysis of the steady-state thermal and thermomechanical models. In conducting a thermal analysis and thereafter importing the results into a corresponding thermomechanical analysis, the concurrent appearance of thermal and mechanical phenomena (for example delamination of the fire protection material, deformation of the connection and temperature increase) cannot simultaneously be depicted due to the sequential nature of the un-coupled simulation. This was improved upon in conducting the coupled transient analysis, although for only one type of fire protection and one assigned thickness (GYP30). Moreover, the loading combinations and magnitudes selected only provide a limited insight into the particular scenario-based effects of fire on the steel connection investigated in the study. While the static, concentrated load represents a relevant potential scenario, the equally important effects of dynamic loads on the steel beam are not examined.

The research investigates the time-dependent effects of delamination under fire, while the steady-state models are restricted with no evolution of the fire event with time. The established conductance of the materials in the models also may not signify the correct conditions of reality, since fire and its conduction through materials occurs with various mechanisms, such as convection and radiation, which are beyond the scope of this study.

While the results from the initial structural model of this study are verified against an existing FEA model featured in Abdalla et al (2015), as mentioned previously in the chapter, there exists scope for further verification of the thermal and thermomechanical models analysed in this dissertation. The ability to authenticate these models is limited in this research, due to the lack of existing experimental data on this topic.

### 3.8 Summary

In this chapter, the methodology followed in the research process was discussed. The steel substructure that forms the crux of the investigation was adopted from a similar study conducted by Abdalla et al (2015). The selection of Abaqus FEA software as the method by which to conduct the analyses was detailed and the steps of the Abaqus simulation procedure were defined. The use of numerical models in investigating the research topic was verified by studies done by Daryan and Yahyai (2009) and Abdalla et al (2015). The types of analyses performed using Abaqus were described as steady-state and transient analyses. The process of creating and executing the Abaqus steady-state and transient analyses was elaborated on and each of the developed models was described. Steady-state simulations were conducted on developed mechanical, thermal and uncoupled thermomechanical models, where the mechanical model was established as verification against existing literature. The method of generating coupled thermo-structural transient analyses on thermomechanical models in real time, towards investigating delamination, was outlined. The limitations experienced in conducting the study and using the Abaqus FEA software, was evaluated and expressed. This chapter has provided the vital premise for presenting the results obtained and discussions of the outcomes in the following Chapter 4.

# Chapter 4

---

## 4 Steady-State Analysis Results and Discussion

### 4.1 Introduction

This chapter will provide the results obtained for the steady-state analyses conducted in accordance with the aims, objectives and methodologies outlined in previous chapters. The results presented are derived from the mechanical, thermal and thermomechanical numerical analyses performed with Abaqus. Maximum temperatures and temperature distributions developed in the steel connection from the thermal analyses are illustrated and discussed. Force-displacement diagrams were produced to quantify the results of the thermomechanical analyses and comparisons between the various models are drawn. Yielding of the connection at elevated temperatures is also depicted and the fire resistance offered by each material is quantified. The effects of fire protection and associated factors are assessed and compared.

### 4.2 Chapter 4 List of Abbreviations

#### 4.2.1 Steady-state Models and Thermal Load Cases

BM-LC1-CONTROL	:	Thermal load applied to top flange of steel beam - no fire protection (control model).
BM-LC1-CONC50	:	Model with beam fire protection - heat flux applied to fire protection top flange - 50mm concrete protection.
BM-LC1-GYP50	:	Model with beam fire protection - heat flux applied to fire protection top flange - 50mm gypsum protection.
BM-LC1-GYP30	:	Model with beam fire protection - heat flux applied to fire protection top flange - 30mm gypsum protection.
FULL-LC1-CONTROL	:	Thermal load applied to top flange of steel beam, extending over the steel joint - no fire protection (control model).
FULL-LC1-CONC50	:	Model with fire protection on the overall steel connection - heat flux applied to fire protection top flange and joint - 50mm concrete protection.

FULL-LC1-GYP50	:	Model with fire protection on the overall steel connection - heat flux applied to fire protection top flange and joint - 50mm gypsum protection.
FULL-LC1-GYP30	:	Model with fire protection on the overall steel connection - heat flux applied to fire protection top flange and joint - 30mm gypsum protection.
FULL-LC2-CONTROL	:	Thermal load applied to all flanges of the steel beam and column - no fire protection (control model).
FULL-LC2-CONC50	:	Model with fire protection on the overall steel connection - heat flux applied to beam and column fire protection flanges - 50mm concrete protection.
FULL-LC2-GYP50	:	Model with fire protection on the overall steel connection - heat flux applied to beam and column fire protection flanges - 50mm gypsum protection.
FULL-LC2-GYP30	:	Model with fire protection on the overall steel connection - heat flux applied to beam and column fire protection flanges - 30mm gypsum protection.
FULL-LC3-CONTROL	:	Thermal load applied over the entire structure on all external steel surfaces - no fire protection (control model).
FULL-LC3-CONC50	:	Model with fire protection on the overall steel connection - heat flux applied to all external fire protection surfaces - 50mm concrete protection.
FULL-LC3-GYP50	:	Model with fire protection on the overall steel connection - heat flux applied to all external fire protection surfaces - 50mm gypsum protection.
FULL-LC3-GYP30	:	Model with fire protection on the overall steel connection - heat flux applied to all external fire protection surfaces - 30mm gypsum protection.

### 4.3 Mechanical Model

Initially, a purely structural model was solved to determine the vertical displacements at the point of application of the concentrated load (shown previously in Figure 3-4, at 1.58 metres along the beam). These vertical displacements were caused by the

vertical, static, incrementally-applied 200kN point load on the steel beam. The explanation for selecting this magnitude of force was discussed in Chapter 3 subsection 3.4. The result of this analysis is illustrated in Figure 4-1 by the force-displacement diagram derived from the output data in Abaqus. These results were verified against the outcomes of the study conducted by Abdalla et al (2015). The output data obtained from Abaqus that was used to develop the force-displacement graph is presented in Appendix C: Table C-1. This serves as a sample of the Excel calculations performed to create the force-displacement diagrams, in the dissertation.

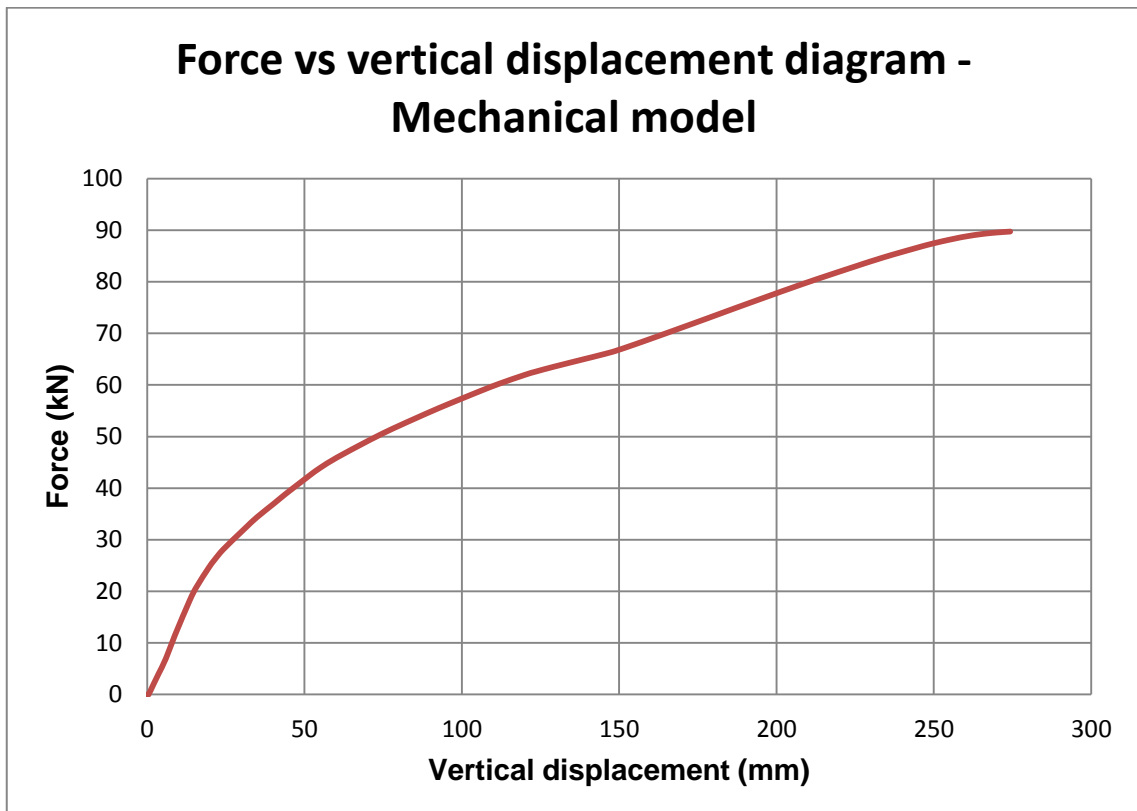


**Figure 4-1: Force-displacement diagram for the mechanical model**

The result displayed by Figure 4-1 clearly indicates a non-linear curve, which is expected since a full von Mises plasticity model was used to depict damage of the structural steel connection. Failure of the steel connection is depicted as the graph tends towards the horizontal at a force of approximately 90kN. This force is less than half of the applied concentrated load, which is expected since the magnitude of the 200kN force was primarily selected to allow the behaviour of the connection to develop from linear to non-linear. The maximum force of 90kN is verified against the FEA study conducted by Abdalla et al (2015), where an ultimate force of approximately 100kN was observed for the same steel connection and loading. Since the FEA model of

Abdalla et al (2015) was verified by experimental research conducted by Badarneh (2004), the mechanical model of this dissertation, by extension, describes reality to a reasonable degree.

At a force of 90kN, the corresponding vertical displacement of the beam, at the particular node at which the concentrated force is applied, reaches a maximum of 274mm. This deflection is far exceeds the allowable deflection; thus, failure of the steel connection essentially occurs at a lower load. Figure 4-2 illustrates the comparison between the original shape at 0kN (grey) and the final deformed shape at 90kN (green) of the steel beam in the connection. The criteria for determining failure of steel connection in the FEA mechanical and thermomechanical models, is denoted by separation of the steel parts, leading to openings at the connected interfaces, as the vertical point load was increased. Yielding of the connection occurred together with an increase in vertical displacement of the beam, as the point load was increased in the model. This yielding and separation experienced by the steel parts in the FEA at failure is shown in Figures 4-3 (a); (b) and 4-4 (a); (b). From a numerical perspective, when the force-displacement diagrams tend towards the horizontal, numerical instabilities arise due to negative eigenvalues of the tangent stiffness matrix. Then, analysis is terminated.

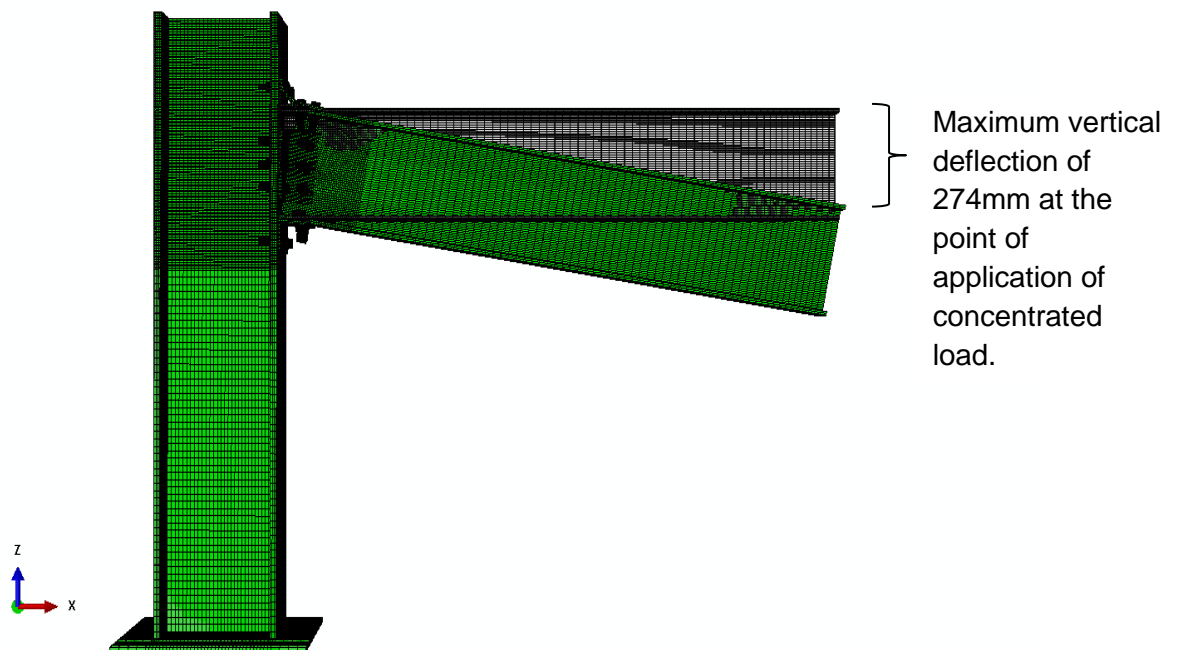


**Figure 4-2: Superimposed original shape (grey) and final deformed (green) shape of steel beam under structural loading**

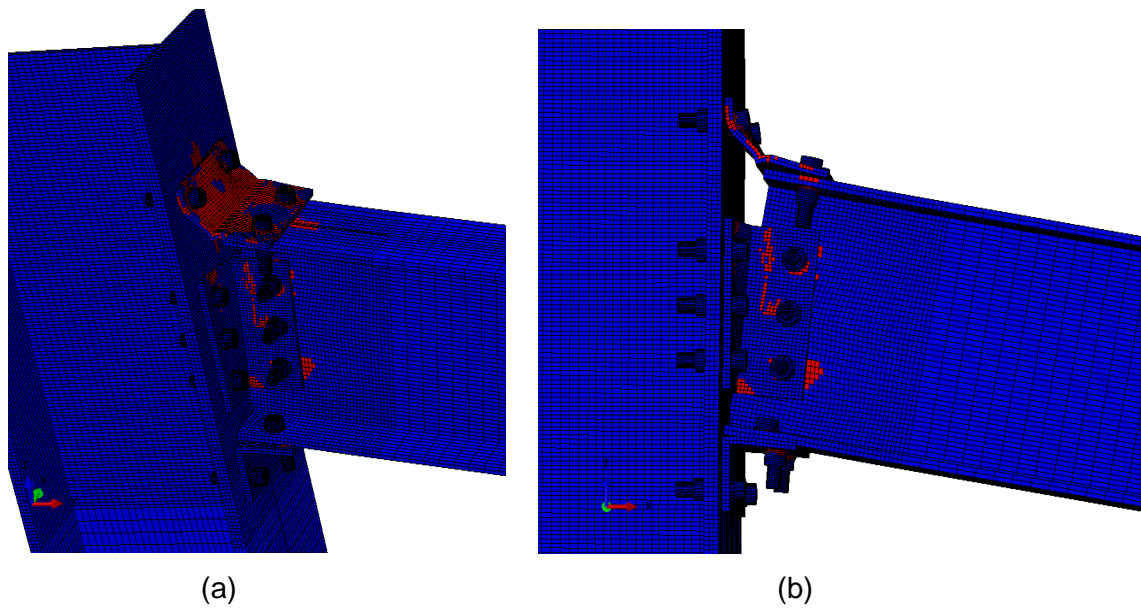


**Figure 4-3: Steel connection indicating: (a) yielding at failure (in red); (b) openings at failure**

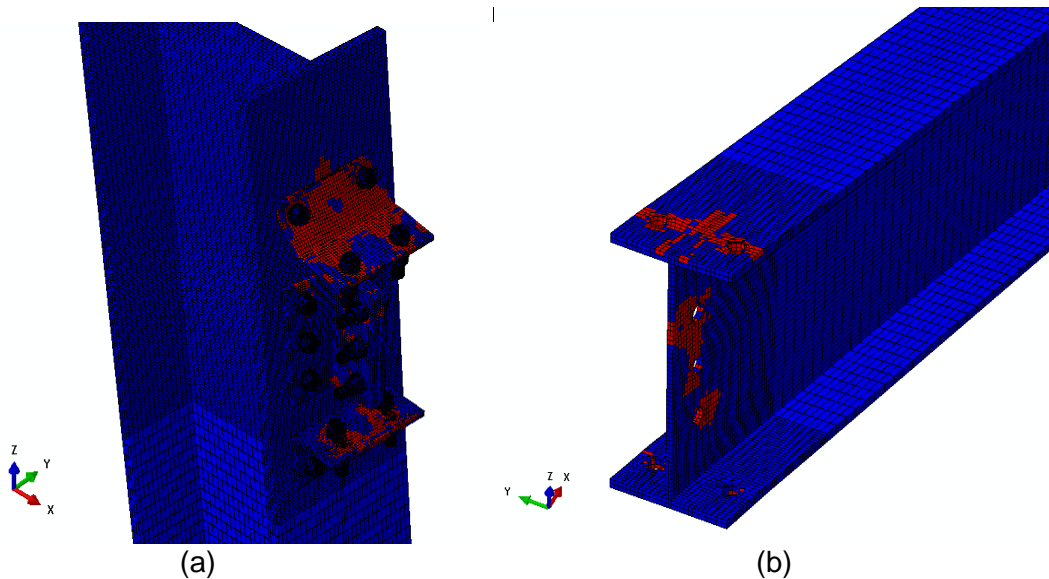


**Figure 4-4: Yielding (in red) of steel connection at: (a) column and angles; (b) beam**

Yielding of the steel parts (indicated in red in the figures) occurred with an increase in applied loading in the FEA and caused openings to occur in the interfaces between the parts, displayed in Figures 4-3 and 4-4. The top angle experienced the greatest deformation and largest separation from other parts, seen in Figure 4-3 (a) and (b). This result is expected and is verified against laboratory experimental research done by Badarneh (2004). The maximum opening value observed at the top angle in the FEA was 42.23mm. The remaining angles, that are the two web angles and seat angle, incurred smaller openings and suffered less yielding than the top angle, shown in Figure 4-4 (a) and (b). This behaviour presents the importance of joints, particularly the

top angle, in determining the overall performance of a steel connection. Since proper unilateral contact-friction interfaces were accounted for between the angles and attached steel parts in the FEA, the behaviour observed in these results is accurately indicative of realistic, non-linear effects on a steel connection.

#### **4.4 Thermal Models – Qualitative Results**

The results of the thermal analyses describe the response of the steel connection to an applied thermal load, with and without fire protection, for three load cases. These results were imported into the corresponding thermomechanical analyses as a predefined temperature field in Abaqus. A comprehensive description and layout for each steady-state thermal and thermomechanical models is presented in Table 4-1.

Table 4-1: Compilation of steady-state thermal and thermomechanical models

FIRE PROTECTION COVERAGE	THERMAL LOAD CASE	CONTROL / PROTECTION	FIRE PROTECTION MATERIAL	PROTECTION THICKNESS (mm)
BM (Fire protection on the beam)	LC1 <i>2kW/m<sup>2</sup> Surface heat flux applied to beam top flange</i>	Control (No fire protection)	Not Applicable (N/A)	
		BM-Fire Protection	CONCRETE	50 (CONC50)
			GYPSUM	50 (GYP50)
		30 (GYP30)		
FULL (Fire protection on the overall connection)	LC1 <i>2kW/m<sup>2</sup> Surface heat flux applied to beam top flange</i>	Control (No fire protection)	(N/A)	
		FULL-Fire Protection	CONCRETE	50 (CONC50)
			GYPSUM	50 (GYP50)
		30 (GYP30)		
FULL (Fire protection on the overall connection)	LC2 <i>2kW/m<sup>2</sup> Surface heat flux applied to beam and column flanges</i>	Control (No fire protection)	(N/A)	
		FULL-Fire Protection	CONCRETE	50 (CONC50)
			GYPSUM	50 (GYP50)
		30 (GYP30)		
FULL (Fire protection on the overall connection)	LC3 <i>2kW/m<sup>2</sup> Surface heat flux applied to all external surfaces</i>	Control (No fire protection)	(N/A)	
		FULL-Fire Protection	CONCRETE	50 (CONC50)
			GYPSUM	50 (GYP50)
		30 (GYP30)		

The standard thermal load applied to all models was  $2\text{kW/m}^2$ , suitably chosen as comparison to current literature adopting the same loading, such as an investigation performed by Tsapara et al. (2013). The load cases described in the second column are applied directly onto the steel connection for the control models and applied to the parallel surface of protection in the fire-protected models. While the first column of Table 4-1 describes the extent of coverage of fire protection, the third column describes control models that did not incorporate any fire protection materials in the analysis with fire applied directly to the steel, in accordance with the load cases. This is compiled as such for ease of grouping of comparable results.

In this study, the effect of fire protection on the structural behaviour of the steel connection under sequential thermal and structural loading is investigated; thus, the results obtained in the purely thermal analyses are quantitatively presented. This dissertation presents the thermal analyses results in terms of temperature distribution diagrams that indicate N11 output (Nodal Temperatures), which are actual temperatures in Celsius degrees obtained from the Abaqus FEA outputs. Although the quantitative NT11 (Nodal Temperatures in  $^{\circ}\text{C}$ ) varied according to the applied thermal load case (LC1, LC2 and LC3), each of the fire-protected models portrayed analogous temperature developments within each load case. Figures 4-5, 4-6, 4-7 and 4-8 illustrate the representative temperature distribution for all fire-protected models, namely CONC50, GYP50 and GYP30, for each applied loading condition (LC1, LC2, LC3).

- **Fire-protected Models: BM-LC1 (heat load applied to protection top flange)**

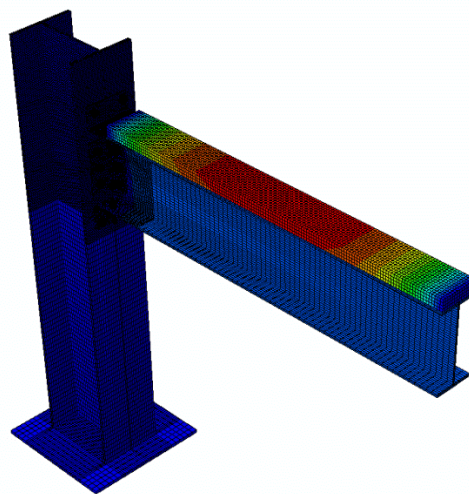


**Figure 4-5: Representative, general temperature distribution for BM-LC1 fire-protected models**

- Fire-protected Models: FULL-LC1 (heat load applied to protection top flange)

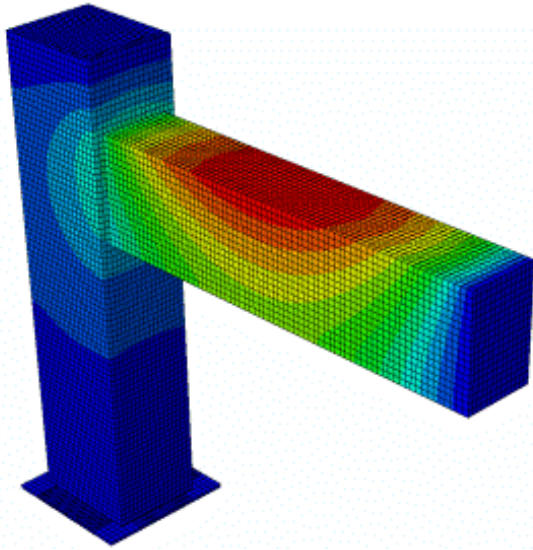


Figure 4-6: Representative, general temperature distribution for FULL-LC1 fire-protected models

- Fire-protected Models: FULL-LC2 (heat load applied to protection parallel to beam and column flanges)

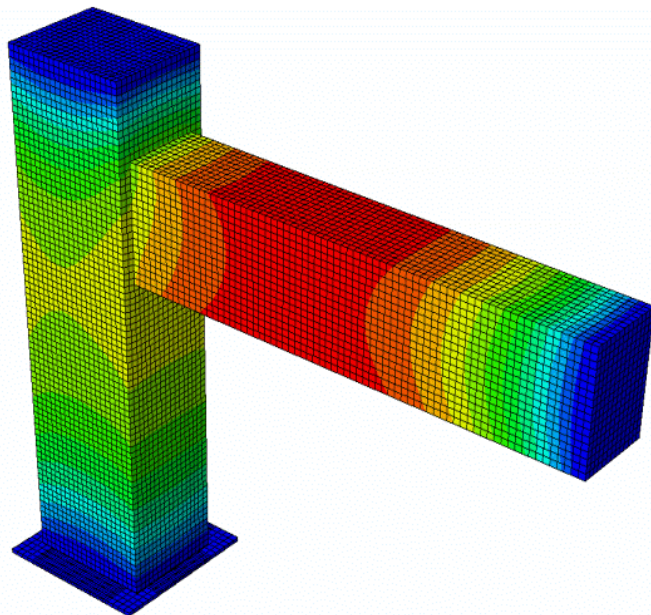


Figure 4-7: Representative, general temperature distribution for FULL-LC2 fire-protected models

- **Fire-protected Models: FULL-LC3 (heat load applied to all external protection surfaces)**

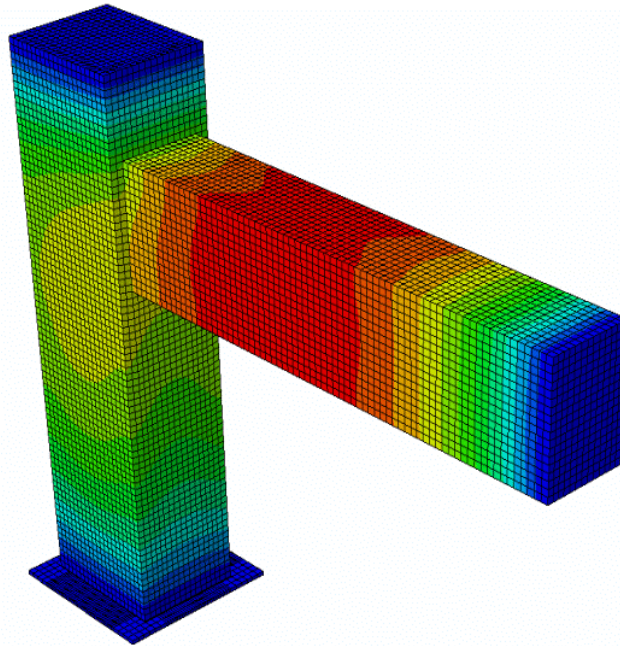


Figure 4-8: Representative, general temperature distribution for FULL-LC3 fire-protected models

#### 4.5 Uncoupled Thermomechanical Models – Quantitative Results

The results of the thermal analyses were imported into the corresponding thermomechanical models as a predefined field. A static point load of 200kN was applied to the beam in all models, as previously discussed. This refers to the uncoupled thermo-structural analyses performed. The sequence and layout of the thermomechanical results follows similarly to that presented in Table 4-1. However, the essential difference is the omission of imported fire protection in the fire-protected models: the CONC50, GYP50 and GYP30 names remain purely as labels to distinguish the various models. As mentioned previously in Chapter 3, the fire protection materials should not influence the structural stability of the connection; therefore, the thermal effects of the materials are only integrated from the imported thermal predefined field. The results of the uncoupled thermomechanical analyses are presented by quantitative NT11 outputs (Nodal Temperatures in °C) developed in the respective models under the various thermal loading conditions. Two maximum temperature outputs were obtained: first, the ultimate steel temperatures at failure of each of the models (nodal temperatures as depicted in the relevant figures), and secondly, the maximum temperature recorded in the steel for approximately the same

applied structural load (a load which varies per LC1, LC2 and LC3). Thus, for the latter temperatures, the maximum temperature of the control model at failure in each load case (BM-LC1, FULL-LC1, FULL-LC2 and FULL-LC3) was used as the criterion to compare the temperatures of the subsequent fire-protected models, developed at approximately the same applied load at which the control model tended to fail.

The main results obtained from the thermomechanical models are presented in comparative force-displacement diagrams to evaluate and compare the effects of thermal loading on the structural system. This is assessed from the non-linear analysis using the global equation (2-16) given in Chapter 2:  $\{F\} = [K]\{d\}$ . Additionally, the results are derived from models with the adaptation of von Mises plasticity: plastic stress-strains shown in Figure 2-8 and the tangent stiffness matrix, in the framework of the Newton-Raphson incremental-iterative procedure, at elevated temperatures, were used to build the global stiffness matrix  $[K]$ . The deformed shapes of the steel connection under structural loading is typically represented by Figure 4-2. The vertical displacements plotted in the force-displacement diagrams are measured at the point of application of the concentrated vertical load, that is: vertical displacements are measured at the node in the FEA model at which the 200kN force was applied (at 1.58 metres along the beam, displayed in Figure 3-4 in the previous chapter).

Failure of the steel connection was determined at the point at which the linear relationship of the force-displacement graphs ended and the linear curves started becoming horizontal. This occurs due to both the structural applied load and induced thermal loading on the system. The maximum temperatures at failure in each of the models (indicated by the NT11 temperature distribution figures) were obtained from Abaqus, where failure of the steel connection was determined at the instance of non-zero output for plastic strains (PEEQ) in the steel beam (thus, failure of the steel beam).

#### 4.5.1 Results for BM Coverage – Load Case 1

The uncoupled thermomechanical analysis on an unprotected and BM-protected steel connection was obtained for LC1. In this scenario, the imported thermal loading as a predefined field is characterised by:

- Thermal load of  $2\text{kW/m}^2$  applied to steel beam or fire protection top flange.

The resulting maximum steel temperatures (Nodal Temperatures, NT11) and distributions in the models with and without fire protection at failure, for the uncoupled thermomechanical BM-LC1 models, are displayed in Figures 4-9, 4-10, 4-11 and 4-12. Thereafter, the results of these analyses performed with and without fire protection are presented by the corresponding force-displacement curves in Figure 4-13.

- **Control Model – No Fire Protection**

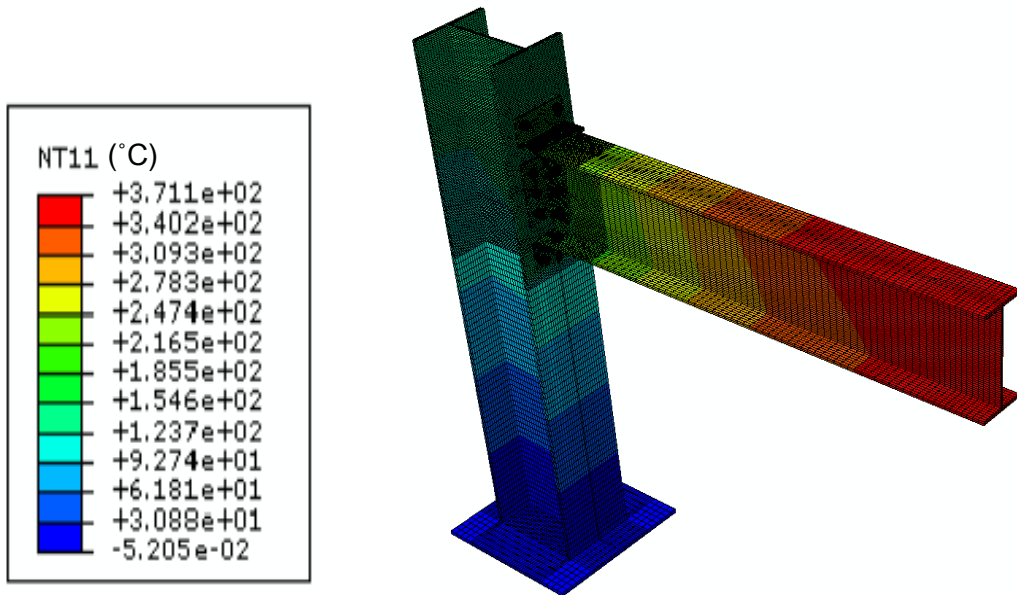


Figure 4-9: Temperature distribution (°C) in the BM-LC1-CONTROL model at failure

- **Concrete 50mm Fire Protection**

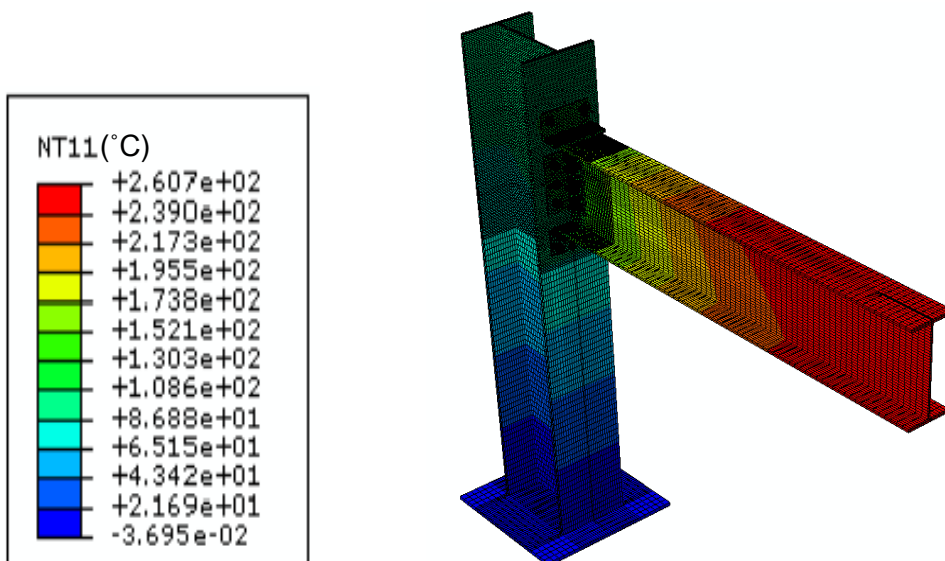


Figure 4-10: Temperature distribution (°C) in the BM-LC1-CONC50 model at failure

- Gypsum 50mm Fire Protection

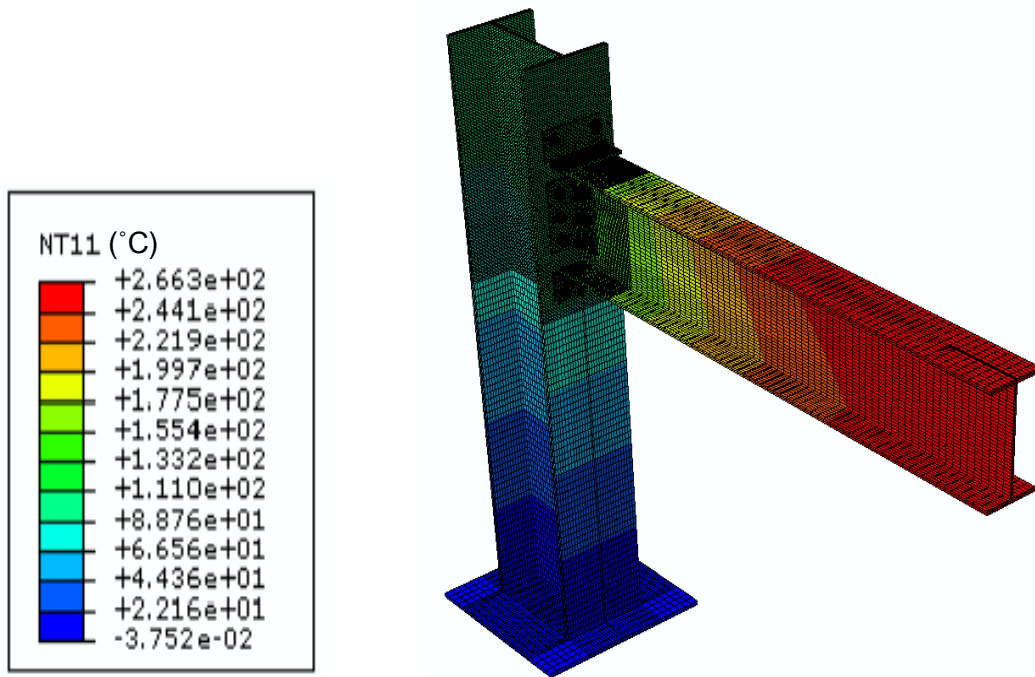


Figure 4-11: Temperature distribution (°C) in the BM-LC1-GYP50 model at failure

- Gypsum 30mm Fire Protection

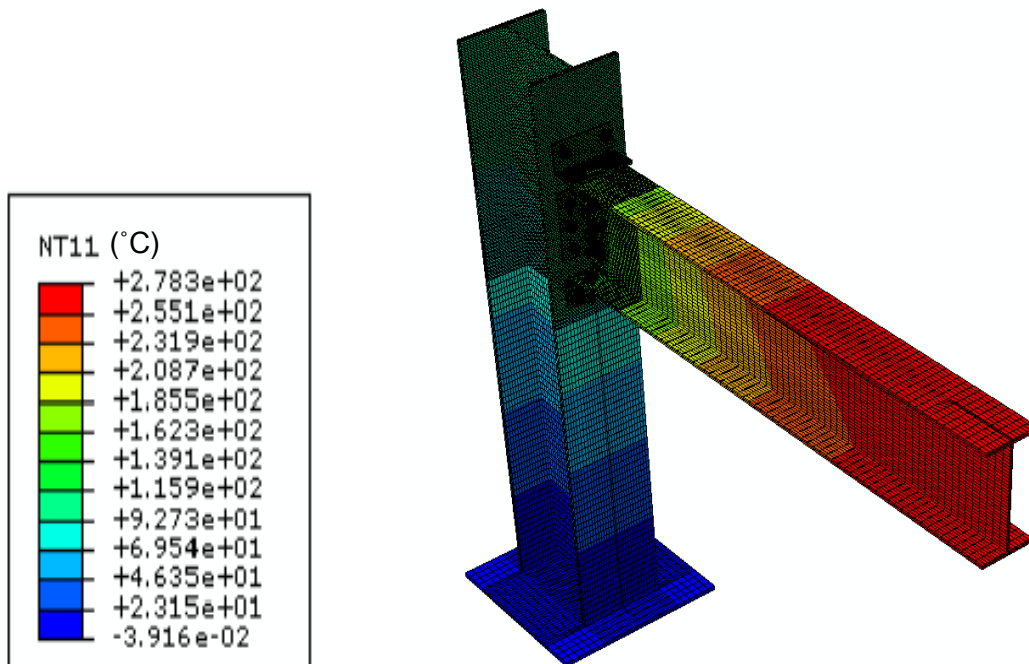


Figure 4-12: Temperature distribution (°C) in the BM-LC1-GYP30 model at failure

## Thermomechanical Models for BM-LC1

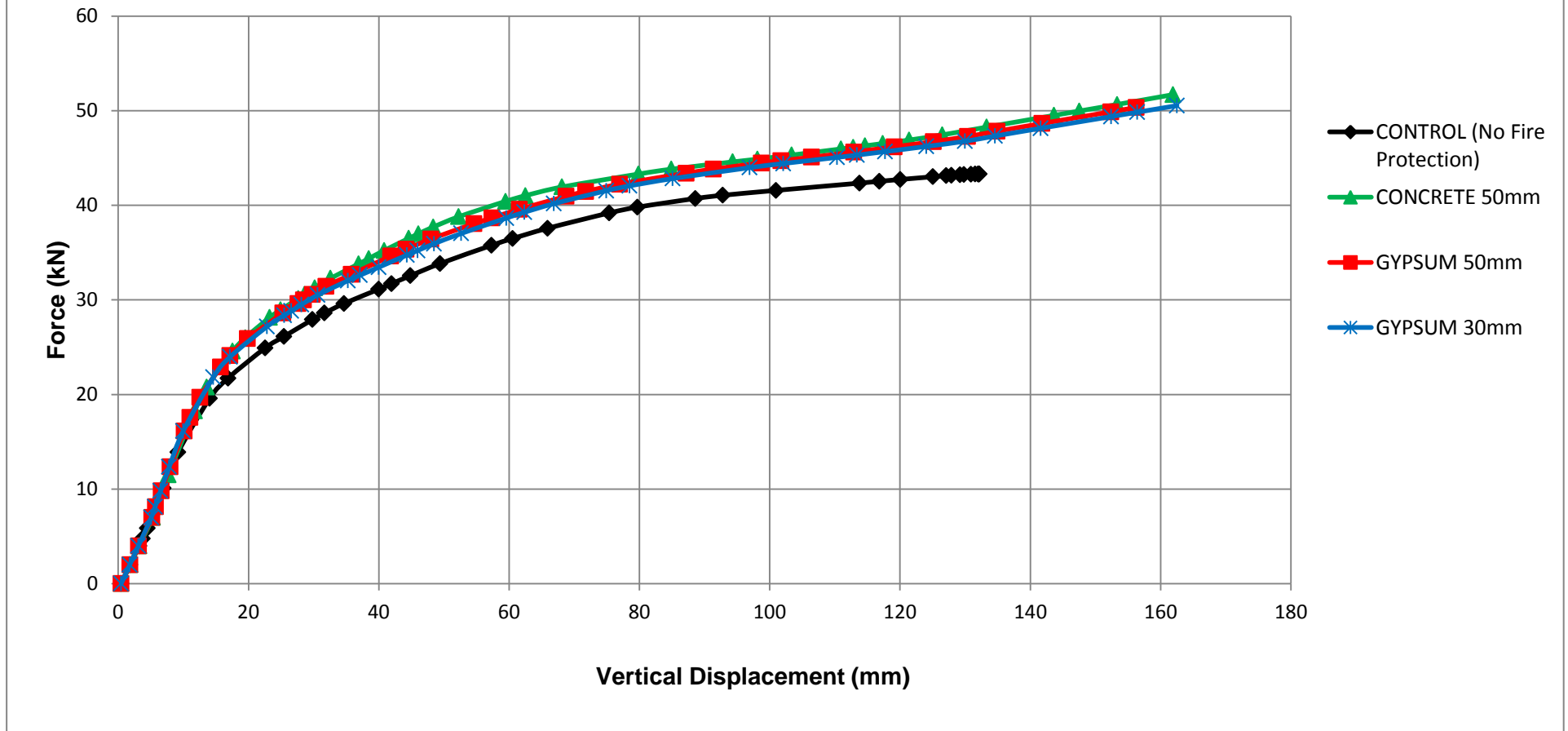


Figure 4-13: Force-displacement curves for steady-state Thermomechanical BM-LC1 models

The force-displacement curves for each model displayed in Figure 4-13 indicate the clear non-linear behaviour of the steel connection. The curves indicate a gradual increase in force with corresponding vertical displacements at the point of application of the point load on the steel beam. The models with fire protection perform distinctly better than the model without protection, under uncoupled thermomechanical loading. This is attributed to the fact that the curves obtained from all the models with protection are higher than the curve of the protected model, shown in Figure 4-13, indicating a greater stiffness and ultimate strength for the protected structures. A summary of the results depicted by Figures 4-9 to 4-13 are provided in Table 4-2.

**Table 4-2: Summarised comparison of fire protection materials for BM-LC1 models**

<b>A</b>	<b>B</b>	<b>C</b>	<b>D</b>
<b>Unprotected/ Fire-protected</b>	<b>Thickness (mm)</b>	<b>Maximum Temperature in Steel at Failure* (°C)</b>	<b>Approximate Ultimate Force** (kN)</b>
Unprotected (Control)	N/A	371	21.72
CONCRETE	50	261	26.00
GYPSUM	50	266	22.90
GYPSUM	30	278	21.84

\*Maximum temperature in steel at failure of the steel beam, shown in Figures 4-9, 4-10, 4-11 and 4-12, for Column D force.

\*\*Column D values were obtained from Abaqus output and verified against Figure 4-13.

As displayed in Figure 4-9 and Table 4-2, the maximum temperature experienced in the unprotected steel connection at failure was 371°C, in the beam. This is relatively high, as expected, since the high thermal conductivity property of steel causes intense temperatures to develop in the steel when exposed to direct fire. The maximum temperatures in column C indicate that CONC50 achieved the lowest maximum steel temperature at failure of the steel beam, when compared to GYP50 and GYP30. The 50mm concrete protection model developed an ultimate steel temperature of 261°C, which is slightly less than both the 50mm and 30mm gypsum models. Furthermore, 50mm gypsum performs marginally better than 30mm gypsum protection, since heat recorded at failure in the GYP50 model is 12°C less than the GYP30 model. This small variation in temperature can be attributed to the 20mm decrease in protection thickness

in the GYP30 model, thereby providing a thinner barrier between the steel and applied thermal load, allowing greater heat transfer thereto.

The improved behaviour of the fire-protected models, compared to the unprotected model, is attributed to the fire protection materials resisting the applied thermal load. The correlation between the thermal results in Table 4-2 and force-displacement curves in Figure 4-13 for each protection material can be observed. The fire protection materials that sustain the lowest maximum temperatures in the steel connection result in stronger systems and thus, the steel substructure exhibits improved behaviour in the force-displacement curves and an increase in the ultimate force of the connection (Column D in Table 4-2). This relationship is governed by the plastic stresses and strains that occur in the steel substructure as a result of elevated temperatures, where higher temperatures cause greater damage. This can be seen in the CONC50 model, which develops the lowest maximum temperature of 261°C and requires the greatest force (approximately 26kN) to induce failure of the system.

In Figure 4-13, for an ultimate force of 22kN in the control mode, the corresponding maximum vertical displacement is approximately 16mm, at the point on the beam at which the concentrated force is applied. In comparison, CONC50, GYP50 and GYP30 models fail at forces of approximately 22-26kN, with corresponding maximum vertical displacements of about 20mm. This demonstrates the increased strength of the connection in its ability to support a higher load when fire protection is applied. The thermal load prevents the steel connection from supporting the full 200kN applied load.

Another significant result of the thermomechanical analyses on the BM-LC1 models is the resulting damage to the steel connection at elevated temperatures, due to yielding of the members under the applied loads. This result was determined from the Equivalent Plastic Strain output (PEEQ) in Abaqus. The PEEQ output is shown in Figure 4-14 and 4-15 for the unprotected and GYP30-protected thermomechanical model, selected as a representative protection material. The majority of the yielding that occurs in the steel connection is focused at the point of application of the structural 200kN point load on the beam and at the joint between the beam-column. As previously mentioned, failure of the connection is indicated by non-zero values for the plastic strain distribution.

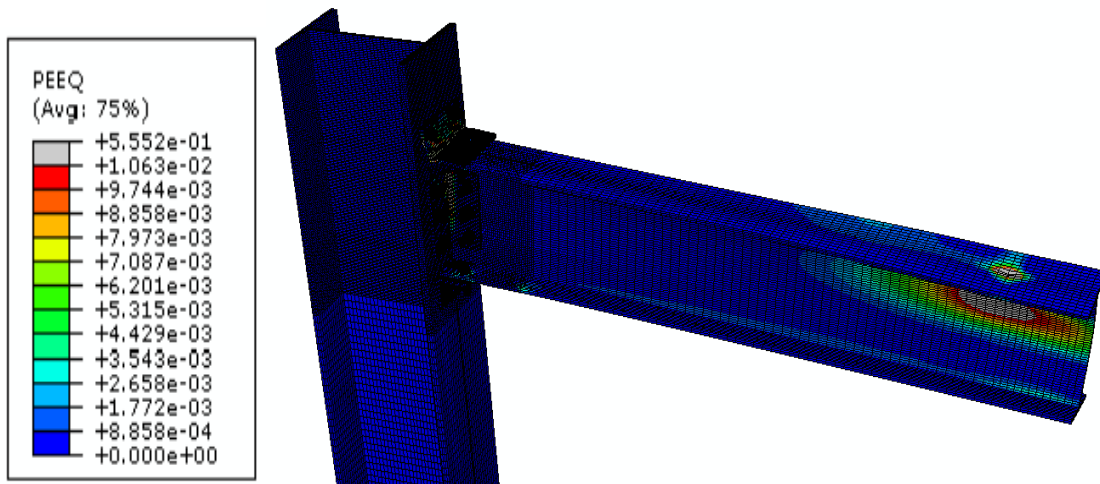


Figure 4-14: Equivalent Plastic Strains for BM-LC1 unprotected model

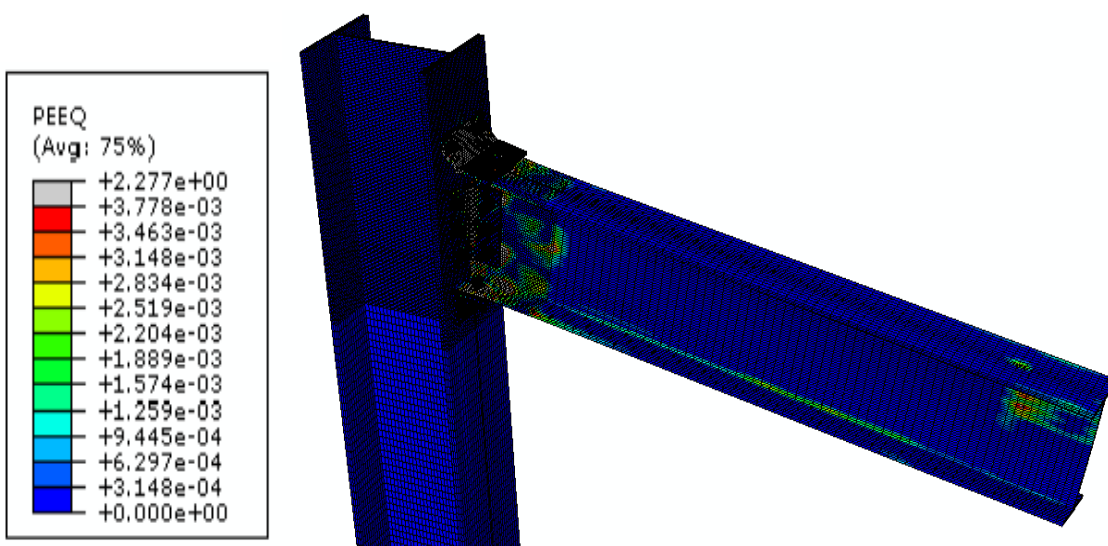


Figure 4-15: Equivalent Plastic Strains for BM-LC1-GYP30 fire-protected model

#### 4.5.2 Results for FULL Coverage – Load Case 1

Uncoupled thermomechanical analyses on models with and without fire protection were conducted for FULL coverage of the steel connection under LC1. In this scenario, the imported thermal loading as a predefined field is characterised by:

- Thermal load of  $2\text{kW/m}^2$  applied to beam or top flange of the fire protection.

The subsequent ultimate steel temperatures incurred in the models with or without fire protection, at failure, for the uncoupled thermomechanical FULL-LC1 analyses are displayed in Figures 4-16, 4-17, 4-18 and 4-19. The derived, corresponding force-displacement curves for these analyses and models are then presented in Figure 4-20.

- Control Model – No Fire Protection

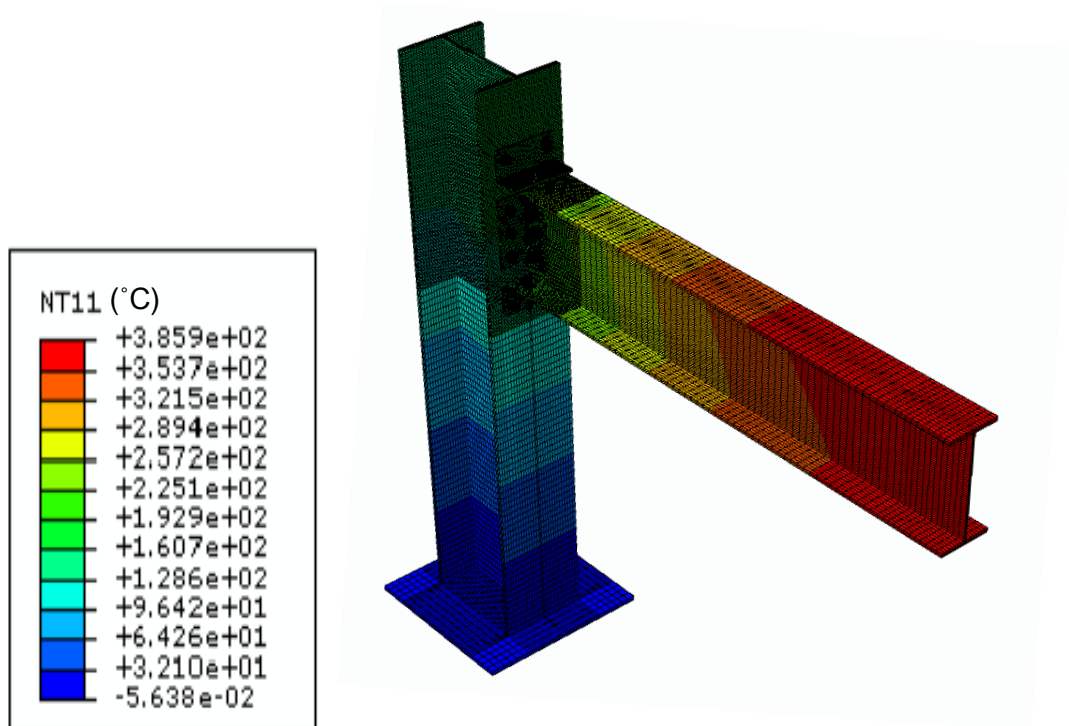


Figure 4-16: Temperature distribution (°C) in the FULL-LC1-CONTROL model at failure

- Concrete 50mm Fire Protection

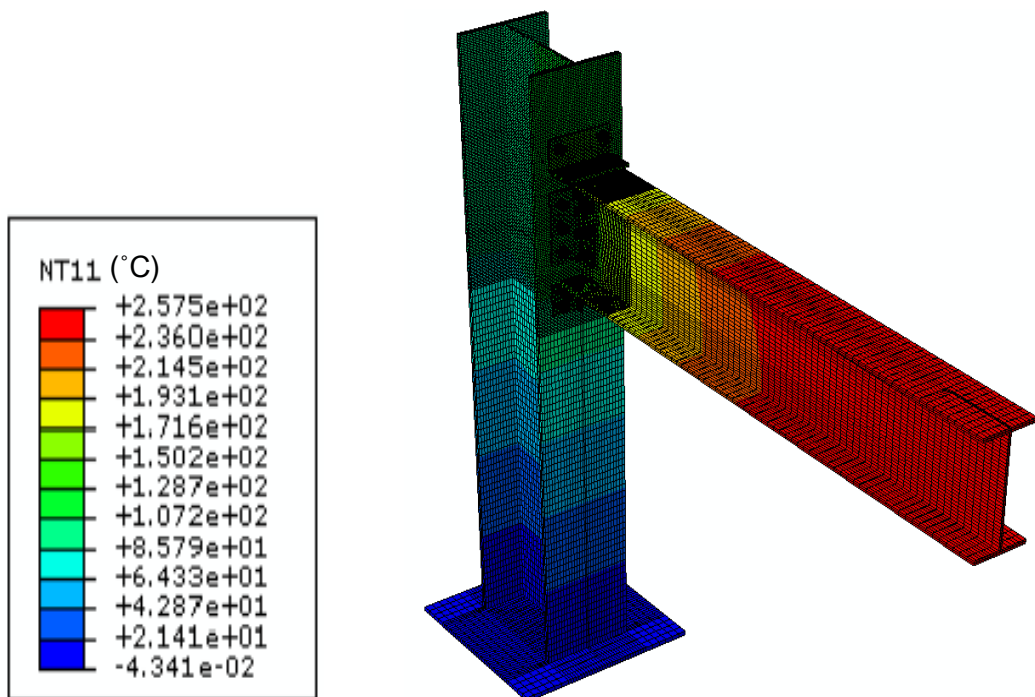


Figure 4-17: Temperature distribution (°C) in the FULL-LC1-CONC50 model at failure

- Gypsum 50mm Fire Protection

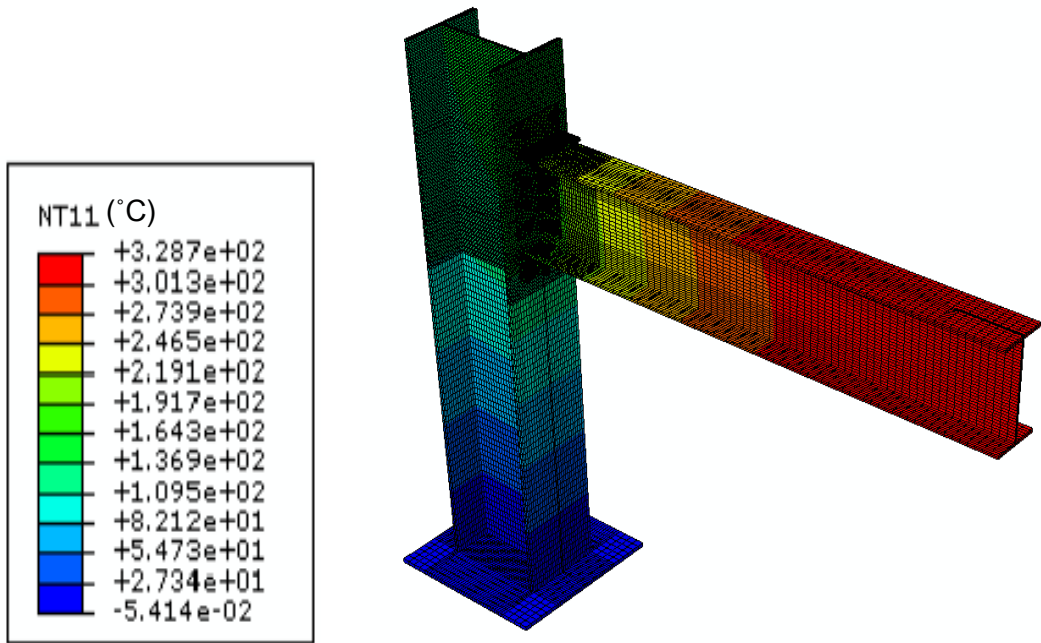


Figure 4-18: Temperature distribution (°C) in the FULL-LC1-GYP50 model at failure

- Gypsum 30mm Fire Protection

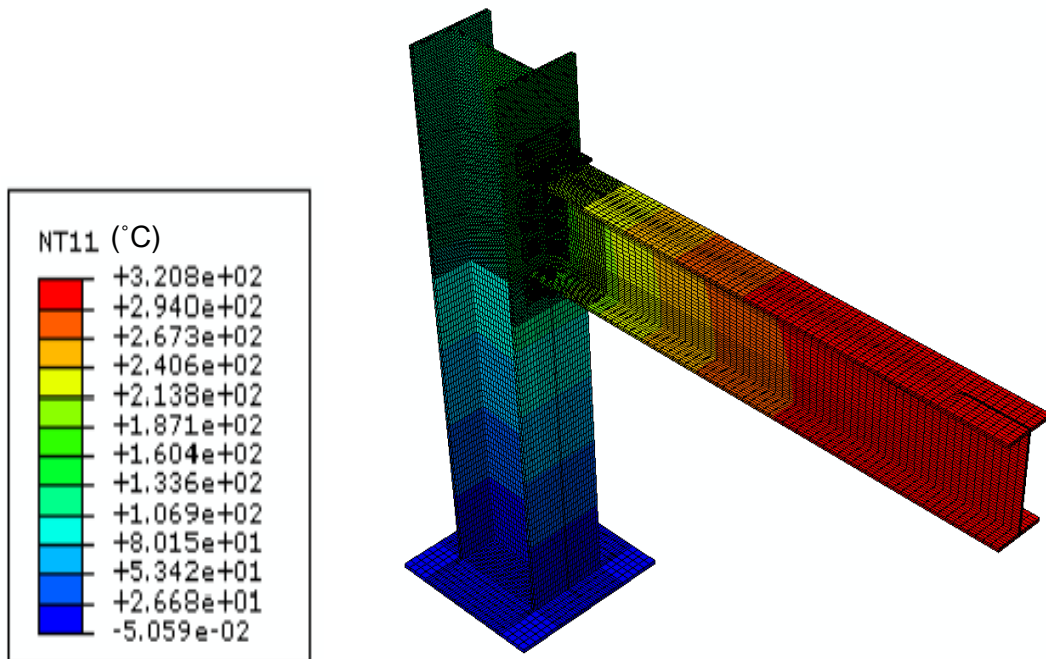


Figure 4-19: Temperature distribution (°C) in the FULL-LC1-GYP30 model at failure

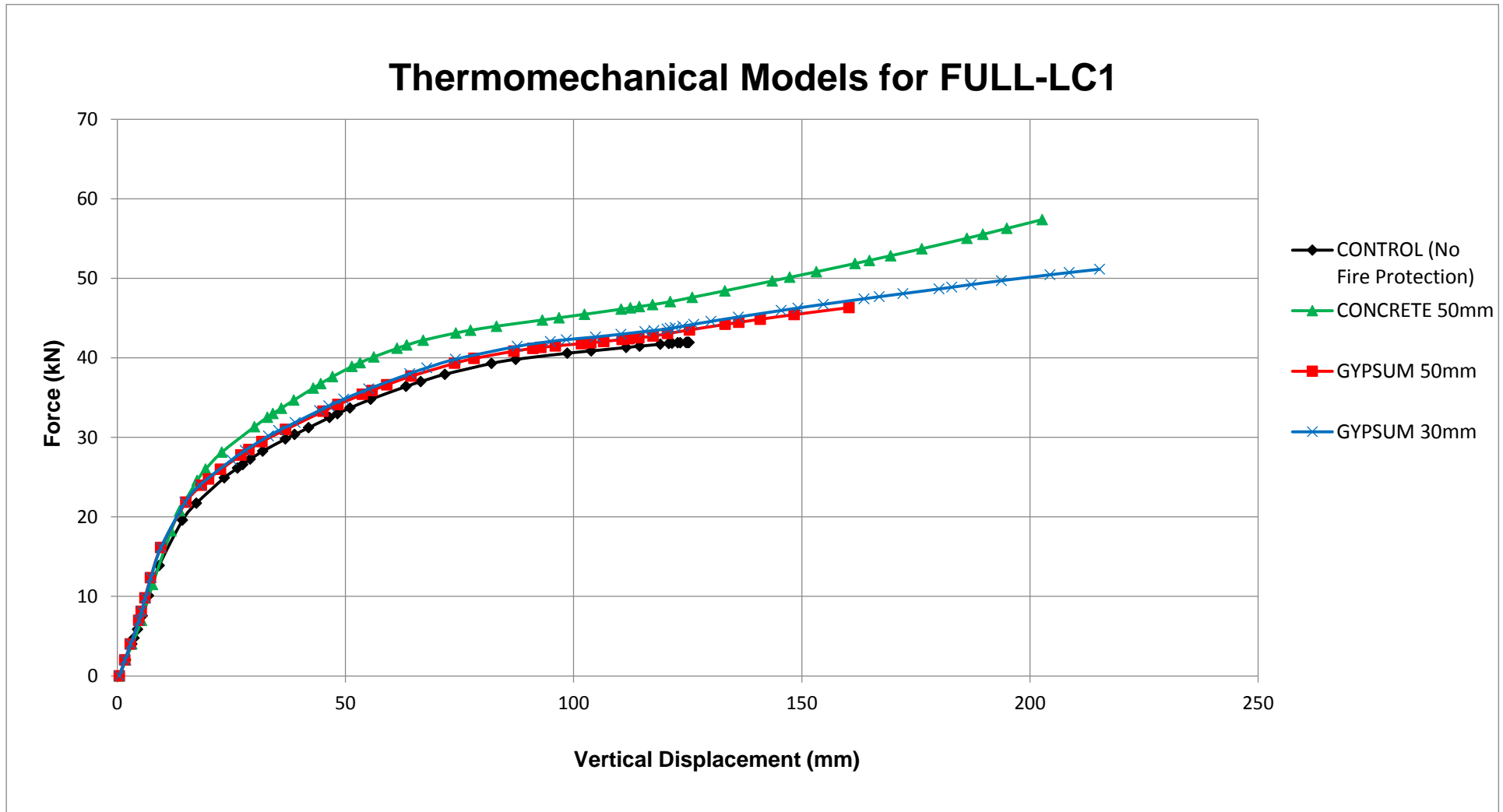


Figure 4-20: Force-displacement curves for steady-state Thermomechanical FULL-LC1 models

The non-linear behaviour of the steel connection under uncoupled thermomechanical loading is evident in Figure 4-20. Similarly to BM-LC1, a gradual increase in force is observed and the results exhibit an improved behaviour in the fire-protected models in comparison to that of the unprotected model. The results shown by Figures 4-16 to 4-20 are summarised and compared in Table 4-3.

**Table 4-3: Summarised comparison of fire protection materials for FULL-LC1 models**

<b>A</b>	<b>B</b>	<b>C</b>	<b>D</b>
<b>Unprotected/ Fire-protected</b>	<b>Thickness (mm)</b>	<b>Maximum Temperature in Steel at Failure* (°C)</b>	<b>Approximate Ultimate Force** (kN)</b>
Unprotected (Control)	N/A	386	21.72
CONCRETE	50	258	31.34
GYPSUM	50	329	21.84
GYPSUM	30	321	21.84

\*Maximum temperature in steel at failure of the steel beam, shown in Figures 4-16, 4-17, 4-18 and 4-19, for Column D force.

\*\*Column D values were obtained from Abaqus output and verified against Figure 4-20.

From Figure 4-16 and Table 4-3, it can be seen that the ultimate steel temperature experienced in the model with no fire protection was 386°C, recorded at failure. As discussed previously, this temperature is expected for the thermal properties that steel possesses. The temperatures developed in this control model differ to that of BM-LC1 since the applied thermal load was extended to the part of the joint connecting the top beam flange to the column flange. In the BM-LC1 control model, the heat flux was applied to the surfaces that would be covered by protection in the ensuing fire-protected models, which did not extend to the part of the joint in the beam-to-column connection. Thus, while the summarised results in Table 4-2 and 4-3 indicate similarities between the BM-LC1 and FULL-LC1 analyses, they are not identical. Hence, the slight increase in maximum temperature of 15°C in the control model of FULL-LC1 compared to BM-LC1 at failure is anticipated, since the thermal load is applied over a greater surface area, increasing the areas of heat transfer to the steel.

From column C, 50mm concrete protection incurs the lowest heat (258°C) in the steel connection at failure, compared to the gypsum-protected models. The difference

between the recorded temperatures at failure between the fire-protected models is attributed to the various associated factors of thermal conductivity material properties and thermal conductance at the interface, which should be further investigated. Despite the 20mm reduction in thickness between the gypsum-protected models, GYP30 and GYP50 experience almost identical, high temperatures at failure of the steel beam. Furthermore, the same ultimate force of 22kN incurred in both the models is further indication that 30mm gypsum could be deemed as effective in providing fire resistance to the steel connection as 50mm gypsum protection.

The control model fails under an applied force of 22kN, with a corresponding ultimate vertical displacement of 20mm, at the point on the beam where the concentrated force is applied. This is similar behaviour to that observed in the BM-LC1 control model, which provided support for the same magnitude of applied force and similar displacement. In comparison to the BM-LC1 scenario, where the fire-protected models supported loads of approximately 22-26kN, FULL-LC1 50mm concrete protection offers support of an additional 5kN, while GYP50 and GYP30 behave fairly similarly in both scenarios. These differences are relatively small when compared to the overall applied load of 200kN, thus indicating that under the specific loading scenario of LC1, providing either BM or FULL fire protection coverage typically yields similar results.

Furthermore, there is evidence of correlation between the maximum steel temperatures experienced in the connection from Table 4-3 and the behaviour of the connection under thermomechanical loading, in Figure 4-20. The CONC50 model experienced the lowest temperature development in the steel (258°C), allowing it to support a greater force up to 32kN, with a corresponding displacement of about 30mm. In comparison, GYP50 and GYP30 suffer higher steel temperatures (329°C and 321°C respectively) and therefore fail at lower forces of approximately 22kN. However, all models with fire protection perform slightly better under the applied uncoupled thermomechanical loading for FULL-LC1 than the unprotected model. Both 50mm concrete and 30mm gypsum board protection induce better performances of the steel connection and behave similarly, as deduced in the BM-LC1 scenario.

#### **4.5.3 Results for FULL Coverage – Load Case 2**

FULL coverage of the steel connection under LC2 was examined by conducting uncoupled thermomechanical analyses on unprotected and fire-protected models. In this scenario, the imported thermal loading as a predefined field is characterised by:

- Thermal load of  $2\text{kW/m}^2$  applied to beam and column flanges/ parallel fire protection flanges.

The resulting maximum temperatures experienced by the steel connection, in the models with and without fire protection, for the uncoupled thermomechanical FULL-LC2 scenarios are exhibited in Figures 4-21, 4-22, 4-23 and 4-24. A graph displaying the resulting, derived force-displacement curves follows thereafter, in Figure 4-25.

- **Control Model – No Fire Protection**

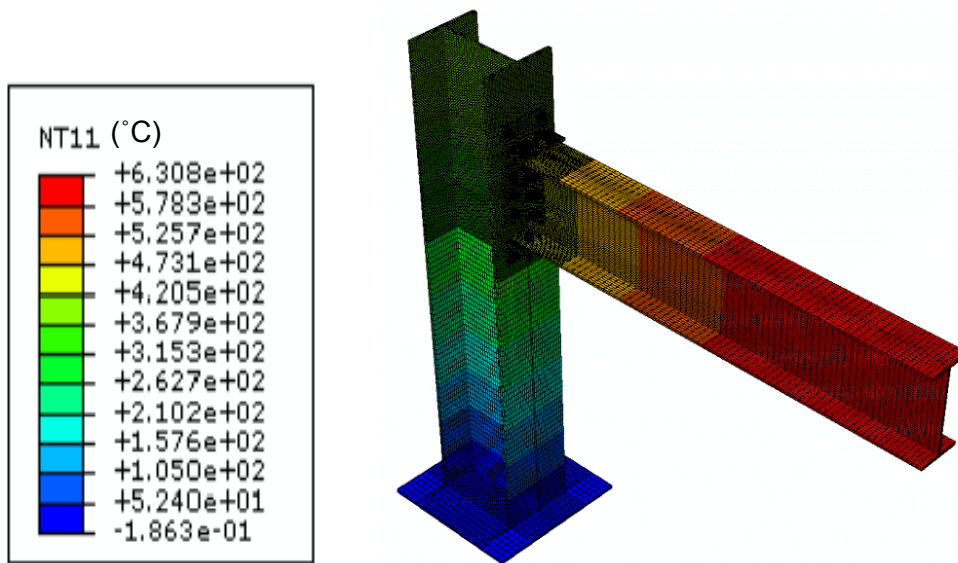


Figure 4-21: Temperature distribution (°C) in the FULL-LC2-CONTROL model at failure

- **Concrete 50mm Fire Protection**

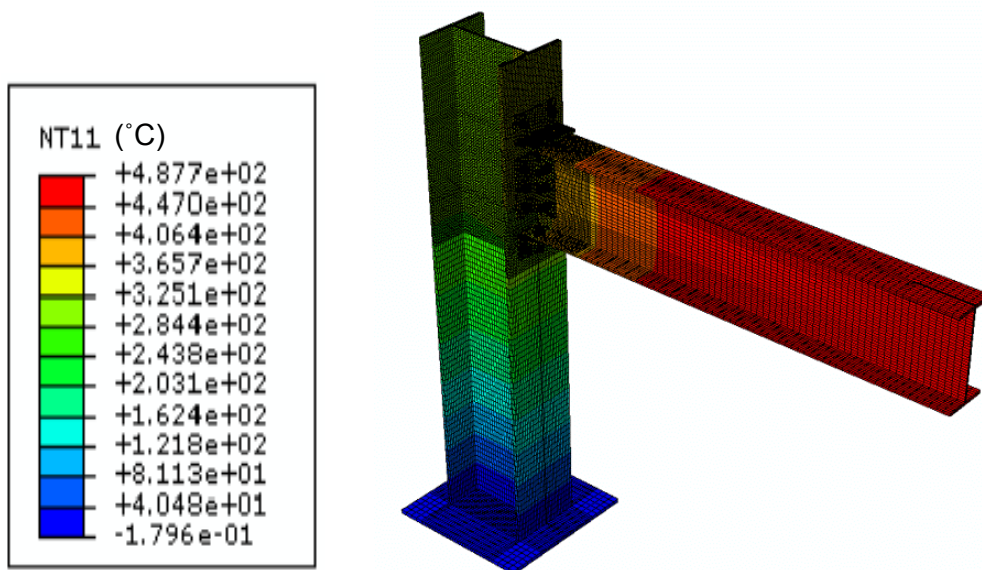


Figure 4-22: Temperature distribution (°C) in the FULL-LC2-CONC50 model at failure

- Gypsum 50mm Fire Protection

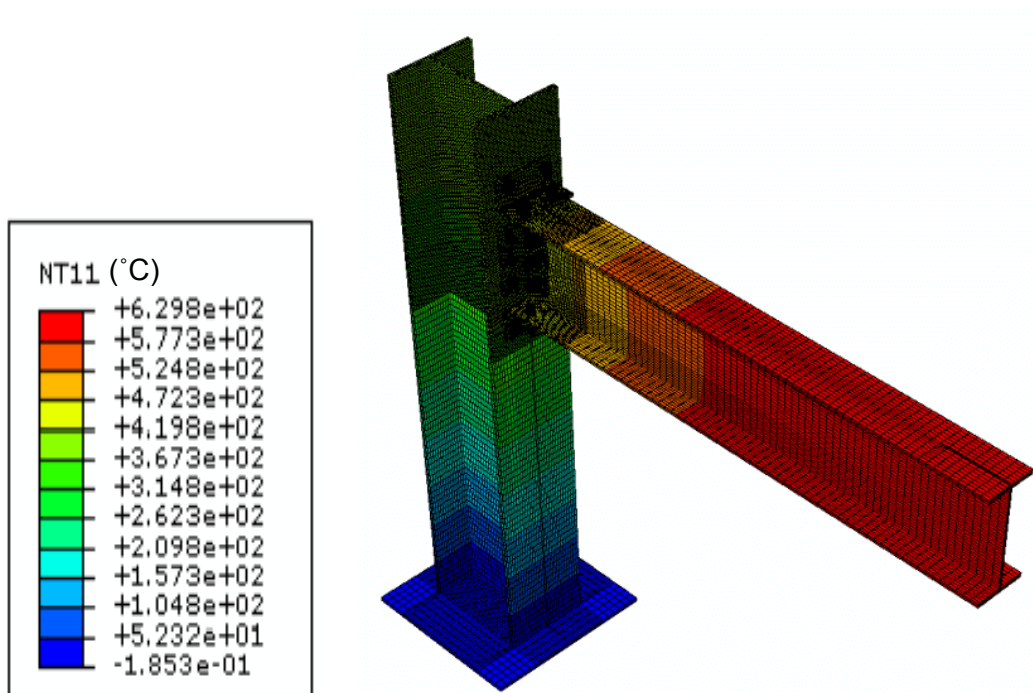


Figure 4-23: Temperature distribution (°C) in the FULL-LC2-GYP50 model at failure

- Gypsum 30mm Fire Protection

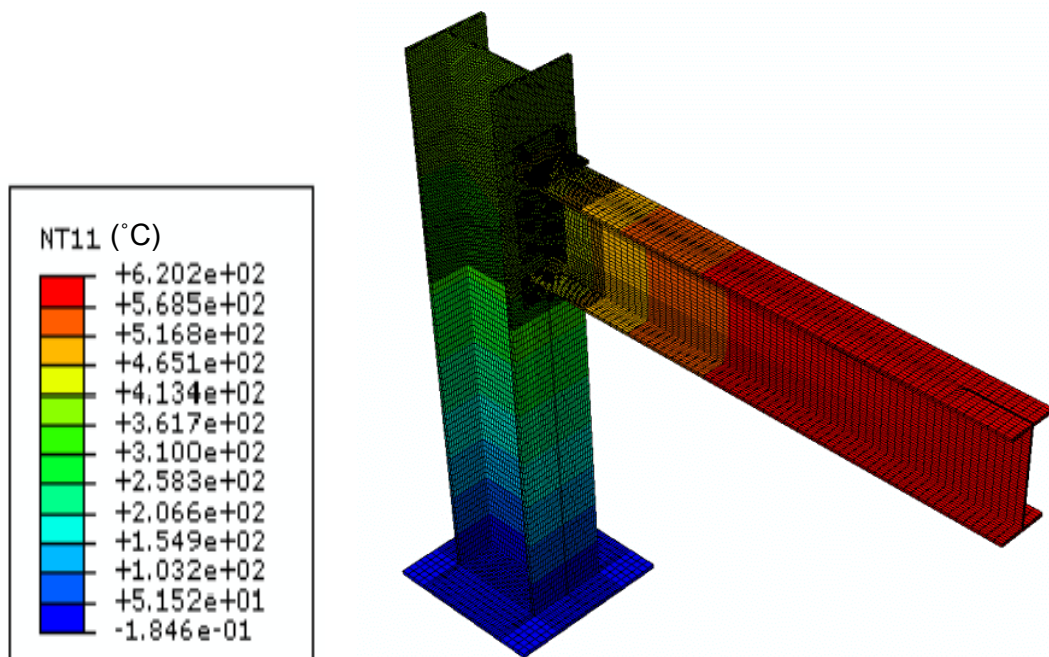


Figure 4-24: Temperature distribution (°C) in the FULL-LC2-GYP30 model at failure

## Thermomechanical Models for FULL-LC2

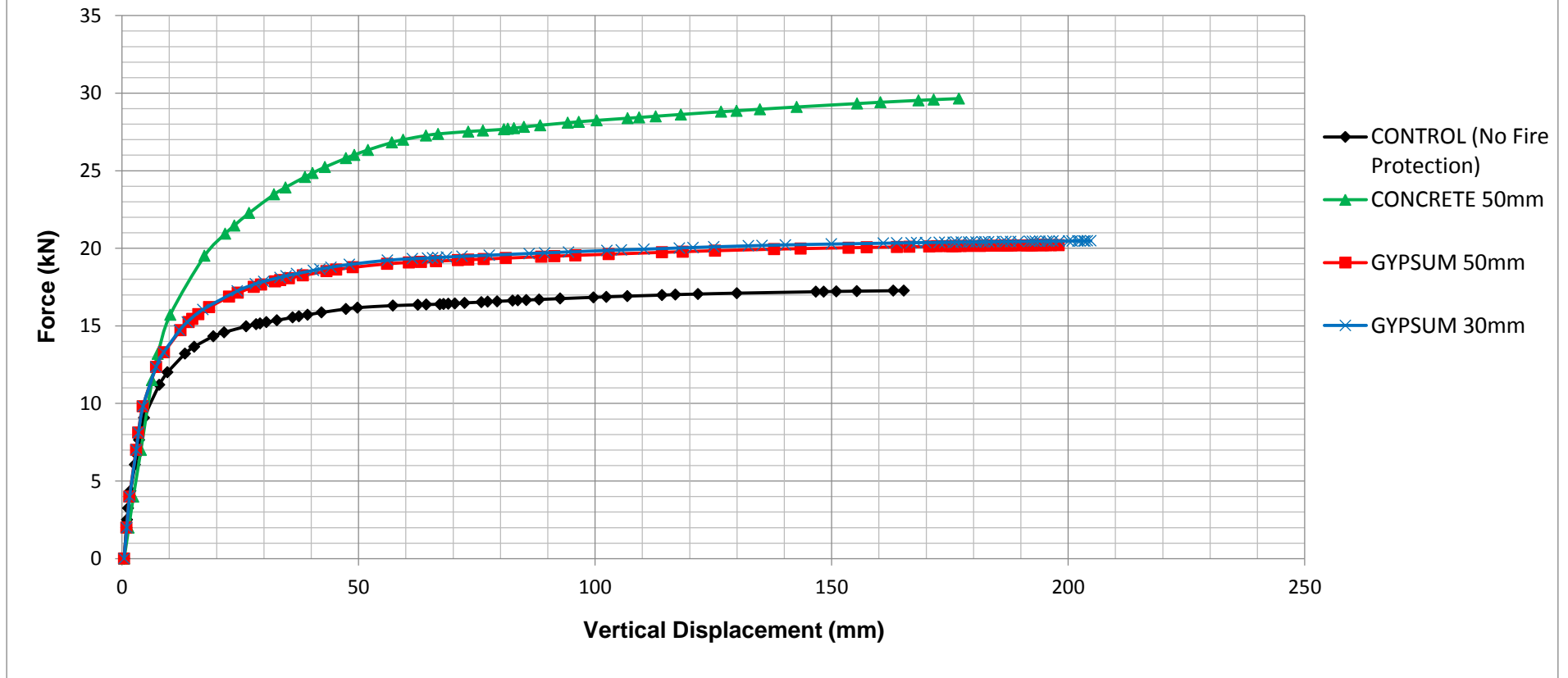


Figure 4-25: Force-displacement curves for steady-state Thermomechanical FULL-LC2 models

Under uncoupled, non-linear thermomechanical analysis, the intense thermal load (of LC2) causes variations in the effect of protection materials on steel behaviour, seen in Figure 4-25. In this scenario, there is a diminished but existing improved effect of fire protection on the steel connection structural performance under elevated temperatures. This is emphasised and indicated by the difference in the force-displacement curves between the models with and without fire protection, as well as the maximum temperatures incurred in the steel connection at failure. Initially, the shapes of the curves in Figure 4-25 indicate that the increasing applied force induces relatively small vertical deformations. However, the connection reaches failure quickly thereafter: for small increasing increments in applied force, large vertical displacements in the steel beam are observed. Furthermore, the improvement in the behaviour of the fire-protected models on the steel connection is clearer in this scenario, compared to the FULL-LC1 scenario where fire is applied to one surface only. Thus, as previously determined in the analogous model temperature distributions, for more severe fire phenomena, the role of the fire protection materials becomes increasingly important. A summary of the results obtained in the FULL-LC2 analyses is provided in Table 4-4.

**Table 4-4: Summarised comparison of fire protection materials for FULL-LC2 models**

<b>A</b>	<b>B</b>	<b>C</b>	<b>D</b>
<b>Unprotected/ Fire-protected</b>	<b>Thickness (mm)</b>	<b>Maximum Temperature in Steel at Failure* (°C)</b>	<b>Approximate Ultimate Force** (kN)</b>
Unprotected (Control)	N/A	631	12.05
CONCRETE	50	488	20.94
GYPSUM	50	629	14.70
GYPSUM	30	620	14.70

\*Maximum temperature in steel at failure of the steel beam, shown in Figures 4-21, 4-22, 4-23 and 4-24, for Column D force.

\*\*Column D values were obtained from Abaqus output and verified against Figure 4-25.

In this scenario of FULL-LC2 control models, significantly higher temperatures were developed in column C than the FULL-LC1 unprotected scenario. This is due to the fact that the thermal load was applied to more steel and fire-protected surfaces in the imported thermal analyses, thereby intensifying the heat transfer to the steel in the FULL-LC2 models. Therefore, fire protection in scenarios of an increased fire event, is

a critical element since a greater improvement in performance can be seen between the protected and unprotected models, compared to the FULL-LC1 scenario. Moreover, it can be observed from Table 4-4 that with the increase in protected surfaces exposed to heat, the difference between the maximum temperatures experienced at failure between the control model and gypsum-protected models (50mm and 30mm) is diminished. GYP50 and GYP30 protection perform almost identically in this situation at failure, while concrete offers a reduction in maximum steel temperatures at failure by approximately 141°C compared to the gypsum protection materials.

The control model fails at a much-reduced force, when compared to the other scenarios, of about 12kN, reaching an ultimate vertical displacement of 10mm in the steel beam at the point of application of the point load. In comparison, the FULL-LC1 unprotected model reached an ultimate force of 22kN, which is approximately double the force at which the FULL-LC2 model fails at. The decreased strengths of the FULL-LC2 models are attributed to the fact that the same thermal loading is applied to multiple surfaces of the connection in LC2, thus leading to increased temperatures experienced in the steel connection, documented in Table 4-4.

The improved effects of the CONC50, GYP50 and GYP30 fire protection materials are similarly decreased in comparison to the corresponding FULL-LC1 fire-protected models. From Figure 4-25, the steel connection with 50mm concrete protection fails at a force of almost 21kN, indicated as the best-performing protection material in the FULL-LC2 scenario. For a force increment of approximately 2kN, from 21kN to 23kN in the CONC50 curve, the steel beam deflects a further 10mm vertically. Similar observations are made with respect to GYP50 and GYP30, both of which result in a fairly identical performance of the steel substructure and fail at a force of roughly 15kN. The slight difference in fire resistances offered by 50mm and 30mm gypsum protection contributes to the similar behaviour of the steel connection with those protection materials incorporated. From Figure 4-25, the steel substructure fails at fairly low forces, for both the models with and without fire protection, in comparison to the BM-LC1 and FULL-LC1 conditions. This is expected due to the increased surfaces subject to the intense heat flux in this scenario and subsequent yielding of the steel members at elevated temperatures.

#### 4.5.4 Results for FULL Coverage – Load Case 3

Uncoupled thermomechanical analyses on models with and without fire protection were conducted for FULL coverage under LC3. In this scenario, the imported thermal loading as a predefined field is characterised by:

- Thermal load of  $2\text{kW/m}^2$  applied to all external surfaces of the beam/ fire protection.

The resulting maximum steel temperatures in the unprotected model and fire-protected models for the uncoupled thermomechanical BM-LC3 models are displayed in Figures 4-26, 4-27, 4-28 and 4-29. Thereafter, the comparative force-displacement curves derived from these analyses are presented in Figure 4-30. These diagrams illustrate the comparison between the models with and without fire protection in this scenario.

- **Control Model – No Fire Protection**

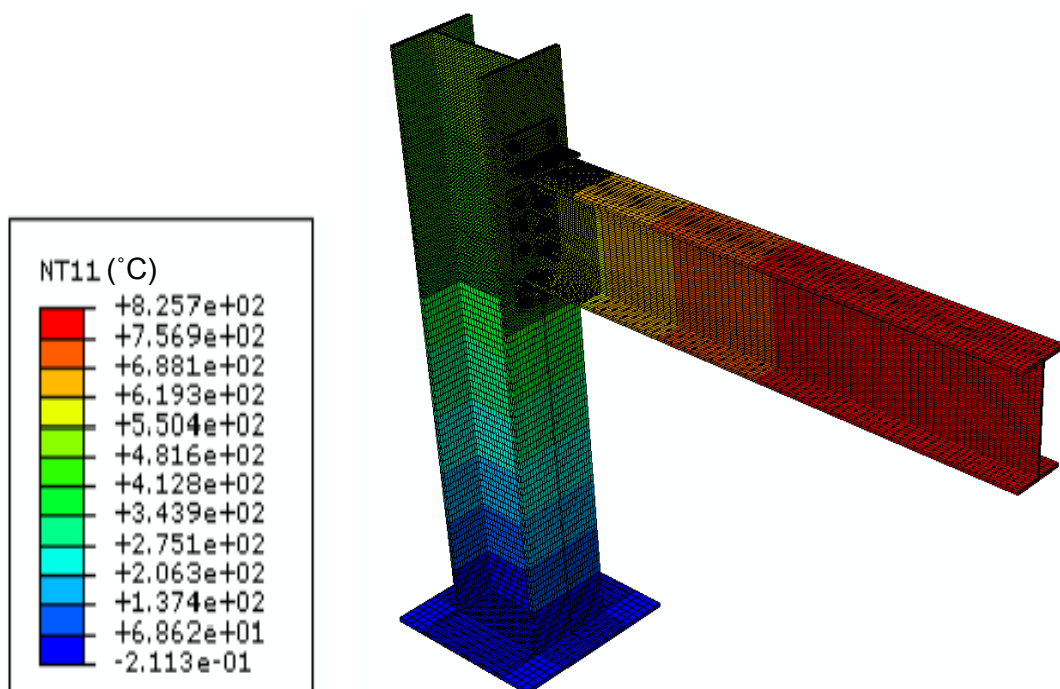


Figure 4-26: Temperature distribution (°C) in the FULL-LC3-CONTROL model at failure

- Concrete 50mm Fire Protection

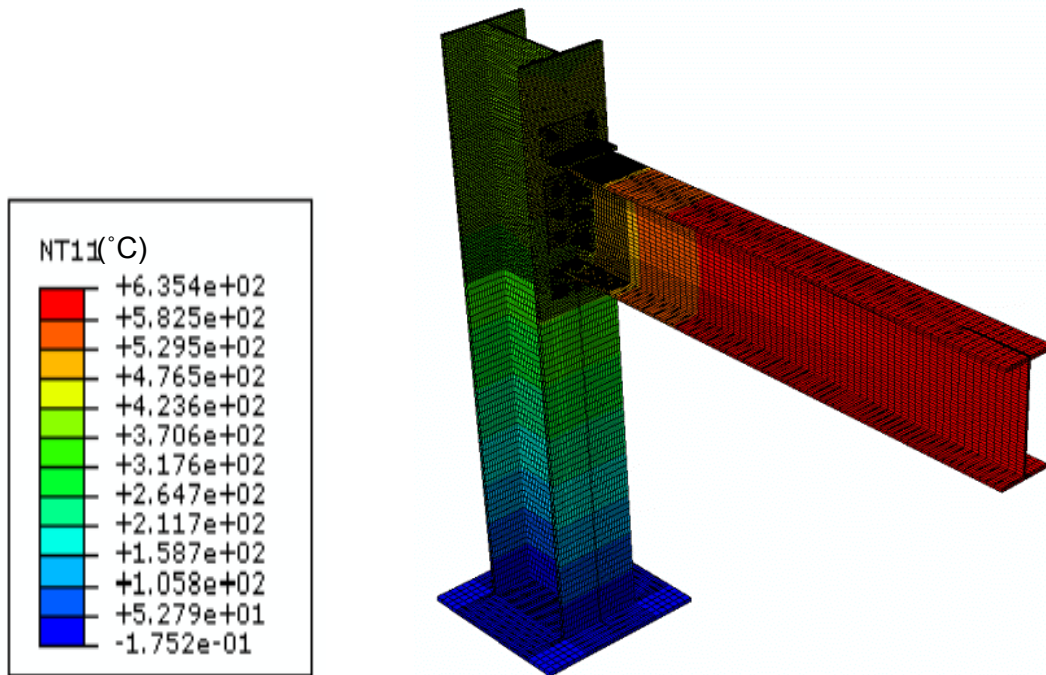


Figure 4-27: Temperature distribution (°C) in the FULL-LC3-CONC50 model at failure

- Gypsum 50mm Fire Protection

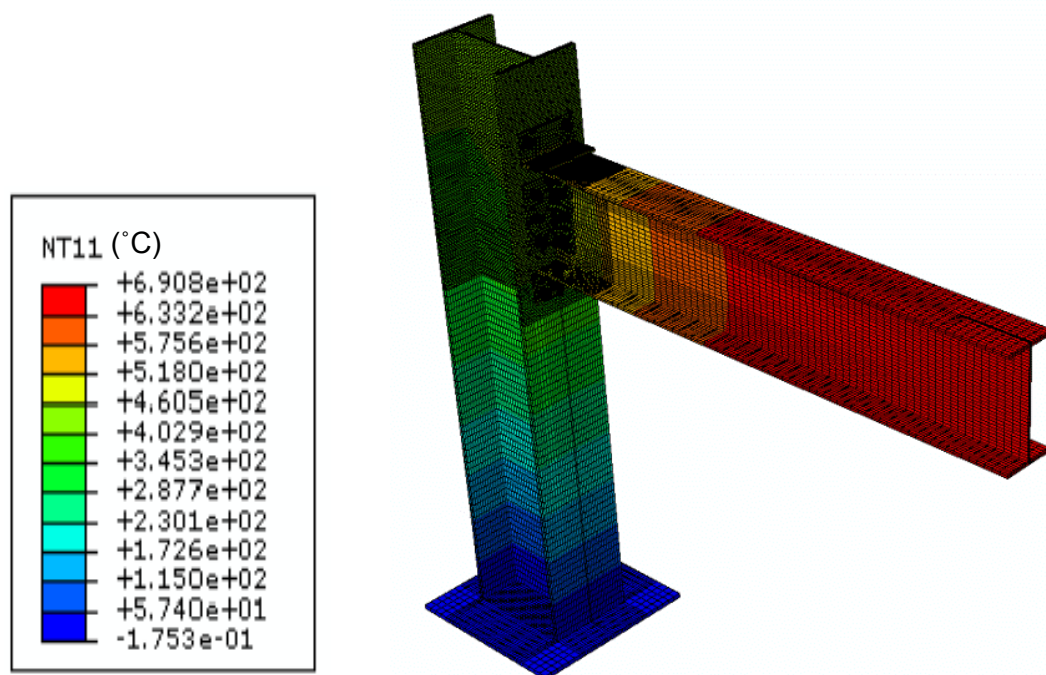


Figure 4-28: Temperature distribution (°C) in the FULL-LC3-GYP50 model at failure

- Gypsum 30mm Fire Protection

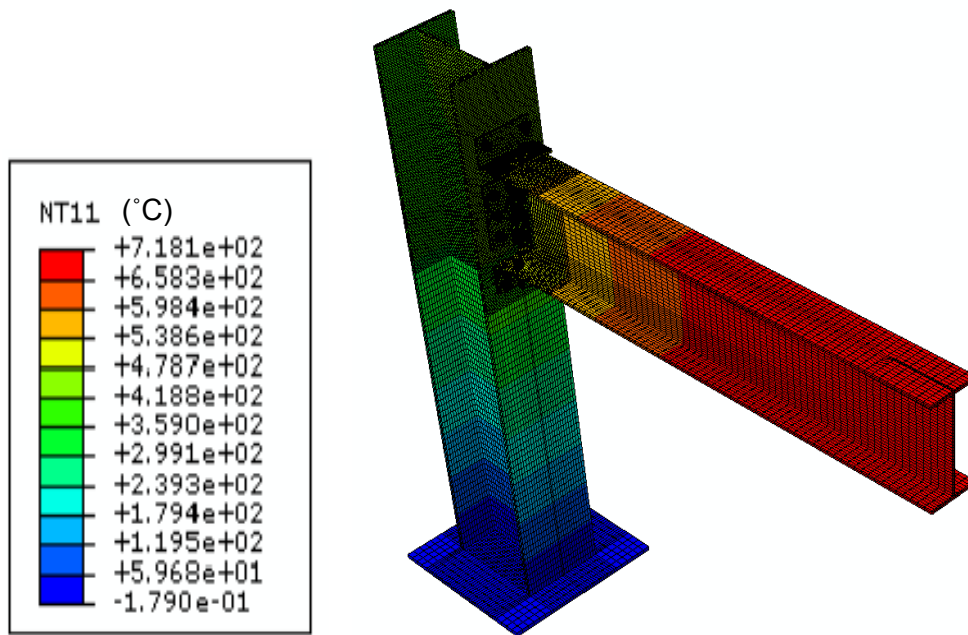


Figure 4-29: Temperature distribution (°C) in the FULL-LC3-GYP30 model at failure

## Thermomechanical Models for FULL-LC3

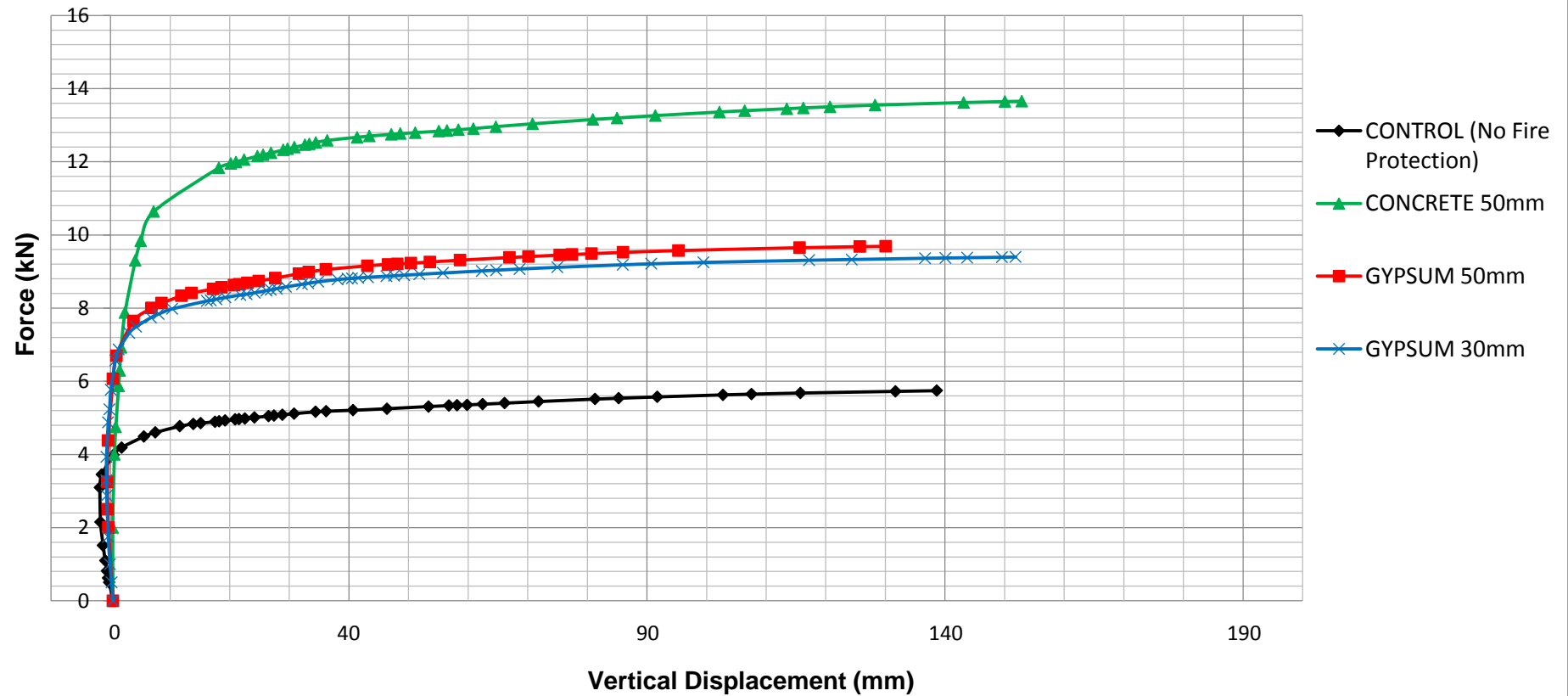


Figure 4-30: Force-displacement curves for steady-state Thermomechanical FULL-LC3 models

Analysis of LC3 for the FULL coverage of the numerical models presents further distinguished differences in the effects of fire protection on the steel connection performance, displayed in Figure 4-30. Additionally, even greater improvement in the strength is observed in the fire-protected models, in comparison to the unprotected model. The heat transfer that occurs on an increased number of surfaces induces failure of the steel connection under diminished structural loads. The shapes of the curves derived in the FULL-LC3 analysis are similar to those obtained in the FULL-LC2 analysis, except that failure occurs at smaller forces in all the models, by comparison. This is due to an increase in the surfaces exposed to direct fire in the FULL-LC3 models, resulting in weaker systems. A summarised comparison of the results obtained and displayed in Figures 4-26 to 4-30 is provided in Table 4-5.

**Table 4-5: Summarised comparison of fire protection materials for FULL-LC3 models**

<b>A</b>	<b>B</b>	<b>C</b>	<b>D</b>
<b>Unprotected/ Fire-protected</b>	<b>Thickness (mm)</b>	<b>Maximum Temperature in Steel at Failure* (°C)</b>	<b>Approximate Ultimate Force** (kN)</b>
Unprotected (Control)	N/A	826	3.98
CONCRETE	50	635	9.84
GYPSUM	50	691	6.69
GYPSUM	30	718	6.57

\*Maximum temperature in steel at failure of the steel beam, shown in Figures 4-26, 4-27, 4-28 and 4-29, for Column D force.

\*\*Column D values were obtained from Abaqus output and verified against Figure 4-30.

The previously established trend of the performance of each of the fire protection materials is further reiterated by the results in Table 4-5. That is, all the fire-protected models indicate superior performance to the unprotected model under elevated temperatures given in column C, by preventing excessive temperature development in the steel. At failure, the differences in the maximum steel temperatures between the fire-protected models indicate a reduction from the maximum potential failure temperature experienced in the unprotected model: CONC50, GYP50 and GYP30 result in reductions of 191°C, 135°C and 108°C respectively. These are significant reductions observed at failure for each fire-protected model, indicating the increasing significance of designing for fire protection of steel members. In this scenario, the

severe thermal load was applied to all external surfaces of the models with and without fire protection, presenting even further amplified behaviour of the steel connection under the loading, hence the larger differences in ultimate steel temperatures at failure are observed.

The uncoupled thermomechanical analysis of FULL-LC3 presents a control model that fails at a force of approximately 4kN. In comparison to the FULL-LC1 and FULL-LC2 models, the FULL-LC3 model indicates a substantial decrease in the force required to induce failure of the steel beam. This is due to the heightened heat intensity on a greater number of surfaces, when compared to the previous thermal load case scenarios, which results in a rapidly weakened system. The 50mm concrete protection best maintains structural integrity of the system in comparison to GYP50 and GYP30, up to a force of approximately 10kN. As previously ascertained, 50mm and 30mm gypsum protection result in similar behaviour of the steel connection: a fairly low 27°C difference in ultimate steel temperature at failure and negligible difference in ultimate force is displayed in Table 4-5. The documented decreased load bearing capacity of the steel connection is expected since the structural system is weakened by the effects of temperature, where elevated temperatures on each external surface causes aggravated yielding of steel members according to the von Mises plasticity model. Thus, for the given thermal load, FULL-LC3 results indicate that CONC50, GYP50 and GYP30 fire protection ultimately affords significant protection to the steel connection, following the sequential thermal and thermomechanical analyses.

The PEEQ output from Abaqus for the Equivalent Plastic Strain incurred in the models is considered for this load case since it presents fire loading on multiple surfaces. This damage to the steel connection can be observed in Figures 4-31 and 4-32 for the unprotected and GYP30-protected thermomechanical models, selected as a representative protection material. The PEEQ result for LC3 was chosen since it represents the case where the fire was applied to all the exterior surfaces in the preceding thermal models. The yielding that occurs in the steel connection is focused primarily on the bottom flange of the model with no fire protection, due to large deformations and temperatures leading to yielding of the seat angle. In the fire-protected model, the yielding is concentrated along the line of the applied structural 200kN force on the beam and at the beam-column joint.

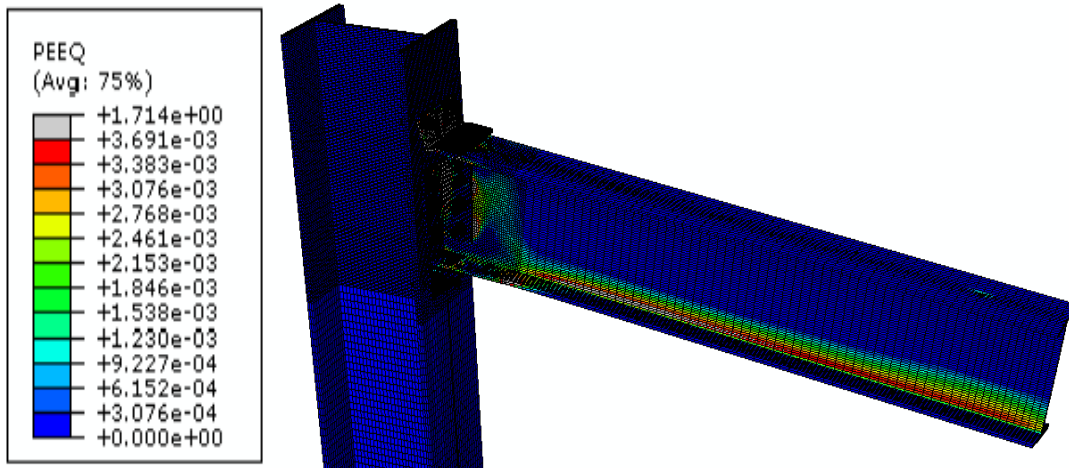


Figure 4-31: Equivalent Plastic Strains for FULL-LC3 unprotected model

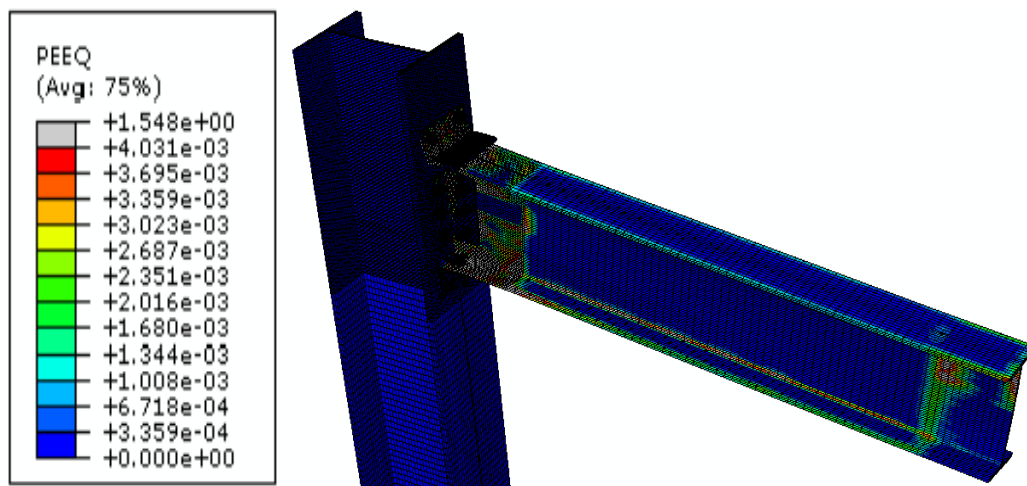


Figure 4-32: Equivalent Plastic Strains for FULL-LC3-GYP30 fire-protected model

#### 4.5.5 Results for Fire Resistance Offered by Protection Materials

The maximum temperature results of each of the model cases presented in Table 4-2, 4-3, 4-4 and 4-5 were obtained at failure of the steel beam, indicated by non-zero PEEQ output in Abaqus and the force-displacement graphs becoming horizontal. These results presented a comparison of the behaviour of the steel connection with fire protection materials to the control models without protection, for varying ultimate forces. As mentioned previously, additional results for maximum temperatures in the steel connection were obtained for approximately the same applied structural load (a load which depends on the ultimate forces of the control models per LC1, LC2 and LC3). These results allowed for a numerical evaluation of fire resistance offered by the concrete and gypsum protections and are depicted per model load case by Figures 4-33, 4-34, 4-35 and 4-36.

For these results, the maximum temperature of the control model at failure in each load case (BM-LC1, FULL-LC1, FULL-LC2 and FULL-LC3) was used as the criterion to compare the temperatures of the subsequent fire-protected models, developed at approximately the same applied load at which the control model tended to fail. This allowed for direct comparison between the models within each load case for the highest temperatures incurred in the steel, whereas the temperatures at failure of each of the models varied according to the total load carrying capacity of each model. The maximum steel temperatures in the fire-protected models presented in these results were obtained from Abaqus output.

#### 4.5.5.1 Fire Resistance Results for BM-LC1

As previously determined, the approximate ultimate force of the control model of BM-LC1 was 22kN, as displayed in Table 4-2. Figure 4-33 indicates the maximum temperature in the steel and fire resistance offered by the concrete and gypsum protection materials within BM-LC1 for approximately the same applied force of 22kN (the load at which the control model fails).

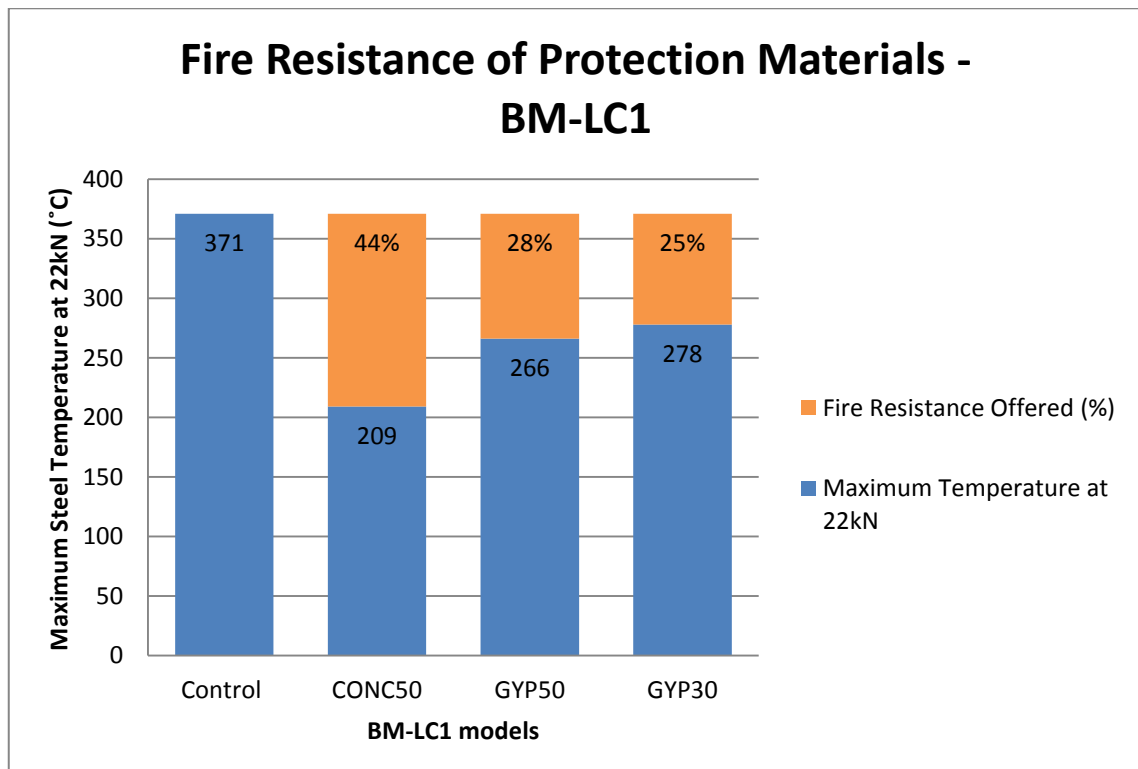


Figure 4-33: Fire resistance offered by protection materials for BM-LC1

From Figure 4-33, it can be seen that 50mm concrete protection limits the exposure of the beam to heat most effectively, compared to the other protection materials, resulting

in a maximum temperature suffered by the beam of 209°C. This temperature was recorded in the CONC50 model for approximately the same applied load that caused failure in the control model (22kN). This result indicates a 162°C reduction in maximum temperature in the steel beam from the control model to the CONC50 model. Thus the concrete protection, due to its low thermal conductivity, adds approximately 44 per cent fire resistance to the applied thermal load of the uncoupled thermomechanical analysis, for the same applied structural load. Furthermore, Figure 4-33 indicates that 50mm concrete protection offers a greater fire resistance than the gypsum protection for the same thickness, which develops a maximum steel temperature of 266°C and affords a significantly less percentage of fire resistance (28 per cent compared to 44 per cent in the CONC50 model). This can be attributed to intrinsically-different thermal behaviours of the protection materials and the variation in the respective thermal conductance between the protection and steel interfaces of each material.

Between the gypsum protection results in Figure 4-33, the GYP30 model experiences a similar ultimate temperature to that of the GYP50 model for the same applied structural load – a difference of 12°C exists between the models. This small variation can be attributed to the 20mm decrease in protection thickness in the GYP30 model, thereby providing a thinner barrier between the steel and applied thermal load and allowing greater heat transfer thereto. Compared to the unprotected model however, both gypsum fire protections prove successful in limiting the fire exposure of the steel parts, offering significant reductions in maximum temperatures experienced in the steel. For GYP50, the maximum steel temperature incurred is decreased by approximately 28 per cent from the highest temperature experienced in the steel connection with no fire protection. Similarly for GYP30, the maximum temperature recorded indicates a 25 per cent decrease from the ultimate steel temperature in the unprotected model, for approximately the same applied point load.

#### **4.5.5.2 Fire Resistance Results for FULL-LC1**

Table 4-3 previously indicated the approximate ultimate force of the control model of FULL-LC1 as 22kN, analogous to that of BM-LC1. This is expected since the fire scenario between these model cases is similar. Figure 4-34 graphically displays the maximum steel temperature and derived fire resistance offered by protection materials within FULL-LC1, at the point in the analyses at which a load of approximately 22kN was applied.

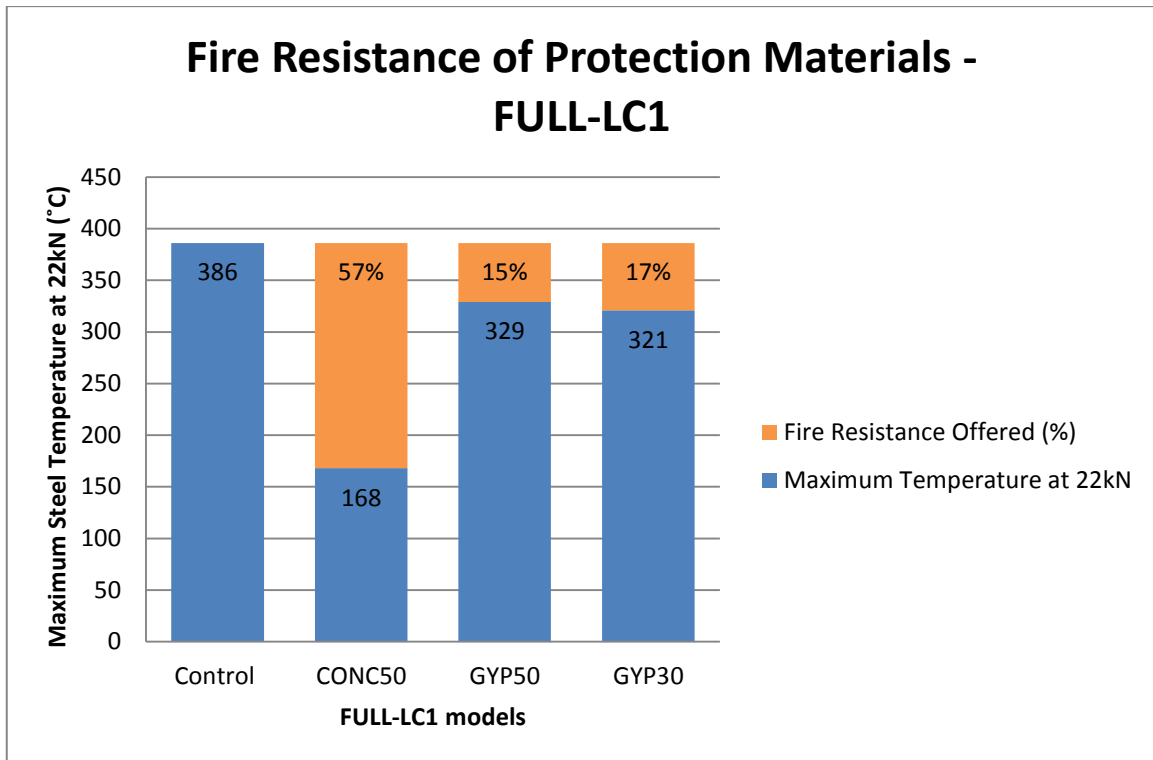


**Figure 4-34: Fire resistance offered by protection materials for FULL-LC1**

Figure 4-34 indicates that all the models with fire protection demonstrate improved fire resistance to the applied thermal load when compared to the maximum steel temperature for the same applied structural load, obtained in the unprotected model. While all fire-protected models offer adequate fire resistance, applying a 50mm concrete fire protection to the steel connection proves to be the most effective fire resisting strategy for FULL-LC1. This is shown by the 57 per cent fire resistance offered by CONC50, which experiences a maximum steel temperature of 168°C compared to a significantly higher 386°C in the unprotected model, for a 22kN force. The potential maximum temperature incurred in the control model was more than halved due to the addition of 50mm concrete protection on the overall steel connection, for the same point load. In comparison, GYP50 and GYP30 protection performed less adequately than CONC50 in resisting temperature build up in the steel connection, achieving 15 per cent and 17 per cent fire resistance to the temperature of the unprotected model respectively. This significant difference between maximum developed temperatures with concrete and gypsum protection is attributed to the different thermal material properties of both materials, in conjunction with the varying thermal properties of the interface between each material and the steel.

While GYP30 is less effective than CONC50 in preventing the rise of temperatures in the steel, it performs slightly better than the GYP50 model for the same applied structural load, shown by Figure 4-34. The result is noteworthy in indicating that 30mm gypsum performs similarly to 50mm gypsum protection, when subject to the same thermo-structural loading for the FULL fire protection. As previously mentioned, to further explain this occurrence, more research should be conducted in the future to investigate how heat is spread through different materials' interfaces.

#### 4.5.5.3 Fire Resistance Results for FULL-LC2

The FULL-LC2 control model indicated failure at an applied load of 12kN, as shown in Table 4-4. The corresponding maximum steel temperatures of the fire-protected models at an applied load of 12kN in the analyses are depicted in Figure 4-35 and the calculated fire resistance offered by the protection materials is indicated, for FULL-LC2.

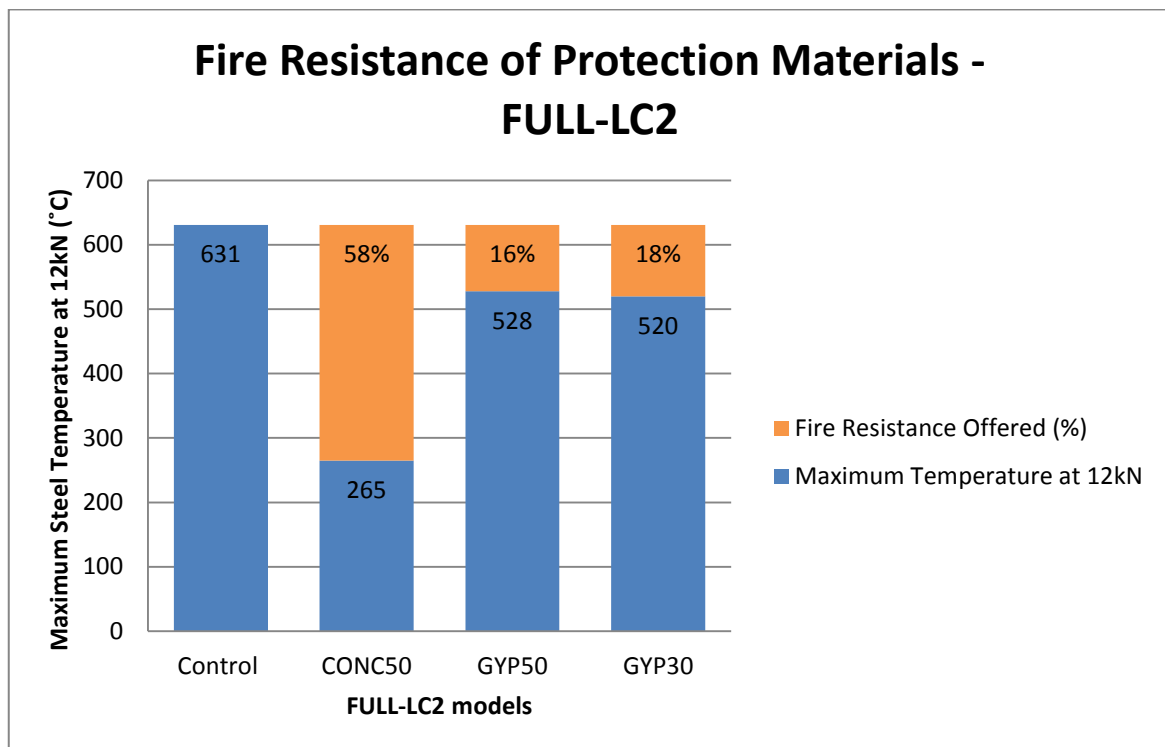


Figure 4-35: Fire resistance offered by protection materials for FULL-LC2

Similarly to FULL-LC1, Figure 4-35 indicates that 50mm concrete protection proved most effective in limiting temperature development in the steel connection and provided 58 per cent fire resistance to the ultimate steel temperature in the model with no fire protection of 631°C. Both GYP50 and GYP30 reduced the potential maximum steel temperature by 103°C and 111°C respectively, affording approximately the same fire

resistance to the overall steel connection. The CONC50, GYP50 and GYP30 fire-protected models all afford slightly increased fire resistance to the steel connection for thermal loading applied to the column and beam flanges, compared to loading solely on the beam flange (FULL-LC1). Thus, the incorporation of fire protection is observed to be increasingly important with further improved fire resistance offered under more intensified loading conditions.

#### 4.5.5.4 Fire Resistance Results for FULL-LC3

Table 4-5, shown previously, indicates the ultimate force of the FULL-LC3 control model as approximately 4kN. For this same applied load (4kN) in the analyses of the fire-protected models, the maximum temperatures developed in the steel connection are displayed in Figure 4-36, inclusive of the resulting approximate fire resistances offered by each protection material.

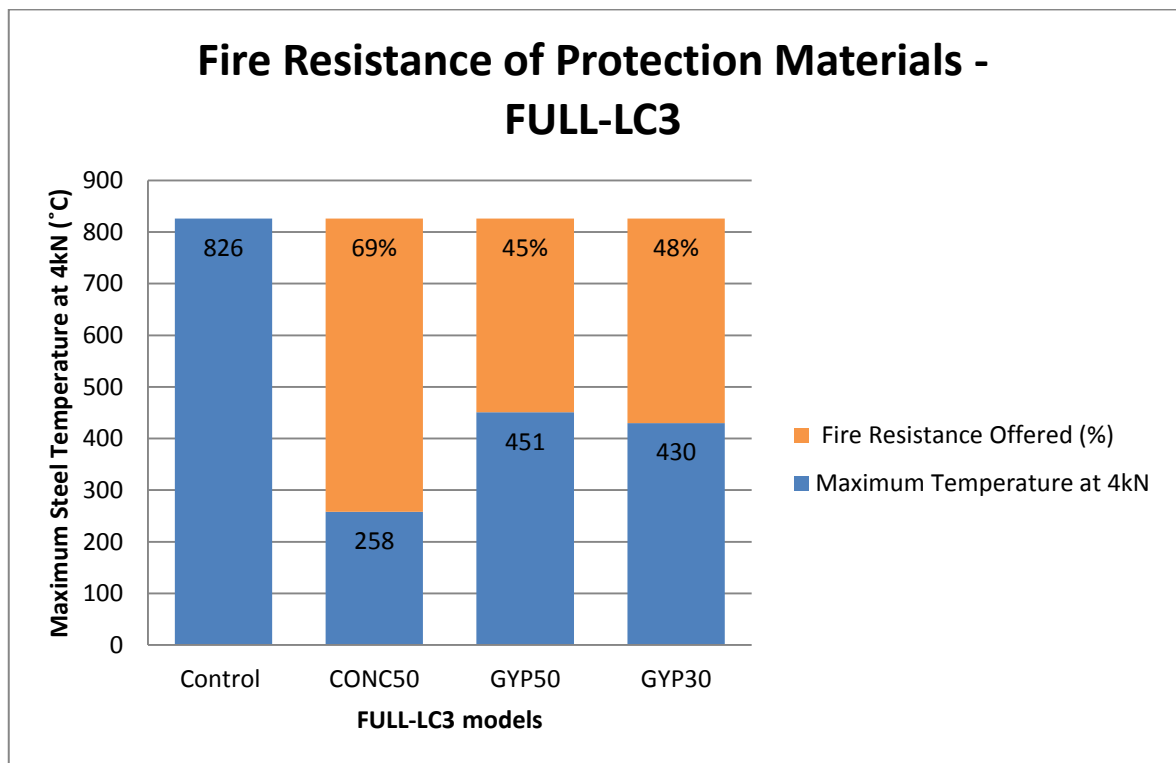


Figure 4-36: Fire resistance offered by protection materials for FULL-LC3

From Figure 4-36, 50mm concrete protection affords a significantly high fire resistance of 69 per cent for approximately the same load (4kN) that induces a maximum steel temperature of 826°C in the model with no fire protection. The GYP50 and GYP30 fire-protected models reduce the potential ultimate steel temperature by almost half its magnitude in the unprotected model, for the same applied load of 4kN. Although the

temperature developments in some of the fire-protected models are lower than those in the FULL-LC2 and FULL-LC1 models, the criterion used to obtain the comparable results was previously mentioned. Thus, comparisons between the models with fire protection are confined to each load case for the fire-protected models, for approximately the same applied load. However, the models with no fire protection across the load cases indicate the maximum temperatures at failure in each model. Therefore, these models display the increase in temperature experienced in the steel due to an increase in the surfaces subject to the applied loading: from LC1 to LC2 and finally, LC3 for FULL fire protection. The role of fire protection in strengthening the thermo-structural system is further reiterated by the results of Figures 4-33 to 4-36. With an increase in the intensity of the fire scenario, the fire resistance offered by the protection materials becomes increasingly important, thus motivating the need to incorporate such protection in structural steel connections.

#### 4.6 Summary

In this chapter, the results of the steady-state analyses performed on the steel connection under elevated temperatures were presented in accordance with part of the aims and objectives outlined in Chapter 1. The results were achieved by adopting the methodology defined in Chapter 3. The initial mechanical model result was determined and verified against previous literature. The results of the sequential thermal and thermomechanical analyses for models with and without fire protection were presented and discussed. The maximum temperatures in the steel connection at failure in each model were described and compared. The temperatures incurred by the connection at failure increased progressively across the model cases from LC1 to LC2 and the highest steel temperatures were experienced in LC3 models, due to an increase in surfaces exposed to direct fire. The uncoupled thermomechanical results were presented by force-displacement curves for each model to graphically represent the effect of fire protection on the behaviour of the steel connection under fire conditions. The 50mm concrete protection required the largest applied load to induce failure in the steel connection and incurred the lowest temperatures in the steel across all models. Gypsum fire protection resulted in improved behaviour of the connection at failure. Thicknesses of 50mm and 30mm resulted in similar behaviour of the steel system under sequential thermo-structural loading. Gypsum proved less effective than concrete as a fire protection material in all cases. Damage to the steel connection was depicted in the equivalent plastic strains that developed in the beam and joint of the steel connection. The fire resistance offered by each protection material was evaluated

for approximately the same applied load. Concrete protection afforded the steel connection the greatest resistance to fire when compared to gypsum protection of 50mm and 30mm. With an increase in the intensity of the fire scenario, the fire resistance offered by the protection materials became increasingly important, thus motivating the need to incorporate such protection in structural steel connections. The subsequent Chapter 5 will present and discuss the results from the coupled temperature-displacement transient analysis, investigating delamination.

# Chapter 5

---

## 5 Transient Analysis Results and Discussion

### 5.1 Introduction

The purpose of this chapter is to provide the results obtained in the transient analyses conducted in accordance with the aims, objectives and methodologies outlined in preceding chapters. The results of the coupled temperature-displacement transient analyses conducted on the steel connection, with and without fire protection, will be presented. The occurrence and effect of delamination during a fire event evolving in real time will be investigated. The force-displacement curves derived from the coupled thermomechanical analyses using Abaqus will be displayed. The delamination phenomenon will be quantified and the eventual damage or destruction to the fire protection will be assessed, with respect to time.

### 5.2 Chapter 5 List of Abbreviations

#### 5.2.1 Transient Models and Thermal Load Case

TRANS-BM-LC1 control model: Transient analysis – thermal load applied to top flange of steel beam – no fire protection (control model).

TRANS-BM-LC1 initial fire-protected model :

Transient analysis – thermal load applied only to top of fire protection material parallel to steel beam top flange – 30mm gypsum protection.

TRANS-BM-LC1 final fire-protected model :

Transient analysis – thermal load applied to top of fire protection material parallel to steel beam top flange and gradually applied directly to steel beam with the occurrence of delamination – 30mm gypsum protection.

### 5.3 Control Model – No Fire Protection

A transient control model was created in Abaqus, where the temperature distribution due to fire and the structural behaviour of the connection were analysed together in the same simulation. The point load of 200kN was applied linearly over time according to

the force-time curve in Appendix B, Table B-7. Simultaneously, the thermal load was applied according to the standard fire curve in Appendix B, Table B-6 onto the top flange of the steel beam. As previously mentioned, the thermo-structural loading considered in the transient models is denoted by TRANS-BM-LC1. The general temperature distribution of the applied thermal load over real time in the control model is shown in Figure 5-1. Thereafter, the temperature variation in the unprotected steel connection is shown in Figure 5-2 (a), (b), (c) and (d) with respect to periods of real time. The total duration of the fire event considered was 90 minutes (5400 seconds), as discussed in Chapter 3 subsection 3.6.2.

It is noteworthy that in the majority of the related research conducted in the past, the concurrent consideration of mechanical and thermal loading has not been elaborately examined. Most of the published work focuses on the thermal effects on a steel assembly without considering a simultaneously applied structural load. Hence, an investigation into the application of simultaneous thermal and structural loading is presented in this chapter. This, together with the contact conditions used to connect several steel parts, the several non-linearities considered (such as large displacements and plasticity) and the simulation of the fire protection material, increases the complexity of the investigation.

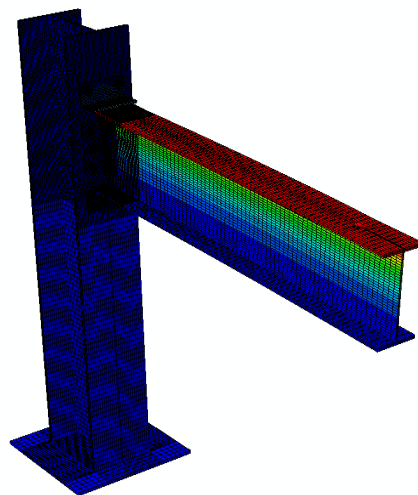


**Figure 5-1: General temperature distribution for TRANS-BM-LC1 control model**

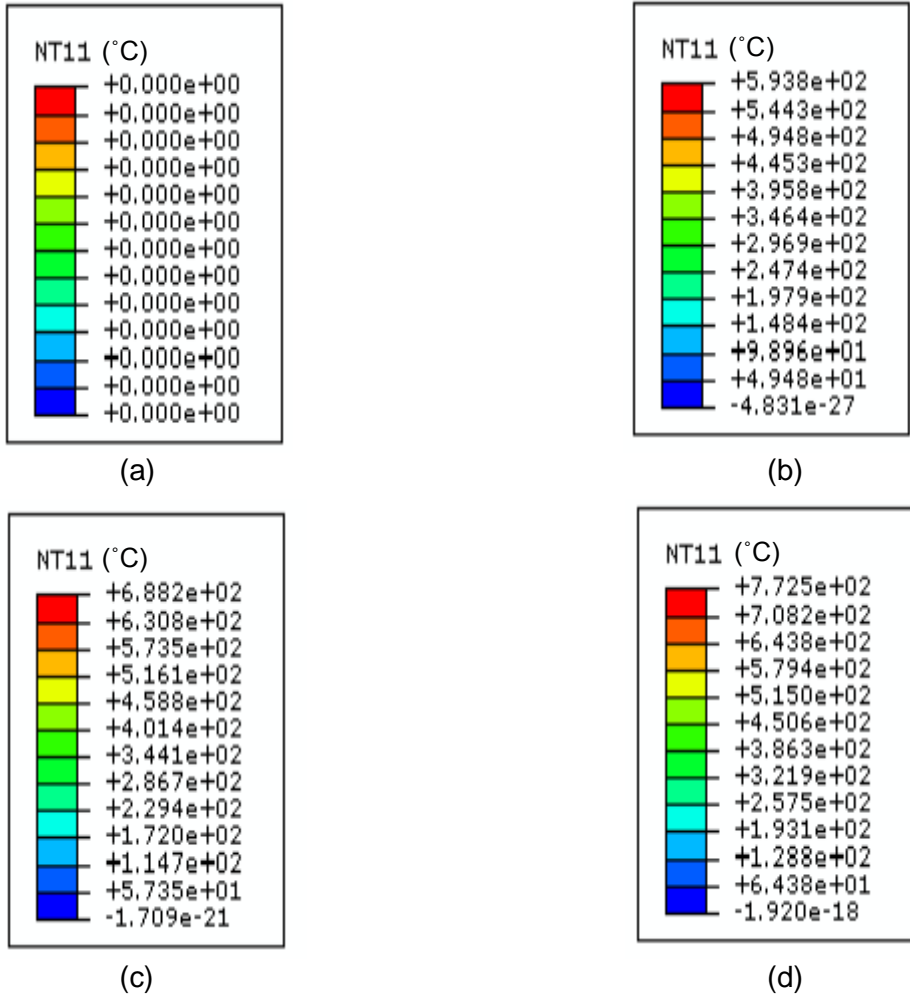


**Figure 5-2: Temperature distribution (°C) in the TRANS-BM-LC1 control model at: (a) 0 minutes; (b) 6 minutes; (c) 11 minutes; (d) 18 minutes, at failure**

From Figure 5-2, it can be seen that over time, an increase in temperatures arises in the steel connection, as expected, from the applied thermal loading. The analysis begins with zero temperatures in the model at 0 minutes. Thereafter at 6 minutes and 11 minutes, the maximum steel temperatures are 594°C and 688°C respectively. The steel connection fails after 18 minutes, with an ultimate steel temperature of 773°C. These temperatures are fairly elevated and increase quickly in the first few minutes due to the high thermal conductivity of steel and absence of a barrier to the applied thermal load. Thus, direct contact between the steel beam and fire is permitted from the outset in this scenario.

Accordingly with the von Mises plasticity model, the elevated temperatures that develop in the first few minutes cause yielding of the steel connection and the substructure incurs damage fairly soon. At approximately 18 minutes in a total analysis time of 90 minutes, the structure reaches its maximum load carrying capacity. This

shows the detrimental effect of not designing for fire resistance, since structural integrity of the steel connection is only maintained for 18 minutes. Furthermore, the transient coupled thermomechanical analysis indicates the effects of real-time fire on the steel connection control model. Therefore, the integrity of the structure is capable of being quantified in terms of real time in the transient analysis. This is related to the main goal of a proper design against fire, defined as the provision of an adequate time period before structural collapse occurs. The force-displacement curve for the coupled temperature-displacement transient analysis of the control mode is displayed in Figure 5-3.

### Thermomechanical Model for TRANS-BM-LC1

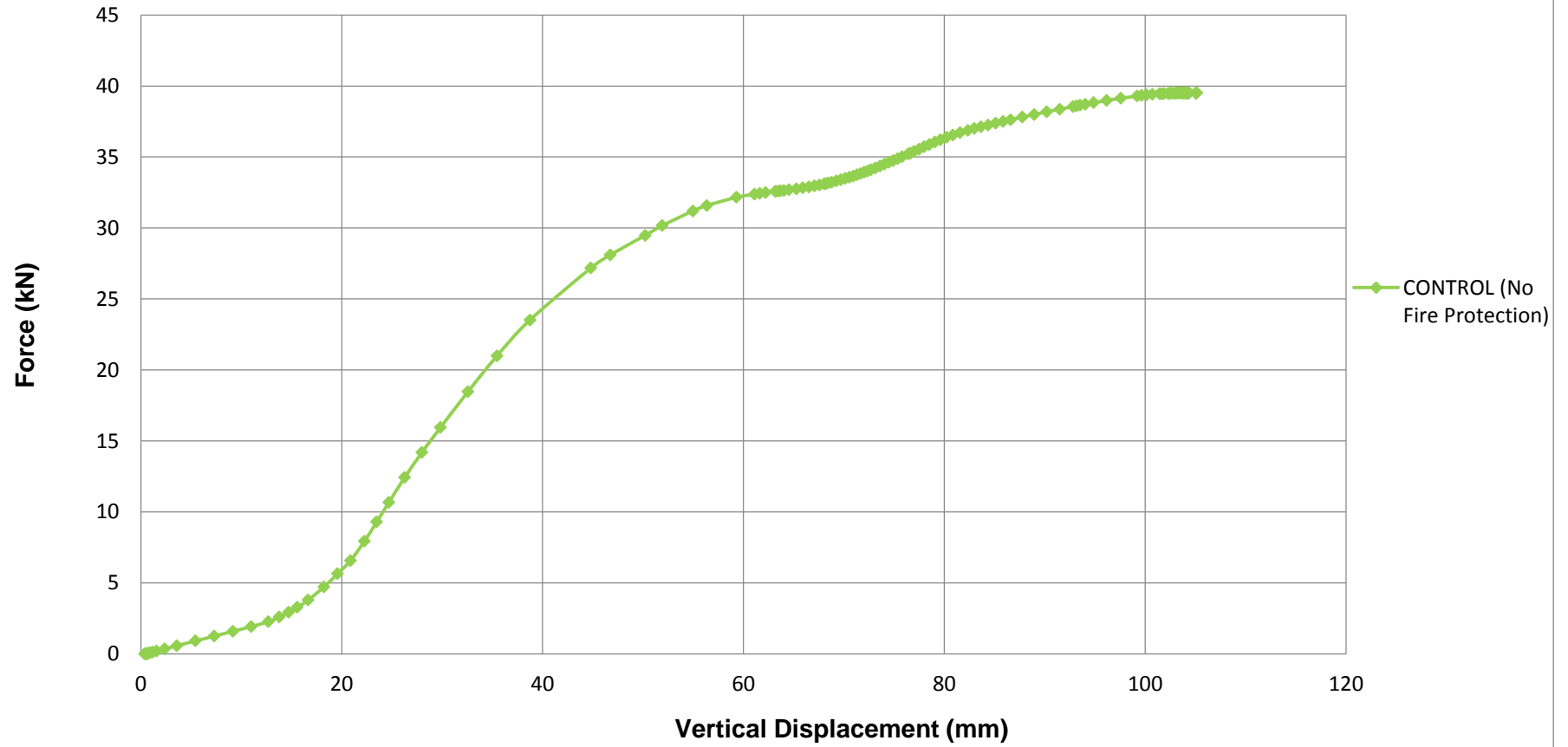
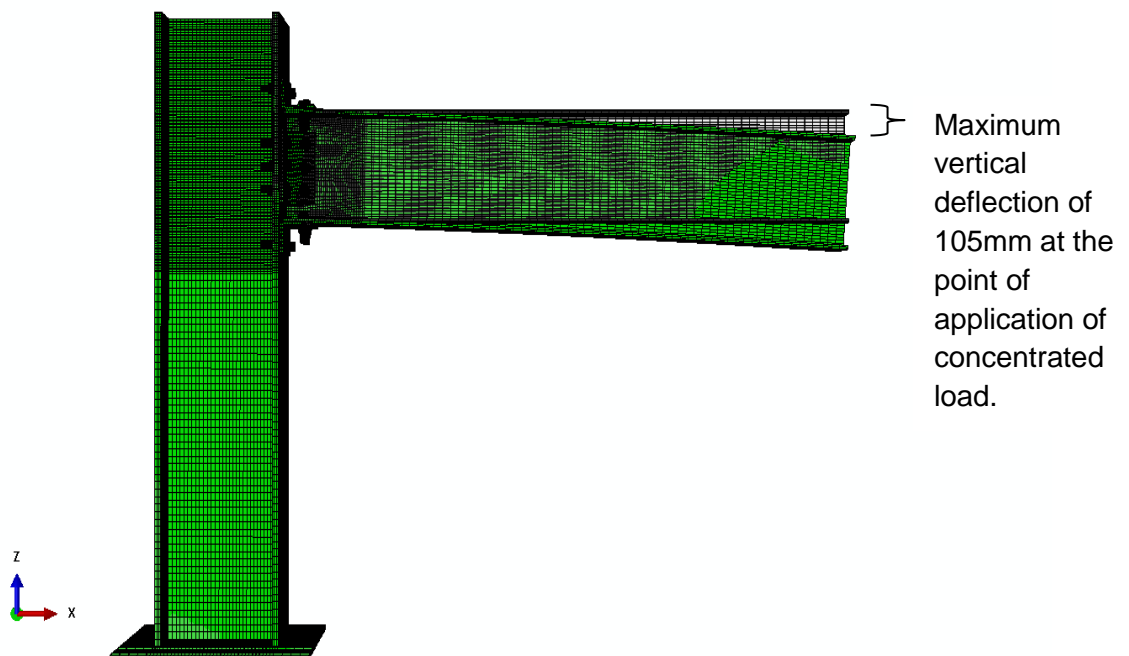


Figure 5-3: Force-displacement curve for coupled Thermomechanical TRANS-BM-LC1 control model

The result depicted by Figure 5-3 indicates the distinct non-linear behaviour of the connection. As the applied structural load and corresponding vertical displacement increases, temperature also increases with time, resulting in yielding of the steel parts. Failure of the steel connection is observed as the curve becomes increasingly horizontal at an applied force of 39kN, with corresponding maximum vertical displacement of 105mm. This indicates that under transient coupled thermomechanical conditions, the unprotected steel connection can support an applied point load of 39kN that occurs at 18 minutes. The purely mechanical steady-state model investigated in Chapter 4 indicates the steel connection supporting a load of 90kN with corresponding 274mm vertical deformation, in Figure 4-1. In the current TRANS-BM-LC1 control model, the added effect from coupled time-dependent thermo-structural loading is assessed in real time, representing a more realistic scenario for the behaviour of the connection. Thus, the importance of conducting investigations into transient coupled thermomechanical is reiterated.

The undeformed shape of the TRANS-BM-LC1 steel connection for 0°C at 0 minutes is compared to the final deformed shape of the connection in Figure 5-4. The final deformed shape is displayed after 18 minutes.



**Figure 5-4: Superimposed undeformed shape (grey) and final deformed (green) shape after 18 minutes of the steel connection for TRANS-BM-LC1 control model**

The result of the Equivalent Plastic Strain output (PEEQ) in Abaqus for the TRANS-BM-LC1 model with no fire protection after 18 minutes is shown in Figure 5-5. This is a significant result of the coupled thermomechanical analyses performed on this model as it depicts the damage to the steel beam at elevated temperatures, due to yielding of the steel members. The maximum yielding that occurs in the steel connection is focused at the point of application of the structural 200kN point load. Further yielding can be observed along the top flange of the beam, due to the applied fire load, and at the joint between the beam-column.

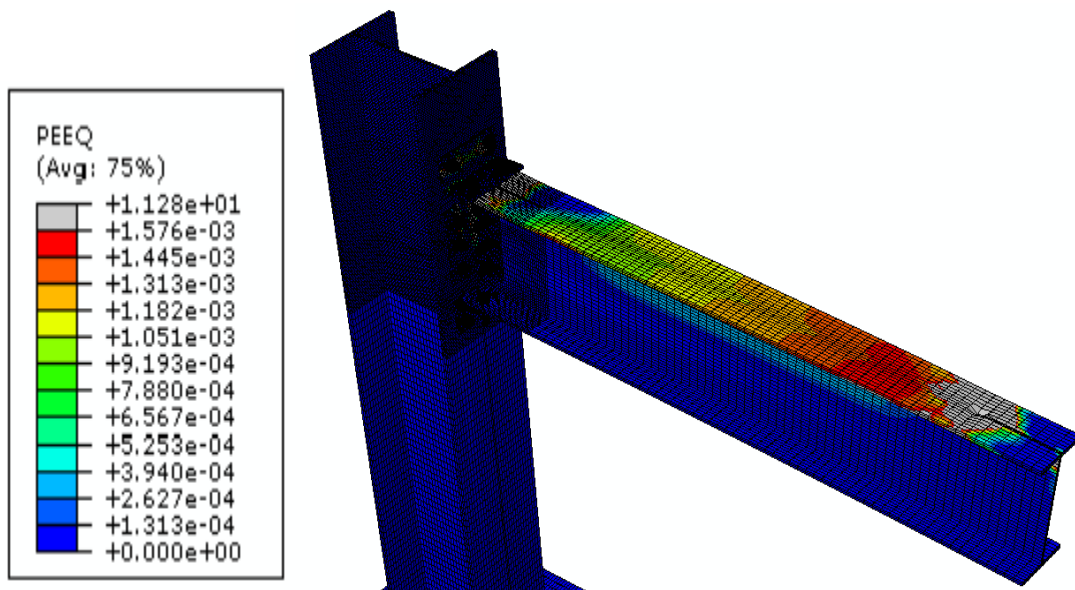


Figure 5-5: Equivalent Plastic Strains for TRANS-BM-LC1 unprotected model at 18 minutes

#### 5.4 Initial Fire-Protected Model

The fire-protected TRANS-BM-LC1 model incorporated 30mm gypsum board protection on the beam flange in a coupled transient thermomechanical analysis. In this initial fire-protected model scenario, the standard fire curve was applied only to the top of the GYP30 protection parallel to the beam top flange. Minimal heat transfer occurred between the fire protection material and the steel connection since delamination occurred between the fire protection material and the steel beam over the 90 minute period. This temperature distribution occurring in the GYP30 protection, formed during analysis, is displayed in Figure 5-6 after complete delamination of fire protection from steel occurred. Thereafter, the temperature variation and progressive delamination in the GYP30-protected steel connection is shown in Figure 5-7 (a), (b), (c) and (d) with respect to periods of real time. This initial fire-protected model scenario was

investigated to obtain the gradual increase in opening between the fire protection material and steel over time.

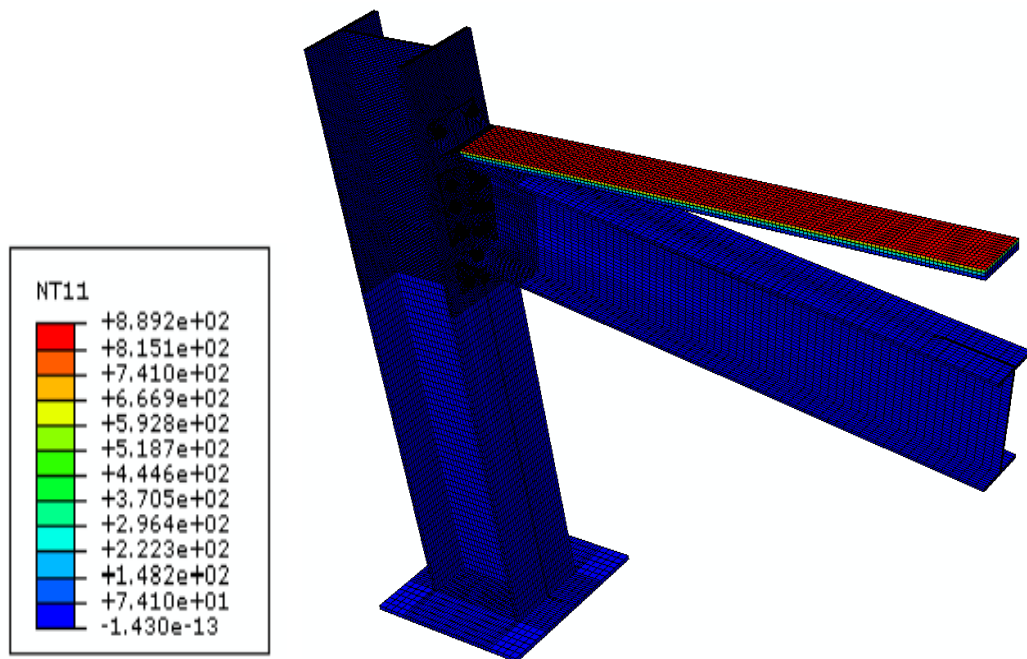
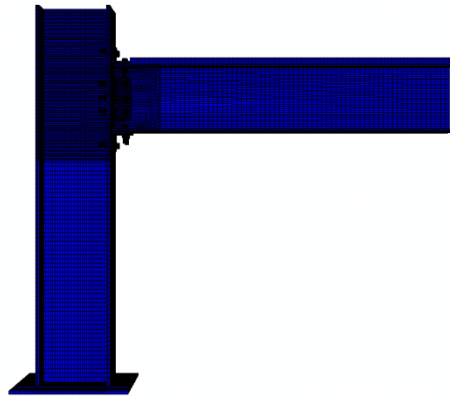
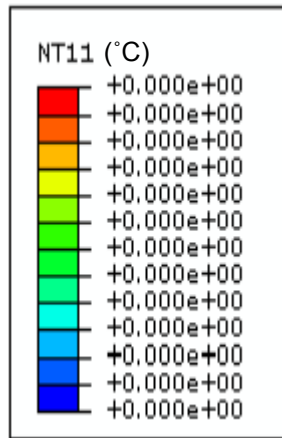
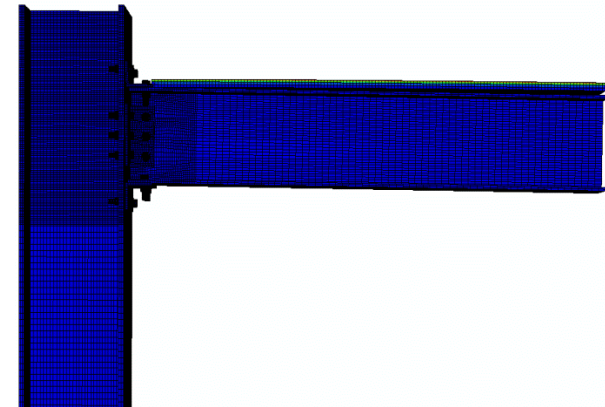
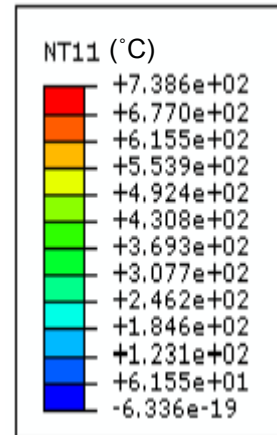


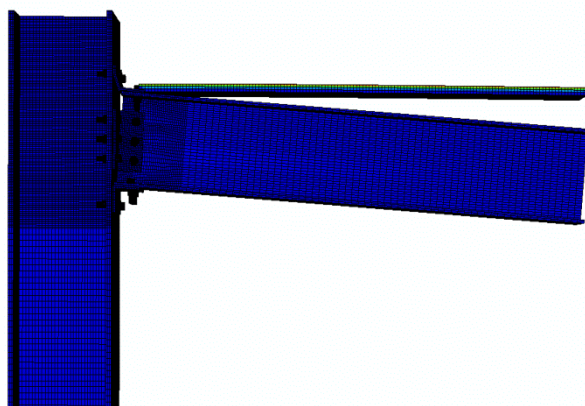
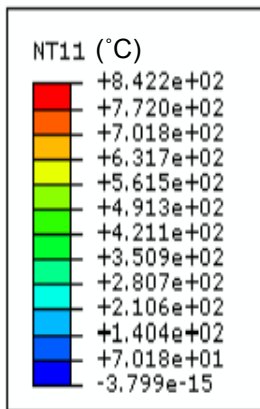
Figure 5-6: Temperature distribution for TRANS-BM-LC1 initial fire-protected model after complete GYP30 delamination, at 41 minutes



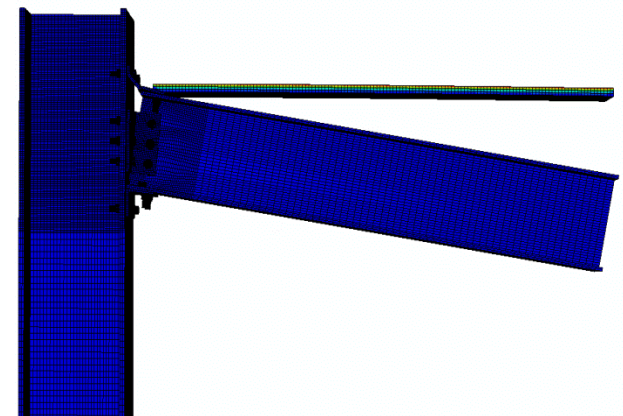
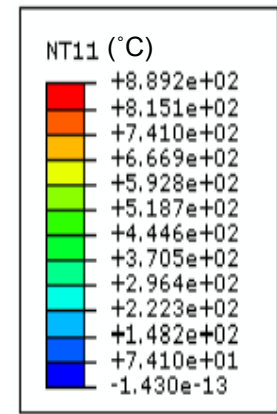
(a)



(b)



(c)



(d)

Figure 5-7: Temperature distribution (°C) and progressive delamination in the initial TRANS-BM-LC1 fire-protected GYP30 model at: a) 0 minutes; b) 15 minutes; c) 30 minutes; d) 41 minutes, after complete delamination

From Figure 5-7, it can be observed that the ultimate temperature of the GYP30 protection progresses from 0°C to 739°C in the first 15 minutes. This is similar to the result obtained in the control model where a maximum temperature of 773°C after 18 minutes was experienced in the steel. However, while the unprotected model fails at 18 minutes, the initial fire-protected GYP30 model experiences complete delamination at 41 minutes, indicating the effect of the fire protection in delaying failure of the connection. It can be seen that temperatures in the actual steel connection remain very low due to the delamination that occurs between the fire protection and the steel beam, thereby preventing heat transfer to the steel from the coupled transient applied thermal load. However, it can be deduced from Figure 5-7 that the GYP30 protection can endure higher temperatures from a temperature-dependent thermal load than the steel connection exposed to direct fire. This can be seen from the temperatures that are developed at 30 minutes and 41 minutes, which is 842°C and 889°C respectively. These temperatures in the GYP30 material are higher than those tolerated by the steel connection with no fire protection, corroborating the fact that GYP30 is efficient in providing fire resistance.

The progressive occurrence of delamination of the fire protection material from the steel connection can be seen in Figure 5-7. From 0 minutes to failure at 41 minutes under coupled transient thermomechanical loading, the increasing gap between GYP30 protection and the steel beam can be observed. The resulting coupled transient force-displacement curve is illustrated by Figure 5-8, in comparison to the TRANS-BM-LC1 control model.

## Thermomechanical Models for TRANS-BM-LC1

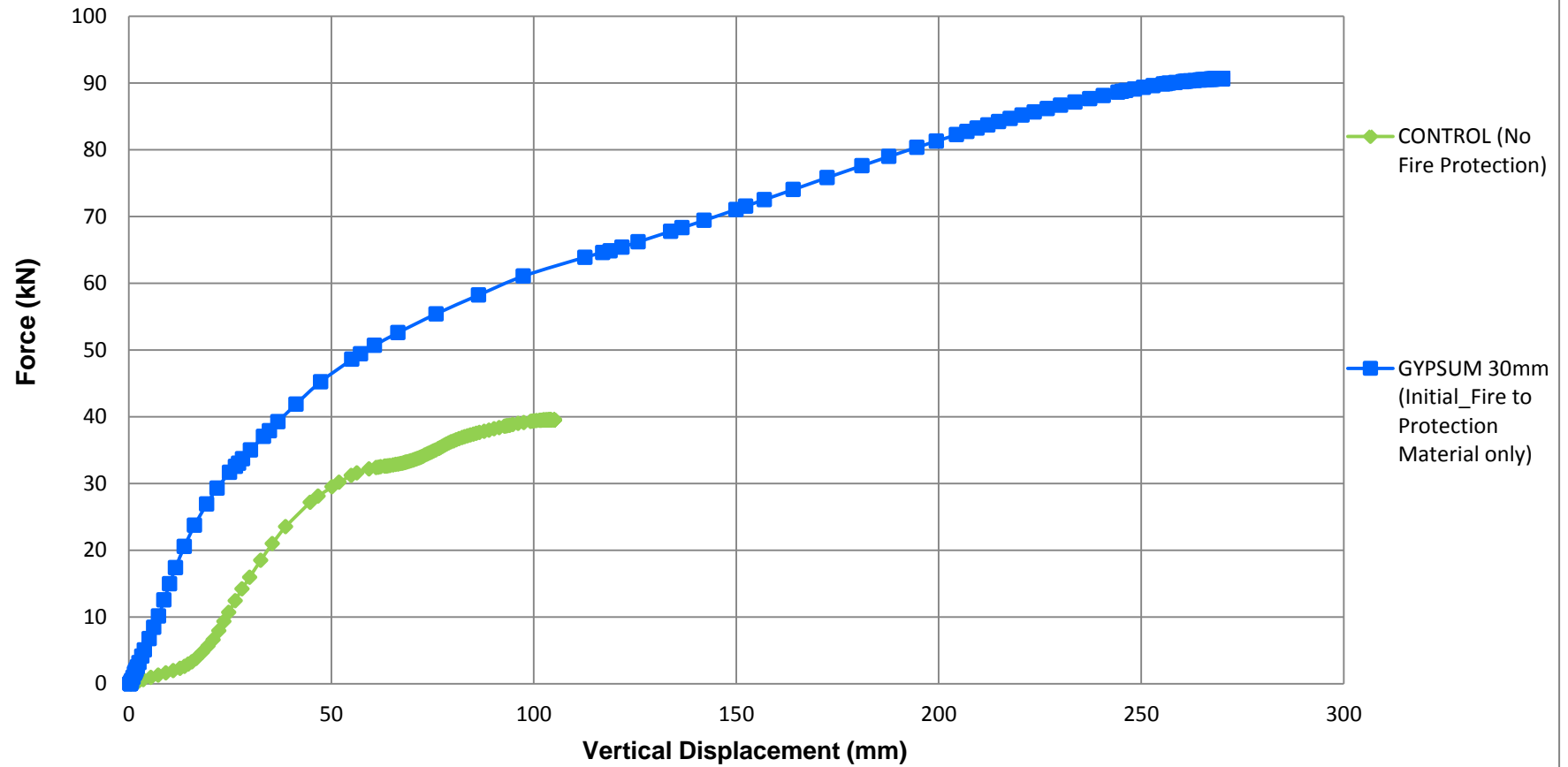


Figure 5-8: Force-displacement curves for coupled Thermomechanical TRANS-BM-LC1 control and initial fire-protected model

As displayed by Figure 5-8, the BM-LC1 initial fire-protected model displays distinct improved behaviour when compared to the unprotected model, since the fire-protected model curve is higher than that of the unprotected model. This improvement is attributed partly to the effectiveness of GYP30 protection in resisting the rise in temperatures in the fire protection over time, thereby maintaining structural integrity for an extended period of time in comparison to the control model. A much greater force is required to cause yielding and failure of the initial fire-protected model under the same coupled transient thermomechanical loading as the control model. The GYP30-protected steel connection tends to failure at a force of approximately 90kN after 41 minutes, with a corresponding maximum vertical deformation of roughly 250mm. In comparison to the model with no fire protection, which fails at a force of 49kN after 18 minutes, the fire-protected model offers increased support of an additional 50kN and maintains structural stability for a significantly longer period of an additional 23 minutes.

However, this scenario does not consider the effect of fire spreading to the steel beam due to the gradual opening between the fire protection and steel beam. Furthermore, damage or destruction to the GYP30 protection due to fire is not encompassed in these results. Thus, a subsequent model is required to account for the realistic coupled transient effects on the overall steel connection.

The PEEQ outcome from the TRANS-BM-LC1 initial fire-protected model (fire applied to the top of the protection only) with GYP30 protection is shown in Figure 5-9. The yielding that occurs in the steel under the coupled thermal-stress loading, at elevated temperatures, is illustrated for this model. Yielding of the steel is less severe than the unprotected model due to the thermal load only being applied to the top of the gypsum protection material parallel to the top flange of the steel beam. Thus, the maximum yielding of the steel occurs at the beam-column joint and at the point of application of the 200kN point load.

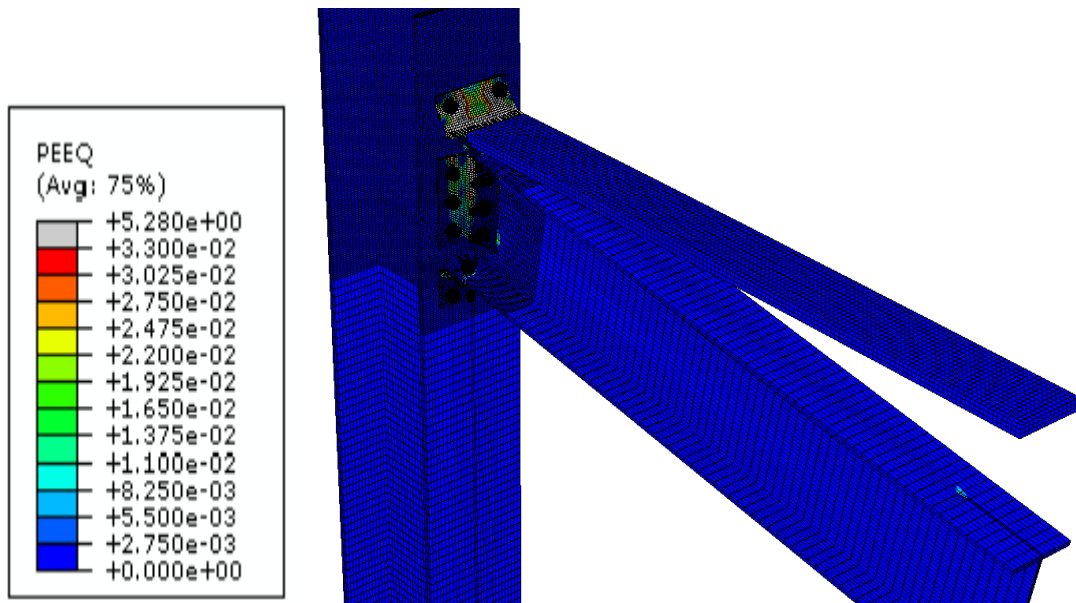


Figure 5-9: Equivalent Plastic Strains for TRANS-BM-LC1 initial fire-protected model at 41 minutes

## 5.5 Final Fire-protected Model – Fire Curve Steel

The results of the initial fire-protected TRANS-BM-LC1 model in subsection 5.3 were used to model a subsequent coupled transient thermomechanical analysis, labelled as the Final Fire-protected Model. This latter model maintained the GYP30 fire protection on the top flange of the steel beam. In the initial model, it was determined that separation of the GYP30 protection from the steel beam gradually occurred over time, with the application of the concentrated force as a force-time curve. The use of the initial transient model results in developing the final model is summarised and presented in Table 5-1.

**Table 5-1: Observations and description of initial and final fire-protected models**

<b>Observations in Abaqus of Initial Fire-protected Transient Model</b>	<b>Translation into Modelling the Final Fire-protected Transient Model</b>
5.1a. Up to approximately 11 minutes, minimal separation occurs between the fire protection and steel beam interfaces (a 0 millimetre gap).	5.1b. The standard fire curve is applied only to the top of the GYP30 protection.
5.2a. After an additional 3 minutes, a 5 millimetre gap is recorded along a measured portion of the steel beam.	5.2b. The standard fire curve continues to be applied to the top of the GYP30 protection and is also applied directly onto the portion of the steel beam with a 5 millimetre gap, measured in 5.2a.
5.3a. At 16 minutes, the 5 millimetre separation between the steel beam and protection material extends further along the beam, as delamination progresses.	5.3b. The transient coupled thermal load continues to be applied as per 5.2b and is further spread directly to the steel beam for a distance measured in 5.3a.
5.4a. After 22 minutes, a minimum 5 millimetre separation between the steel and protection material is experienced throughout the length of the beam.	5.4b. The steel connection fails after 22 minutes, where the fire load makes direct contact with the steel beam over its entire length.

The main difference between the initial and final transient models is that, where the fire condition was previously only applied to the top of the GYP30 material for the entire analysis in the initial model, the final model incorporates the gradual addition of the fire condition to the steel beam itself. Thus, this model takes into account the occurrence of delamination and eventual damage of the board at elevated temperatures by applying the standard fire curve to the top of the protection material and gradually onto the steel beam, as delamination of the protection from the steel occurs. This is an effort towards simulating, as realistically as possible, the evolution of the phenomenon, that is, fire initially makes contact with the protection material, but after a few minutes, evaporation of the water content out of the gypsum board takes place due to elevated temperatures. Additionally, cracking of the board occurs. At this point, the fire protection material is damaged and cannot protect the structure fully. Eventually, the steel is exposed to direct fire, due to this damage incurred by the fire protection. This allows the realistic transient fire scenario to be investigated since fire-spread to the steel beam was accounted for during delamination and heat transfer to the steel beam occurred, as documented in Table 5-1. This temperature distribution occurring in the

GYP30 protection, formed during the coupled temperature-displacement analysis, is displayed in Figure 5-10, after complete delamination of the fire protection material occurred. Thereafter, the temperature variation and progressive delamination in the final GYP30-protected steel connection is shown in Figure 5-11 (a), (b), (c) and (d) with respect to periods of real time.

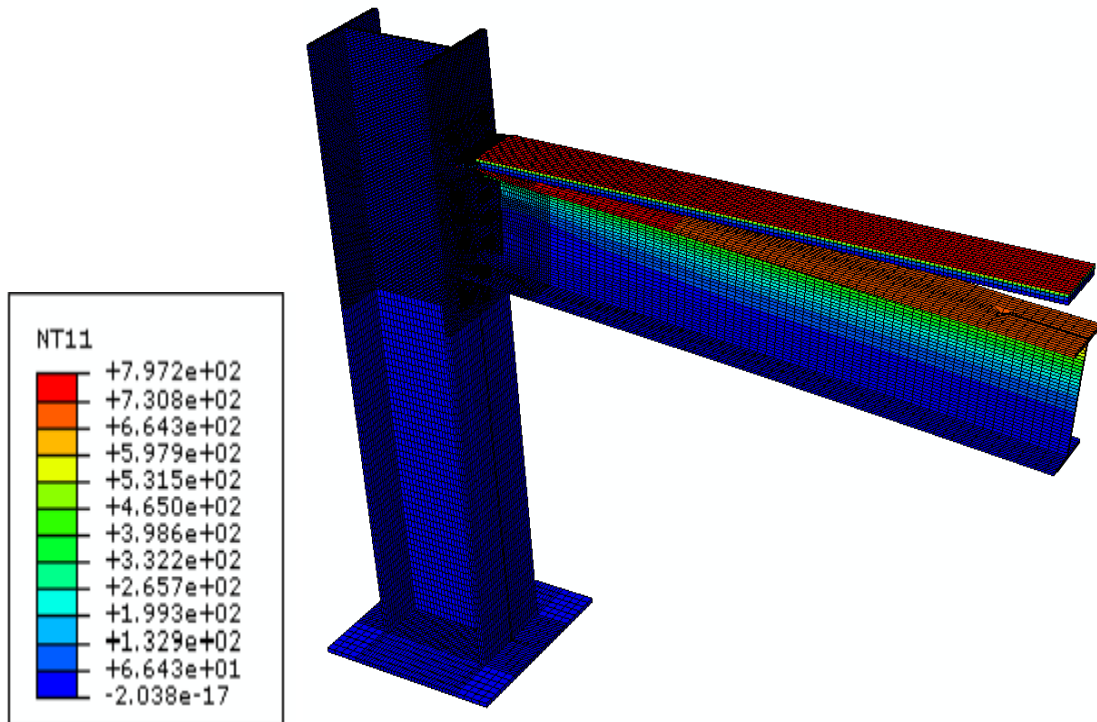
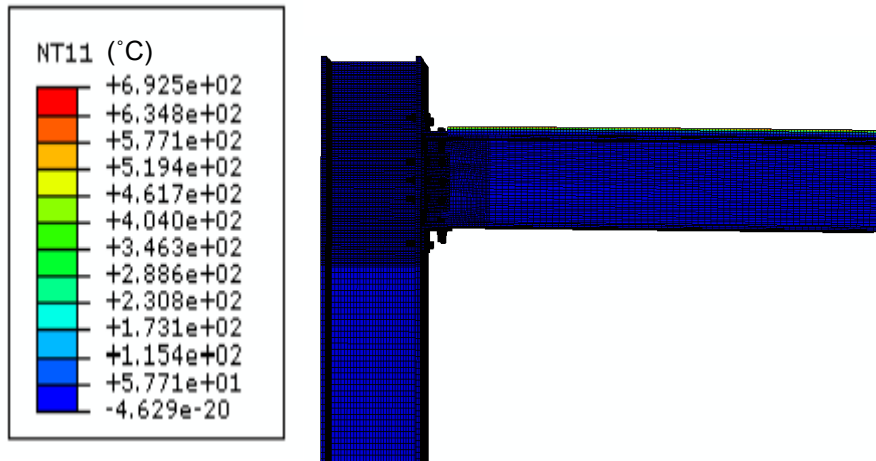
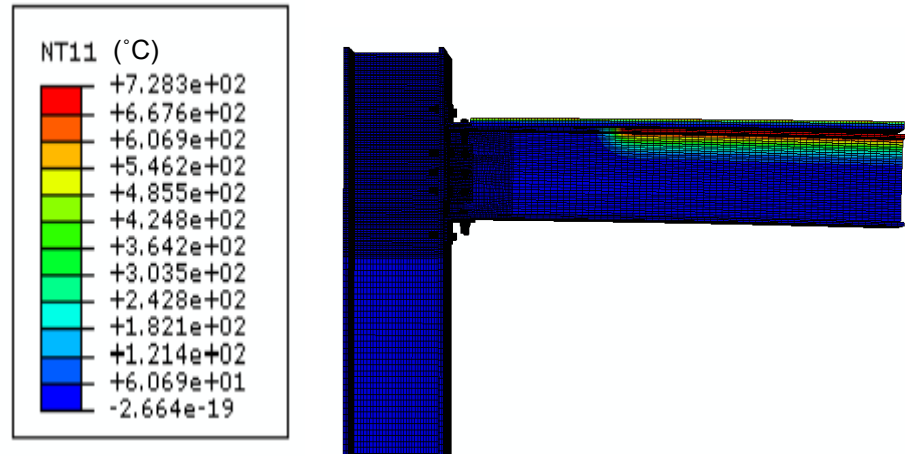


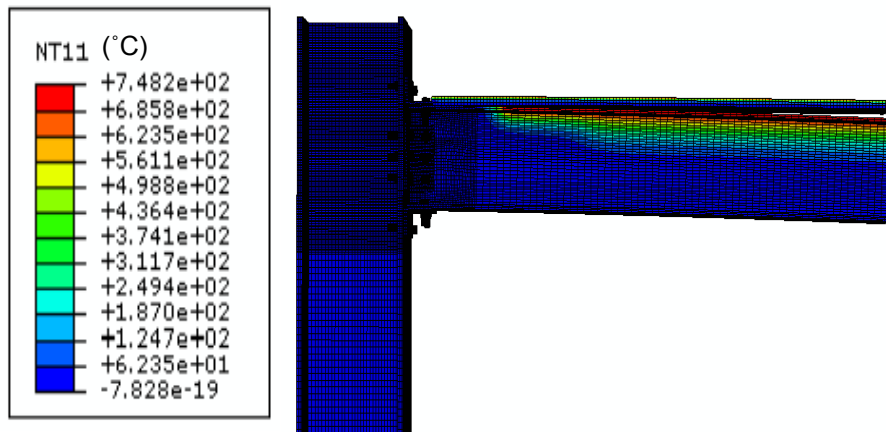
Figure 5-10: Temperature distribution for TRANS-BM-LC1 final fire-protected model after complete GYP30 delamination and additional fire applied to steel beam, at 22 minutes



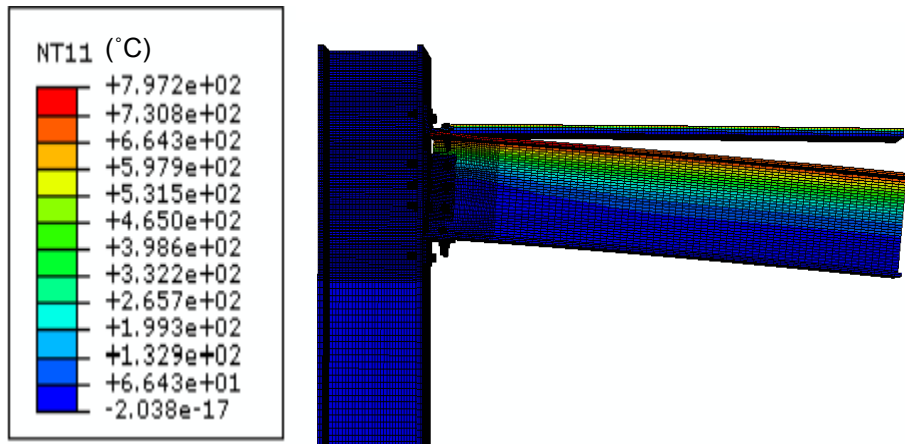
(a)



(b)



(c)



(d)

Figure 5-11: Temperature distribution (°C) and progressive delamination in the final TRANS-BM-LC1 fire-protected GYP30 model at: a) 11 minutes; (b) 14 minutes; (c) 16 minutes; (d) 22 minutes, after complete delamination

The temperature distributions depicted in Figure 5-11 progress from 0°C at the beginning of the analyses, which is depicted previously in Figure 5-7 (a). From Figure 5-11, the maximum temperature in the system at 11 minutes is 693°C, where the coupled transient thermal load is applied on the fire protection since a 0mm gap between the GYP30 protection and the steel beam exists up to 11 minutes. This is in accordance with data describe by Pyro-cote (2017) that states that a temperature of 550°C is reached within 5 minutes in a commercial structural steel building, in the case of a standard time temperature building fire. After an additional 3 minutes, the maximum steel temperature increases to 728°C, where the fire condition is applied onto the length of the steel beam that experience a 5mm opening between the protection and steel beam. At 16 minutes, a maximum steel temperature of 748°C is experienced by the connection due to the progression of delamination and subsequent further application of the transient coupled thermal load along the beam. The steel connection fails after 22 minutes, with an ultimate steel temperature of 797°C. At this point, the thermal load is applied throughout the length of the steel beam since larger gaps exist along the beam between the protection and steel, shown in Figure 5-11 (d).

In comparison to the initial fire-protected model with the transient coupled thermal load applied only on the fire protection, the final fire-protected model develops similar temperatures but fails sooner. While the initial model fails at 41 minutes, the final model is capable of maintaining structural integrity for only 22 minutes. This is expected and attributed to the realistic spread of fire to the protection material with the progression of delamination of the protection material. In contrast to the control model, the TRANS-BM-LC1 final fire-protected model affords the steel connection a few, possibly critical, minutes of additional structural integrity. The resulting comparative coupled transient force-displacement curves between the TRANS-BM-LC1 models are illustrated by Figure 5-12.

## Thermomechanical Models for TRANS-BM-LC1

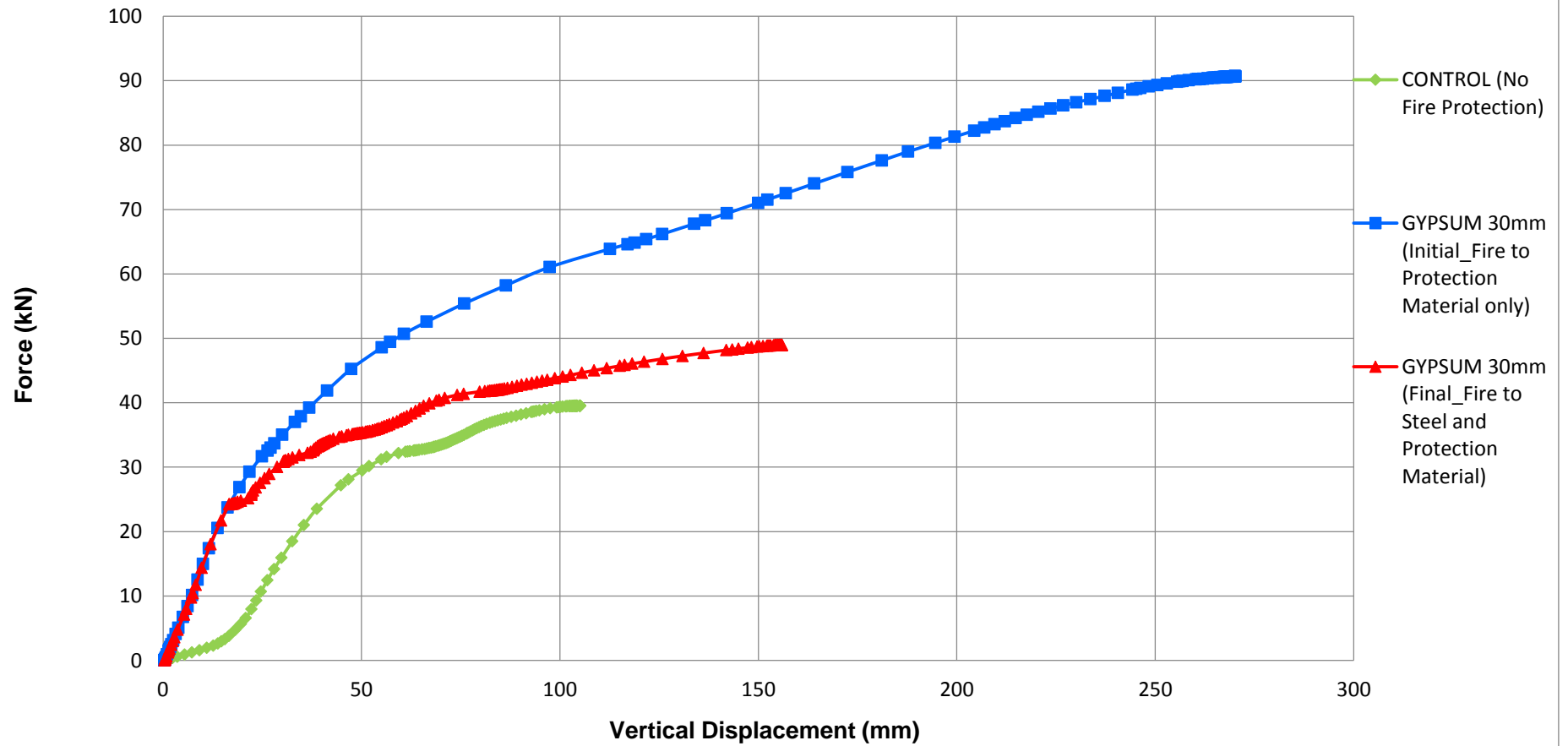


Figure 5-12: Force-displacement curves for coupled Thermomechanical TRANS-BM-LC1 control and fire-protected models

From Figure 5-12, it can be inferred that both TRANS-BM-LC1 models with fire protection indicate an improved performance of the overall steel structure compared to the unprotected model, under transient coupled thermomechanical loading. While the initial fire-protected model displays the superior performance in comparison to the final fire-protected model, it does not represent the realistic fire condition. The fire-protected steel connection would incur progressive delamination and possible destruction of the gypsum protection would permit the spread of fire to the steel beam after some time, thus weakening the structural system. This is evident in the force-displacement curve of the final GYP30-protected model. For the first few minutes where there exists no gap between the fire protection and steel beam, as the initial and final fire-protected model curves behave similarly under the coupled applied force. Thereafter, there is a clear reduction in strength between the two models with fire protection due to the progression of delamination and corresponding realistic spread of fire to the steel beam.

In comparison to the unprotected model, the final fire-protected model presents improved behaviour for some time, despite the eventual spread of fire to the steel beam. The final GYP30 model tends to failure at approximately 48kN with a maximum vertical displacement of 143mm, offering additional load bearing capacity and structural stability for some time compared to the control model. However, it can be seen from Figure 5-12 that after a period of time, the final fire-protected model tends towards the same behaviour as the model with no protection. This behaviour accounts for the damage caused to the gypsum protection and eventual destruction thereof after some time in a fire situation. The damage and destruction caused to the fire protection material will eventually cause failure in the steel connection, similar to the failure that occurs in the unprotected model after some minutes.

The PEEQ output for the TRANS-BM-LC1 final fire-protected model (fire applied to protection material and progressively, the steel beam) is displayed in Figure 5-13. The maximum yielding in the steel connection occurs, once again, at the point of application of the 200kN point load on the steel beam. Further yielding occurs at the joint of the connection due to large deformations that occur in the angles from the applied load. The clear difference in PEEQ output can be seen between the initial and final fire-protected models, where the latter indicates yielding along the flange of the steel beam due to the fire load applied progressively along the length of the beam.

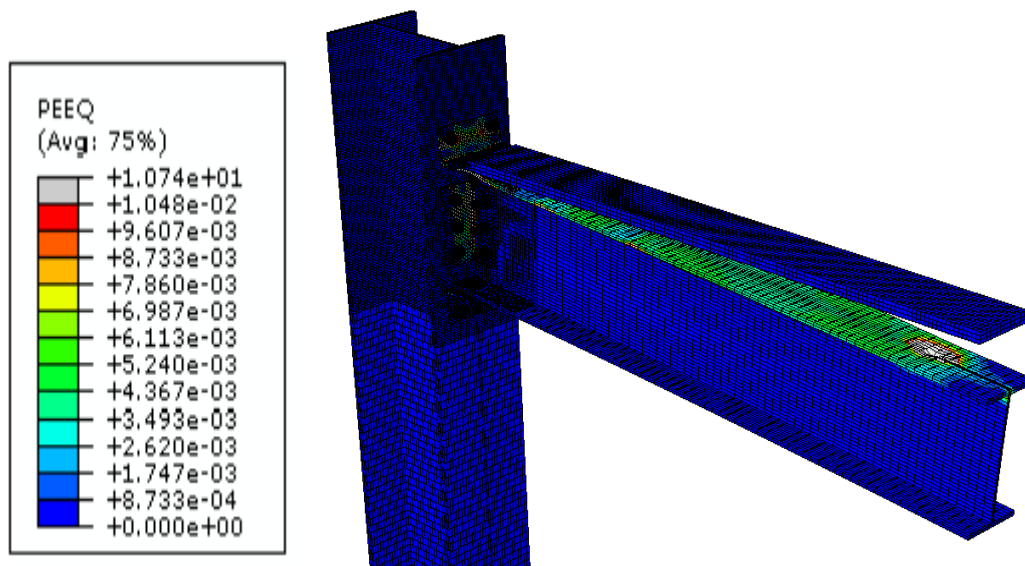


Figure 5-13: Equivalent Plastic Strains for TRANS-BM-LC1 final fire-protected model at 22 minutes

## 5.6 Summary

This chapter provided the results of the coupled transient thermomechanical analyses on the steel connection in accordance with the remaining aims and objectives outlined in Chapter 1. The transient analysis methodology outlined in Chapter 3 was followed. Time-dependent temperature distributions and force-displacement diagrams were obtained and presented for models with and without fire protection. The fire-protected transient models displayed improved behaviour when compared to the unprotected control model that experienced direct fire to the steel beam. The 30mm gypsum protected models incurred lower temperatures in the steel and correspondingly resulted in an increased load bearing capacity of the connection, thus indicating a stronger system than the unprotected model. The effect of progressive delamination on the structural system under coupled temperature-displacement analysis was determined and illustrated. The capacity of the initial fire-protected model to restrict temperature development in the steel and maintain structural integrity of the connection was diminished when the fire event was gradually applied directly onto the steel, through delamination of the GYP30 protection, in the final fire-protected model. Eventual damage of the protection material was accounted for. Furthermore, damage to the steel connection under the time-dependent analyses was displayed by the plastic strains that developed in the beam of the connection, at elevated temperatures. Chapter 6 that follows will offer the main conclusions and recommendations of the steady-state and transient analyses.

# Chapter 6

---

## 6 Conclusions and Recommendations

### 6.1 Introduction

This chapter aims to provide the main conclusions drawn from the research conducted in this study. These deductions will be made from the results recorded from the steady-state and coupled transient analyses of the steel connection under elevated temperatures. The conclusions presented will be established in accordance with the research questions, aims and objectives of the study. Additionally, important findings made through the non-linear investigation into the effect of fire protection and protection material variables will be summarised in this chapter. The key effects of progressive transient delamination and subsequent destruction of fire protection at elevated temperatures examined in the study will be presented. Recommendations for further research on the topic will be provided and concluding remarks of the dissertation will be offered.

### 6.2 Steady-State Analyses

A literature review was conducted in an attempt to determine the existing research and standards regarding fire protection and its effect on steel structures. From this, Abaqus FEA software was selected to conduct the relevant steady-state analyses of various numerical models. A purely structural model was designed and analysed to verify the results against the outcomes of an existing investigation. Thereafter, sequential thermal and thermomechanical analyses were conducted on models with and without fire protection, in various scenarios, to determine the effect of fire protection on the overall structural system. In each scenario, the addition of fire protection to the substructure increased the load bearing capacity of the steel connection, resulting in an improved performance of the connection under elevated temperatures. This occurred as the protection materials offered resistance to the applied fire conditions, thereby limiting the steel temperatures and strengthening the system. The fire protection materials that were investigated were selected as 50mm concrete, 50mm gypsum and 30mm gypsum protection. The improved behaviour of the steel connection was quantified in the comparative force-displacement diagrams derived for each model and in terms of the fire resistance offered by each protection material within the model cases.

The effect of the extent of coverage of the steel connection under similar loading conditions was examined. Two scenarios of coverage were investigated: BM (protection of the top flange of the beam only) and FULL (concealing the entire beam-to-column connection). For load case 1, with applied thermal loading onto the fire protection parallel to the top flange of the beam, FULL coverage offered minimal additional strength to the overall connection. Thus, providing either BM or FULL fire protection coverage typically yields similar results for this load case, where the fire is applied on the protection surface parallel to the flange of the beam. This is expected, since the fire protection applied to the other parts of the connection, are not “activated” against fire, for the FULL-LC1 scenario. Each of the unprotected and fire-protected models in the BM-LC1 scenario resulted in similar maximum temperatures in the steel connection at failure and indicated approximately the same ultimate forces as their analogous models in FULL-LC1. However, when thermal loads are applied to multiple surfaces, in load cases 2 and 3, the total protection resulted in a significantly distinct, improved behaviour in comparison to the unprotected connection. A representation of this was 50mm concrete which afforded a 44 per cent fire resistance to the connection for BM-LC1, which increased to a 69 per cent resistance to fire in FULL-LC3 (all external surfaces exposed to fire), when compared to the unprotected model for the same applied load. Thus, the protection of steel parts becomes increasingly important with the increase in the surfaces that encounter fire. This is noteworthy towards further improving the fire resistance offered by the protection materials under progressively intensified loading conditions, by incorporating fire protection.

As previously mentioned, the fire protection materials under consideration were 50mm concrete, 50mm gypsum board and 30mm gypsum board. Each of these materials resulted in a strengthened connection compared to the unprotected models. This was evident from the comparisons of maximum temperatures incurred in the steel connection at failure and the corresponding ultimate force of the system, displayed by the force-displacement diagrams. Across all model cases, 50mm concrete protection proved to be the most effective in restricting temperature developments in the steel connection, thus affording the highest load-bearing capacity and resulting in the most improved performance of the connection. Concrete protection afforded approximately 50 per cent reduction in temperatures experienced in the steel of all the models, when compared to the unprotected models for the same applied force. In general, 50mm concrete incurred the lowest temperatures in the steel at failure and afforded the system the ability to maintain structural integrity for a force of approximately 1.5 times the ultimate force of the unprotected model in the FULL-LC1 scenario. This margin of

ultimate forces was still evident but reduced for LC2 and LC3 scenarios due to the intensified fire event in these models resulting in rapid failure under the applied thermo-structural loading.

Gypsum protection also resulted in improved behaviour of the steel connection under fire conditions. However, by comparison, both 50mm and 30mm gypsum proved less effective than concrete in reducing the maximum steel temperatures of the connection at failure and indicated failure at loads lower than that of concrete-protected models. Within the gypsum models, the thicknesses of 50mm and 30mm resulted in similar behaviour of the steel system under sequential thermo-structural loading. Under the scenario of BM-LC1, 50mm gypsum offered 28 per cent resistance to fire, while 30mm gypsum offered slightly diminished but similar 25 per cent fire resistance, when compared to the control model for the same applied force. This trend was established across all the subsequent models. The thermal behaviour of different protection materials, the thermal properties of the interfaces between protection-structure and the numerical integration thereof influenced the output of this investigation. Further research is required on this topic.

While the performance of the steel connection with different materials under each loading condition varies, there exists potential for savings to be made in industry. The results determined in the steady-state analyses aid the selection of protection material used for offering fire resistance in the structure, based on the structural requirements and building functionality. Savings can be made from the deduction that providing partial fire protection to a critical element in the substructure can afford similar stability and load bearing capacity to that of covering the entire structure. Thus, this research theoretically aids in the estimation of potential savings by providing information and results on scenario-based research into the behaviour of a steel connection under fire. A more holistic approach, for which complete structural systems need to be examined, shall indicate an optimum configuration for passive fire protection systems in buildings, taking into account financial as well as structural parameters. This remains for future research.

### **6.3 Coupled Transient Analyses**

The literature review conducted indicated deficiencies in current research regarding transient coupled thermo-structural investigations into the behaviour of steel structures under fire and considering fire protection. Abaqus was used to create models with and

without fire protection to investigate the gradual effect of delamination between the protection material and steel surface on the structural system. The coupled structural and thermal loadings were applied for one load case through a force-time curve and standard fire curve, described previously in Chapter 3, respectively. This coupled temperature-displacement analysis offers several advantages, since structural loads and fire events were simultaneously be studied in the same model. Thus, the redistribution of forces due to local failure of some parts of a building in a fire event, as well as failure of the passive protection against fire, are only some cases for which this type of analysis can be useful. On the other hand, the computational effort required for this analysis is higher in comparison with a typical, uncoupled simulation.

An initial fire-protected model was subjected to thermal loading on the fire protection only, while the final fire-protected model was subjected to fire on the protection material and progressive fire on the steel part. Thus, the final fire-protected model considered the deterioration of the fire protection over time under fire conditions and accounted for the spread of fire to the steel after some minutes. This modelling technique can be used as an accurate assessment of the load carrying capacity of protected structural systems in fire conditions. Initially from literature and existing experiments, the thermal behaviour of fire protection materials and the time they resist against fire, are recorded. In the structural model, fire loading is initially applied to the protection but gradually, when the protection is damaged at elevated temperatures, the thermal loads are applied to the steel parts. This procedure takes place in several time steps.

The aforementioned procedure was implemented in the investigation conducted in this dissertation. The fire protection material under investigation was 30mm gypsum, but exactly the same procedure could be similarly applied to concrete protection. From the literature review, it was found that a gypsum board resists fire for the first minutes of a fire event. Thereafter, evaporation of the water from the board and cracking due to elevated temperatures, results in the failure of the protection. At the same time of this failure, the heat load is applied also to the steel parts in the proximity of the board, where the heat load had initially been applied.

The delamination failure mechanism over time, with corresponding temperature distributions from the coupled analysis, in the steel connection with fire protection was illustrated. Force-displacement curves of the models with and without fire protection were obtained and compared. The true, realistic results of the final fire-protected model indicated a clear reduction in strength of the overall connection with the occurrence of

progressive delamination and corresponding fire spread to the exposed steel. Although the fire-protected final model indicated an improved behaviour in the steel connection initially, over time the degradation in strength of the model resulted in similar behaviour to that of the unprotected model. Thus, delamination of the fire protection material and eventual destruction thereof proves to be detrimental to the performance of the steel structure, under elevated temperatures. The gradual destruction of the thermal protection occurs as a result of direct contact between the fire event and the steel, and eventually causes the connection to behave as an unprotected structure.

#### **6.4 Recommendations for Further Research**

- The present study investigates the behaviour of a particular steel substructure and therefore affords limited insight into the behaviour of a larger-scale, global structure. There is scope to investigate other significant steel substructures and overall assemblies in attaining greater accuracy in determining the effects of fire. Furthermore, composite structures and the effects of fire thereon can be analysed.
- In the analyses, static structural forces are considered. Studies can be conducted to include the effects of dynamic and impact loading coupled with simultaneous effects of fire.
- There is scope for additional scenario-based analyses of transient coupled temperature-displacement models and probing of the phenomenon of delamination to be conducted, with the consideration of other fire protection materials and variations in thicknesses.
- Further research can be conducted by means of physical experimental investigations into the topic, towards verifying the thermal, thermomechanical and delamination models of the study.
- The effect of various other commonly used fire protection materials can be investigated, such as intumescent coatings, or spray-applied fire resistant materials. Steady-state and transient analyses can be performed to investigate these other materials.
- Further research can be conducted in modelling a more sophisticated fire event considering other parameters such as radiation, convection and complex thermal conductance at the interface.

The research conducted in this investigation affords engineers, locally and internationally, further insight into the effects of fire on a steel connection and the

delamination phenomenon. Relevant information can be drawn from this dissertation regarding the fire resistance of various protection materials and associated factors on the behaviour of the steel connection under fire. The time-dependent analyses provide effective comprehension of the realistic temperature distributions and structural behaviour of steel connections under elevated temperatures, considering delamination. Coupled with building regulations and designated design codes, the sound analyses presented from the numerical models can be used to optimise the fire design of similar steel connections and substructures.

# References

---

- Abaqus/CAE User's Guide. 2014. Understanding the relationship between models, parts, instances and assemblies. Abaqus Online Documentation. Available from: <http://abaqus.software.polimi.it/v6.14/books/usi/default.htm>. Accessed on: 15 September 2017.
- Abdalla, K.M, Drosopoulos, G.A and Stavroulakis, G.E. 2015. Failure Behaviour of a Top and Seat Angle Bolted Steel Connection with Double Web Angles. *Journal of Structural Engineering*, 141 (7).
- Arablouei, A and Kodur, V. 2015. Dynamic delamination of fire insulation applied on steel structures under impact loading. *International Journal of Impact Engineering*, 83 (15), 11-27.
- Arablouei, A and Kodur, V. 2016. Effect of fire insulation delamination on structural performance of steel structures during fire following an earthquake or an explosion. *Fire Safety Journal*, 84 (16), 40-49.
- Badarneh, M.A. 2004. Unilateral contact problem and prying force in top and seat angle connection with double web angle. M.S. thesis, Jordan University of Science and Technology, Irbid, Jordan.
- Baetu, G, Galatanu, TF and Baetu, SA. 2017. Behaviour of Steel Structures under Elevated Temperature. *Procedia Engineering*, 181 (17), 265-272.
- Beitel, J.J and Iwankiw, N.R. 2004. Historical Survey of Multi-storey Building Collapses Due to Fire. Hughes Associates, Inc. Available from: [https://www.iensenhughes.com/wp-content/uploads/2014/02/White\\_Paper\\_Historical\\_Survey\\_Building\\_Collapse\\_NIST\\_JBeitel-NIwankiw\\_OCT-2006.pdf](https://www.iensenhughes.com/wp-content/uploads/2014/02/White_Paper_Historical_Survey_Building_Collapse_NIST_JBeitel-NIwankiw_OCT-2006.pdf). Accessed on: 9 October 2017.
- Buchanan, A.H and Abu, A.K. 2017. *Structural Design for Fire Safety*. John Wiley & Sons, Ltd. West Sussex. United Kingdom.

Daryan, A.S and Yahyai, M. 2008. Behavior of bolted top-seat angle connections in fire. *Journal of Construction Steel Research*, 65 (9), 531-541.

Daryan, A.S and Yahyai, M. 2009. Modeling of bolted angle connections in fire. *Fire Safety Journal*, 44 (9), 976-988.

*EN1991-1-2: Eurocode 1 – Actions on Structures*. 2002. Draft prEN1991-1-2. General Actions – Actions on structures exposed to fire. European Committee for Standardization. Brussels. Belgium.

*EN1993-1-2: Eurocode 3 – Design of steel structures*. 2001. DD ENV 1993-1-2. General rules – Structural fire design. European Committee for Standardization. Brussels. Belgium.

*EN1993-1-2: Eurocode 3 – Design of steel structures*. 2005. DRAFT prEN1993-1-2. General rules – Structural fire design. European Committee for Standardization. Brussels. Belgium.

Encyclopaedia Britannica. 2017. Specific heat. Encyclopaedia Britannica, Inc. Available from: <https://www.britannica.com/science/specific-heat>. Accessed on: 14 October 2017.

Encyclopaedia Britannica. 2017. Thermal conduction. Encyclopaedia Britannica, Inc. Available from: <https://www.britannica.com/science/thermal-conduction>. Accessed on: 14 October 2017.

Engineering News. 2017. More Fire Protection For Concrete With Adfil Fibres From Chryso. Available from: <http://www.engineeringnews.co.za/article/more-fire-protection-for-concrete-with-adfil-fibres-from-chryso-2017-09-01>. Accessed on 28 November 2017.

FEACompare. 2017. Side by side comparison chart of 78 mechanical Finite Element Analysis (FEA) programs. Available from: <http://feacompare.com/index.html>. Accessed on: 14 September 2017.

Fire Protection Association of Southern Africa (FPASA). 2017. Fire Stats 2015, SA Fire Loss Statistics 2015. FPASA. Gauteng. South Africa.

Franssen, J.M, Kodur, V and Zaharia, R. 2009. *Designing Steel Structures for Fire Safety*. CRC Press Taylor & Francis Group. Florida. United States of America.

Franssen, J-M and Real, P.V. 2015. *Fire Design of Steel Structures*. European Convention for Constructional Steelwork. Mem Martins. Portugal.

Garg, A. C. 2003. Delamination – a damage mode in composite structures. *Engineering Fracture Mechanics*, 29 (5), 557-584.

Geneva Association. 2014. Fire and Climate Risk. No.29. The Geneva Association. Zurich. Switzerland.

Gentili, F. 2013. Advanced numerical analyses for the assessment of steel structures under fire. *International Journal of Lifecycle Performance Engineering*, 1 (2), 159-184.

Gu,L and Kodur, V. 2011. Role of Insulation Effectiveness on Fire Resistance of Steel Structures under Extreme Loading Events. *Journal of Performance of Constructed Facilities*, 24 (4), 277-286.

Gyproc South Africa. 2017. Walls. Available from:  
<https://www.gyproc.co.za/products/walls>. Accessed on: 28 November 2017.

Henderson, B and Graham, C. 2017. Dubai skyscraper fire: Torch Tower residents wake to screams as flames engulf 79-storey building. Telegraph Media Group Limited. United Kingdom. Available from: <http://www.telegraph.co.uk/news/2017/08/03/dubai-skyscraper-fire-1100ft-torch-tower-engulfed-flames/>. Accessed on: 28 November 2017.

Hopkin, D.J, Lennon, T, El-Rimawi, J and Silberschmidt V.V. 2012. A numerical study of gypsum plasterboard behaviour under standard and natural fire conditions. *Fire and Materials*, 36 (2), 107-126.

Kalogeropoulos, A, Drosopoulos, G.A. and Stavroulakis, G.E. 2011. Thermal–stress analysis of a three-dimensional end-plate steel joint. *Construction and Building Materials*, 29 (12), 619-626.

Kodur, V and Arablouei, A. 2015. Effective properties of spray-applied fire-resistive material for resistance to cracking and delamination from steel structures. *Construction and Building Materials*, 84 (15), 367-376.

Lafarge. 2017. Fire Solutions. Available from: [https://www.lafarge.co.za/fire\\_solutions](https://www.lafarge.co.za/fire_solutions). Accessed on 28 November 2017.

Logan, D.L. 2007. A First Course in the Finite Element Method - Fourth Edition, Thomson, Canada, United States of America.

Mandoval. 2017. Fire proofing products. Available from: <http://www.mandovalvermiculite.co.za/fire-proofing-products/>. Accessed on 28 November 2017.

National Fire Protection Association (NFPA). 2016. Fire Loss in the United States During 2015. NFPA Research. Quincy. United States of America.

Nombembe, P. 2017. Millions go up in flames at Cape Town cash and carry warehouse. TimesLIVE. South Africa. Available from: <https://www.timeslive.co.za/news/south-africa/2017-10-28-millions-go-up-in-flames-at-cape-town-cash-and-carry-warehouse/>. Accessed on: 28 November 2017.

Oxford English Dictionary. 2017. Delaminate. Oxford University Press. Available from: <https://en.oxforddictionaries.com/definition/delaminate>. Accessed on: 22 October 2017.

Phan, L.T, McAllister, T.P, Gross, J.L and Hurley, M.J. 2010. *Best Practice Guidelines for Structural Fire Resistance Design of Concrete and Steel Buildings*. Report No.1681. National Institute of Standards and Technology. Maryland. United States of America.

Pyro-cote. 2015. Fire Protective coatings for structural steel. Available from: <http://pyrocote.co.za/> <http://pyrocote.co.za/structuralsteel/>. Accessed on 28 November 2017.

Rogers, C.P and Medonos, S. n.d. Fire Induced Progressive Collapse Analysis of Safety Critical Structures. In: ed. Viridi, K.S, Matthews, R.S, Clarke, J.L and Garas, F.K. *Abnormal Loading on Structures*, 125-136. E & FN Spon, London, United Kingdom.

SANS 10400. Edition 3. 2011. Part T: Fire Protection. SABS Standards Division. Pretoria. South Africa.

Slater, D. 2017. Grenfell Tower – How could we have done the Risk Analysis Differently? Cambrensis Ltd. Cardiff. United Kingdom. Available from: <https://www.researchgate.net/publication/319183242>. Accessed on: 12 October 2017.

Southern African Institute of Steel Construction (SAISC). 2016. *Southern African Steel Construction Handbook*. Eighth Edition. SAISC. Johannesburg. South Africa.

Steelconstruction.info. (2017). Fire protecting structural steelwork. Available from: [http://www.steelconstruction.info/Fire\\_protecting\\_structural\\_steelwork](http://www.steelconstruction.info/Fire_protecting_structural_steelwork). Accessed on: 9 November 2017

Tsapara, K, Drosopoulos, G.A and Stavroulakis, G.E. 2013. Finite Element Analysis of Fire Resistant Reinforcement on End-Plate Steel Connections. *Application of Structural Fire Engineering*. Prague. Czech Republic.

Walls, R.S and Botha, M. 2016. Towards a structural fire loading code for buildings in South Africa. Insights and Innovation in Structural Engineering. Available from: <https://www.researchgate.net/publication/311439884>. Accessed on: 15 October 2017.

Winestone, J. 2010. Steel Buildings in Europe: Multi-Storey Steel Buildings – Part 6: Fire Engineering. Available from: <http://sections.arcelormittal.com/library/design-manuals-steel-building-in-europe.html>. Accessed on: 20 October 2017.

World Life Expectancy. 2014. Fires: Death Rate Per 100,000. World Life Expectancy. Available from: <http://www.worldlifeexpectancy.com/cause-of-death/fires/by-country/>. Accessed on: 3 September 2017.

World Life Expectancy. 2014. Health Profile: South Africa. World Life Expectancy. Available from: <http://www.worldlifeexpectancy.com/cause-of-death/fires/by-country/>. Accessed on: 3 September 2017.

Zingoni, A. 2006. Behaviour, analysis and design of steel structures. *Journal of Constructional Steel Research*, 62 (1-2), 1-3.

# Appendix A

## A.1 Geometry of the Steel Connection Parts

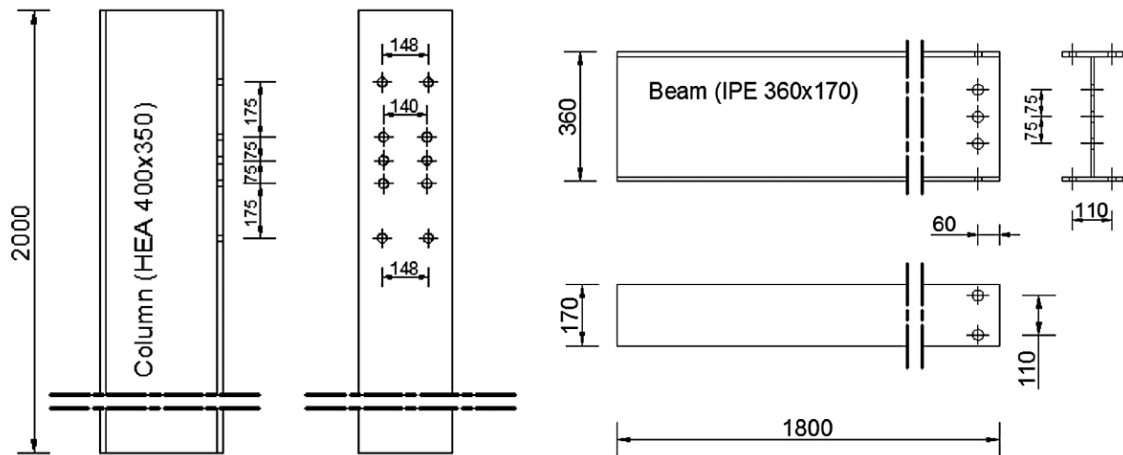


Figure A-1: Geometry of the column and beam steel elements in millimetres (Abdalla et al., 2015)

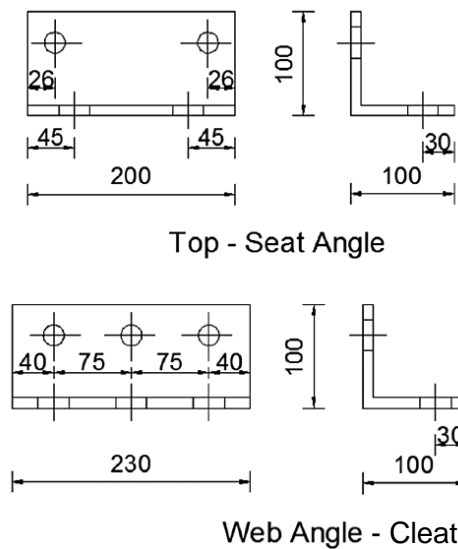


Figure A-2: Geometry of the steel angle elements in millimetres (Abdalla et al., 2015)

# Appendix B

## B.1 Raw Data

Table B-1: Plasticity properties for mechanical model (after EN1993-1-2, 2005)

Steel Connection	Yield Stress (kPa)	Plastic Strain
Steel Parts	300600	0
	445200	0,055301
	522000	0,144940
Steel Bolts	652816,67	0
	778125,00	0,031626
	880000,00	0,089444

Table B-2: Thermal conductivities of fire protection materials for thermal model (after Tsapara et al, 2013)

Temperature (°C)	Thermal Conductivity of Protection Material (kW/m°C)	
	Gypsum	Concrete
20	0,000200	0,000988
100	0,000183	0,000938
200	0,000120	0,000875
300	0,000100	0,000813
400	0,000120	0,000750
500	0,000123	0,000688
600	0,000130	0,000625
700	0,000137	0,000563
800	0,000147	0,000500
900	0,000160	0,000500

Table B-3: Plasticity properties for steel parts in thermomechanical model (after EN1993-1-2, 2005)

Steel Parts (Column, beam, angles and washers)		
Temperature (°C)	Yield Stress	Plastic Strain
20	300600	0
20	445200	0,055300908
20	522000	0,136793942
100	300600	0
100	445200	0,055300908
100	522000	0,136793942
200	242584,2	0
200	300600	0,017575961
200	300600	0,137535276
300	184267,8	0
300	300600	0,017297627
300	300600	0,137256942
400	126252	0
400	300600	0,01693977
400	300600	0,136899085
500	108216	0
500	234468	0,017197427
500	234468	0,137156742
600	54108	0
600	141282	0,016764305
600	141282	0,13672362
700	22545	0
700	69138	0,016257089
700	69138	0,136216404
800	15030	0
800	33066	0,017353294
800	33066	0,137312609
900	11272,5	0
900	18036	0,018021294
900	18036	0,137980609

Table B-4: Plasticity properties for steel bolts in thermomechanical model (after EN1993-1-2, 2005)

Steel Bolts		
Temperature (°C)	Yield Stress	Plastic Strain
20	652816,67	0
20	778125,00	0,03162647
20	880000,00	0,089444
100	631839,28	0
100	631839,28	0,09109792
200	610486,00	0
200	610486,00	0,09078806
300	589820,92	0
300	589820,92	0,09039501
400	506166,80	0
400	506166,80	0,09048954
500	358920,07	0
500	358920,07	0,09132218
600	143439,76	0
600	143439,76	0,09222545
700	65216,67	0
700	65216,67	0,09196574
800	43690,49	0
800	43690,49	0,09207385
900	21495,44	0
900	21495,44	0,09318717

Table B-5: Specific heat of steel (after EN1993-1-2, 2005) and gypsum (Hopkin et al, 2012)

Temperature (°C)	Specific Heat (J/kgK)	
	Steel Parts and Bolts	Gypsum Protection
20	439,80	1000
40	453,35	1000
80	477,16	1000
100	487,62	18000
200	529,76	8000
300	564,74	1000
400	605,88	1000
500	666,50	1000
600	759,92	1000
700	1008,15	1000
735	5000,00	1000
800	803,26	1000
900	650,44	1000

**Table B-6: Data for the standard fire curve (after EN1991-1-2, 2002)**

<b>Time (seconds)</b>	<b>Temperature (°C)</b>
0	20
60	349,213
120	444,504
180	502,289
240	543,887
300	576,410
360	603,117
420	625,776
480	645,455
540	662,846
600	678,427
660	692,539
720	705,436
780	717,310
840	728,312
900	738,560
960	748,153
1020	757,168
1080	765,671
1140	773,718
1200	781,354
1260	788,620
1320	795,550
1380	802,174
1440	808,517
1500	814,602
1560	820,450
1620	826,078
1680	831,502
1740	836,737
1800	841,795
1860	846,688
1920	851,426
1980	856,019
2040	860,476
2100	864,803
2160	869,009
2220	873,100
2280	877,083
2340	880,962
2400	884,744
2460	888,432
2520	892,032
2580	895,547
2640	898,982

2700	902,339
2760	905,624
2820	908,837
2880	911,983
2940	915,065
3000	918,084
3060	921,044
3120	923,946
3180	926,794
3240	929,588
3300	932,331
3360	935,024
3420	937,671
3480	940,271
3540	942,827
3600	945,340
3660	947,811
3720	950,242
3780	952,635
3840	954,990
3900	957,309
3960	959,592
4020	961,841
4080	964,056
4140	966,240
4200	968,392
4260	970,513
4320	972,605
4380	974,668
4440	976,703
4500	978,711
4560	980,692
4620	982,648
4680	984,578
4740	986,484
4800	988,366
4860	990,224
4920	992,060
4980	993,873
5040	995,665
5100	997,435
5160	999,185
5220	1000,915
5280	1002,625
5340	1004,315
5400	1005,987

**Table B-7: Data for force-time curve (developed for transient analyses in Chapter 5 using the time periods of Table B-6)**

<b>Time (seconds)</b>	<b>Force (kN)</b>
0	0
60	2,2
120	4,4
180	6,6
240	8,8
300	11,0
360	13,2
420	15,4
480	17,6
540	19,8
600	22,0
660	24,2
720	26,4
780	28,6
840	30,8
900	33,0
960	35,2
1020	37,4
1080	39,6
1140	41,8
1200	44,0
1260	46,2
1320	48,4
1380	50,6
1440	52,8
1500	55,0
1560	57,2
1620	59,4
1680	61,6
1740	63,8
1800	66,0
1860	68,2
1920	70,4
1980	72,6
2040	74,8
2100	77,0
2160	79,2
2220	81,4
2280	83,6
2340	85,8
2400	88,0
2460	90,2
2520	92,4
2580	94,6
2640	96,8
2700	99,0
2760	101,2

2820	103,4
2880	105,6
2940	107,8
3000	110,0
3060	112,2
3120	114,4
3180	116,6
3240	118,8
3300	121,0
3360	123,2
3420	125,4
3480	127,6
3540	129,8
3600	132,0
3660	134,2
3720	136,4
3780	138,6
3840	140,8
3900	143,0
3960	145,2
4020	147,4
4080	149,6
4140	151,8
4200	154,0
4260	156,2
4320	158,4
4380	160,6
4440	162,8
4500	165,0
4560	167,2
4620	169,4
4680	171,6
4740	173,8
4800	176,0
4860	178,2
4920	180,4
4980	182,6
5040	184,8
5100	187,0
5160	189,2
5220	191,4
5280	193,6
5340	195,8
5400	200,0

# Appendix C

## C.1 Sample Calculation

Table C-1: Sample calculation for force-displacement curve in mechanical model

Output from Abaqus		Calculated force-displacement values	
A	B	C = (A-1) x 200	D = (-1) x (B)
Time step*	Vertical displacement (U) (in metres)	Force (kN)	Vertical Displacement (m)
1,00	-4,41E-04	0,00	4,41E-04
1,01	-2,04E-03	2,00	2,04E-03
1,02	-3,63E-03	4,00	3,63E-03
1,04	-5,98E-03	7,00	5,98E-03
1,06	-8,84E-03	11,50	8,84E-03
1,09	-1,35E-02	18,25	1,35E-02
1,10	-1,56E-02	20,78	1,56E-02
1,12	-1,96E-02	24,58	1,96E-02
1,13	-2,13E-02	26,00	2,13E-02
1,14	-2,42E-02	28,14	2,42E-02
1,16	-2,96E-02	31,34	2,96E-02
1,16	-3,17E-02	32,54	3,17E-02
1,17	-3,49E-02	34,34	3,49E-02
1,19	-4,04E-02	37,05	4,04E-02
1,19	-4,24E-02	38,06	4,24E-02
1,20	-4,55E-02	39,58	4,55E-02
1,21	-5,04E-02	41,86	5,04E-02
1,21	-5,22E-02	42,72	5,22E-02
1,22	-5,52E-02	44,00	5,52E-02
1,23	-6,03E-02	45,93	6,03E-02
1,24	-6,91E-02	48,81	6,91E-02
1,25	-7,25E-02	49,89	7,25E-02
1,26	-7,80E-02	51,52	7,80E-02
1,27	-8,68E-02	53,95	8,68E-02
1,27	-9,02E-02	54,87	9,02E-02
1,28	-9,55E-02	56,24	9,55E-02
1,29	-1,04E-01	58,29	1,04E-01
1,30	-1,07E-01	59,06	1,07E-01
1,30	-1,12E-01	60,22	1,12E-01
1,31	-1,20E-01	61,95	1,20E-01
1,31	-1,24E-01	62,60	1,24E-01
1,32	-1,30E-01	63,58	1,30E-01

1,33E	-1,39E-01	65,04	1,39E-01
1,33	-1,43E-01	65,59	1,43E-01
1,33	-1,48E-01	66,41	1,48E-01
1,33	-1,49E-01	66,72	1,49E-01
1,34	-1,52E-01	67,18	1,52E-01
1,34	-1,55E-01	67,88	1,55E-01
1,34	-1,60E-01	68,92	1,60E-01
1,35	-1,67E-01	70,48	1,67E-01
1,36	-1,78E-01	72,82	1,78E-01
1,37	-1,82E-01	73,70	1,82E-01
1,38	-1,87E-01	75,02	1,87E-01
1,38	-1,96E-01	77,00	1,96E-01
1,39	-2,00E-01	77,74	2,00E-01
1,39	-2,05E-01	78,85	2,05E-01
1,40	-2,13E-01	80,52	2,13E-01
1,42	-2,25E-01	83,02	2,25E-01
1,42	-2,28E-01	83,65	2,28E-01
1,42	-2,32E-01	84,27	2,32E-01
1,43	-2,37E-01	85,21	2,37E-01
1,43	-2,45E-01	86,62	2,45E-01
1,43	-2,47E-01	86,97	2,47E-01
1,44	-2,49E-01	87,32	2,49E-01
1,44	-2,53E-01	87,85	2,53E-01
1,44	-2,57E-01	88,38	2,57E-01
1,44	-2,58E-01	88,51	2,58E-01
1,44	-2,59E-01	88,71	2,59E-01
1,45	-2,62E-01	89,01	2,62E-01
1,45	-2,64E-01	89,15	2,64E-01
1,45	-2,66E-01	89,30	2,66E-01
1,45	-2,67E-01	89,36	2,67E-01
1,45	-2,68E-01	89,44	2,68E-01

\*The time step of Abaqus set for incremental application of the concentrated force, thus not real time. Abaqus provides the time step for five decimal places. The time step figures in the table are provided to two decimal places for simplicity. The calculated column C values are based on the full Abaqus values.